SLK-mediated phosphorylation of paxillin is required for focal adhesion turnover and cell migration

Jennifer Leigh Quizi

Thesis submitted to the Faculty of Graduate and Postdoctoral Studies
In partial fulfillment of the requirements
For the PhD degree in Cellular and Molecular Medicine

Department of Cellular and Molecular Medicine
Faculty of Medicine
University of Ottawa

Supported By:

Dedication:

"What goes beyond is what you see beyond when you know"

Ernest Hemingway

To my entire family: for your loving support and tireless encouragement, I dedicate this work to you.

Acknowledgements:

First and foremost, I'd like to thank my supervisor, Dr. Luc Sabourin for his help and guidance these past 5 years. I truly feel that I would not be the researcher I am today if it was not for the faith and confidence you placed in my abilities. To my committee members, thank you for preparing me to write this thesis and present it to the best of my ability. Your constructive feedback made me strive for better and is the reason I am proud to present the data that is in this thesis. To my lab mates past and present, I'd like to extend my most heart-felt gratitude to you for your comradery, your patience and your suggestions.

To the Center for Cancer Therapeutics, I could not have asked for a better experience than what the environment of this research center has provided me with. Thank you for your tireless dedication to the continuous improvement of this facility and the quality of care that cancer patients receive in Ottawa.

To the Canadian Breast Cancer Foundation, thank you for choosing to believe in our research and my potential to help realize our goal. The friendships I have formed because of the opportunities you have provided me with are truly invaluable. To the National Science and Engineering Research Council and the Ontario Graduate Scholarships in Science and Technology, thank you for your support in my research.

Lastly, to my family and friends: your unwavering support in my education has helped me to become the person that I am today. To my parents, thank you for your faith in my future and your patience as I have strived to achieve it. To my husband Chris, you are my rock and my safe place. Thank you for believing in me and helping me to see my way through… this is as much yours as it is mine.

Abstract:

The precise mechanism regulating focal adhesion disassembly has yet to be elucidated. Recently, we have implicated the Ste20-like kinase SLK in mediating efficient focal adhesion turnover and cell migration in a Rac-1 and FAK-dependent manner. Although an indirect association of this kinase with the microtubule network has been determined, the exact involvement of SLK in the disassembly of the adhesion complex remains unclear. With the identification of the focal adhesion protein paxillin as a substrate of SLK, we show that SLK regulates adhesion turnover through its phosphorylation at S250. Mutation of S250 to a threonine residue ablates SLK phosphorylation of paxillin *in vitro* and results in reduced adhesion turnover and migration *in vivo.* Additionally, our studies demonstrate that overexpression of the paxillin S250T mutation prevents the redistribution of paxillin to the membrane ruffle in migrating cells. The complete loss of polyubiquitylation in the S250T mutant, combined with no observed reduction in S250T protein expression, suggests that S250 phosphorylation is required for a ubiquitin-mediated modification that regulates paxillin redistribution within the cell. Moreover, we show that phosphorylation of S250 is required for paxillin to interact with FAK. An observed accumulation of phospho-FAKY397 in cells overexpressing the paxillin S250T mutant suggests that phosphorylation of S250 is involved in regulating FAK-dependent focal adhesion dynamics. Consequently, our data suggests that SLK regulates adhesion turnover through the phosphorylation of paxillin at S250.

Table of Contents:

List of Figures and Tables:

List of Abbreviations:

(1) AR: Androgen receptor

(2) BSA: Bovine serum albumin

(3) cDNA: Complementary deoxyribonucleic acid

(4) CHO-K1: is a subclone of the parental CHO, or Chinese hamster ovary cell line derived from the ovary of an adult Chinese hamster; these cells are of an epithelial origin and are considered to be adherent.

(5) Ci: Curie

(6) DAB: 3,3'-diaminobenzidine

(7) DAPI: 4',6-diamidino-2-phenylindole

(8) DMEM: Dulbucco's Modified Eagle Medium

(9) DNA: Deoxyribonucleic acid

(10) Drf: Diaphonous-related formins

(11) DTT: Dithiothreitol

(12) EGF: Epidermal growth factor

(13) EGFR: Epidermal growth factor receptor

(14) ER: Estrogen Receptor

(15) Erk1/2: Extracellular signal-regulated kinases 1/2; also known as p44/p42 MAPK

(16) FAK: Focal adhesion kinase

(17) FBS: Fetal bovine serum

(18) FN: Fibronectin

(19) FVB: Friend Virus B-Type

(20) GEF: Guanine nucleotide exchange factor

(21) Glu: glutamic acid

(22) GST: Glutathione-S transferase

(23) HRG: Heregulin

(24) h: Hour

(25) IF: immunofluorescence

(26) IHC: Immunohistochemistry

(27) kb: kilobase

(28) kDa: kilodalton

(29) MAPK: Mitogen-activated protein kinase

(30) MEF: Mouse embryonic fibroblasts

(31) MEF3T3: Mouse embryonic fibroblasts immortalized via the 3T3 protocol

(32) µCi: Microcurie

(33) µl: Microliter

(34) µM: Micromolar

(35) mM: Millimolar

(36) mmol: Millimole

(37) p: phospho

(38) P: position

(39) p130-Cas: p-130 Crk-associated substrate

(40) PBS: Phosphate buffered saline

(41) PCR: Polymerase chain reaction

(42) PFA: Paraformaldehyde

(43) PI3K: Phosphoinositol-3 kinase

(44) PMA: phorbol 12-myrisate 13-acetate

(45) PMSF: Phenylmethylsulfonyl Fluoride

(46) PR: Progesterone Receptor

(47) PVDF: Polyvinylidene difluoride

(48) RING: Really interesting new gene

(49) S: serine

(50) SDS: Sodium Dodecyl Sulphate

(51) SH: Src-homology

(52) SLK: Ste20-like kinase

(53) T: Threonine

(54) TMA: Tissue microarray

(55) TNBC: Triple-negative breast cancer

(56) TRITC: Tetramethylrhodamine-5-isothiocyanate

(57) WASP: Wiskott-Aldrich syndrome protein

(58) Y: Tyrosine

<u>Chapter 1</u>:

General Introduction

Introduction:

Cell Migration

The proper development and maintenance of multicellular organisms is highly dependent on cell migration [1]. *In vivo*, cell migration is a directional, multi-step process that regulates embryonic development, inflammatory response and tissue regeneration [2, 3]. Dysregulation of cell migration has been shown to drive disease progression, contributing to the pathologies of vascular disease, multiple sclerosis and cancer [1, 4].

Directed cell migration is initiated by chemical and physical cues that originate from the extracellular environment [5]. For example, chemotaxis induces migration regulation via gradients of soluble growth factors and/or cytokines such as the platelet-derived growth factor (PDGF), chemokines and bacterial products [2]. In contrast, haptotaxis stimulates migration in response to gradients of extracellular matrix (ECM) proteins such as fibronectin and collagen. However, fibronectin, vitronectin and collagen I are soluble in plasma and in this capacity, have been shown to induce migration through chemotaxis as well [2, 6, 7]. Other guidance cues include but are not limited to: the topography and mechanics of the ECM itself such as cell stretching and/or fluid flow, gradients of light intensity as well as electrostatic and gravitational potentials [3, 5]. Irrespective of the mode of stimulation, directed cell migration requires a polarization of the cell and its components to elicit net cellular movement in a predetermined direction.

Polarized cells are defined by a spatial and functional asymmetry from which the cell develops two, opposing migratory poles. The primary pole or leading edge, can be identified by the formation of localized protrusive structures, whereas the opposing pole or trailing edge, exhibits cellular retraction [7, 8]. Without the acquisition of front-rear polarity, protrusions would be able to form simultaneously in opposite directions, creating a relative cellular tug-of-war which would effectively render migration impossible [9]. At the molecular level, cellular polarization can be regarded as a bi-product of the unequal distribution of signaling molecules, cytoskeletal elements such as actin and tubulin, as well as directed membrane trafficking and redistribution of adhesion receptors to the leading edge [7, 10]. Culminating in the formation and dissolution of focal complexes, a leading and trailing edge emerges and facilitates efficient cell migration. However, the cyclical formation and dissolution of focal adhesions that drives directed migration, is dependent on a co-ordinated, localized, reorganization of the cytoskeleton in order to generate sufficient force to advance the cell in a given direction [7]. Consequently, cytoskeletal dynamics have been shown to play a critical role in each of the four stages involved in acquiring a migratory phenotype: cellular extension, adhesion, contraction and release [2, 7, 8, 11].

The Cytoskeleton and Cellular Extension:

The cytoskeleton is a three-dimensional polymer network composed of actin fibres, microtubules and intermediate filaments [11]. Actin fibres, by mass, are the dominant structural element of actively moving cellular extensions, and are the most abundant protein in a eukaryotic cell [11, 12]. Specifically, lamellipodial extension is regulated by the dynamic polymerization of actin in a Rac1 and Cdc42-dependent manner into branched filament networks. This arrangement of actin provides the force required to push the plasma membrane forward [1, 5, 10, 13, 14]. Like lamellipodia, invadopodia are believed to require an extensively branched actin meshwork, although in the case of invasive structures, sustained branching would be required to propel invadopodia into the underlying matrix (**Figure 1.1 A-C**) [13, 14]. The actin assembly and dendritic nucleation involved in the formation of both lamellipodia and invadopodia have been shown to require the actin nucleator Arp2/3, its activator, N-WASP and the stabilizing actin binding protein cortactin [13-16]. Conversely, the relatively transient and less substantial filopodial membrane extension or ruffle which functions as a pseudo sensory organ that assimilates extracellular stimuli, is made up of bundles of long, cross-linked parallel actin filaments that are nucleated and elongated by the formin family protein, mDia1 and mDia2/DRF3 (**Figure 1.1 A, D & E**) [13-18].

Microtubules have also been shown to play a role in cell polarization and membrane extension. Migratory cells form a stable sub-population of microtubules at the leading edge to reorient the microtubule organizing center (MTOC) between the nucleus and the leading edge to create a polarized microtubule array that directs vesicular trafficking and maintains cell shape [9, 10, 19]. Additionally, disruption of the microtubule network by nocodazole-induced microtubule catastrophe or taxol-mediated microtubule stabilization, results in a depolarized cell morphology and a dramatic reduction in both the rate and directionality of migration [2, 20]. Conversely, release from the stabilizing effects of microtubule antagonists has been shown to induce microtubule regrowth toward the membrane ruffle, activation of Rac1 and the formation of filopodia and lamellipodia [2, 19, 21].

Adhesion, Contraction and Release:

Once formed, membrane protrusions are stabilized by the assembly of, and their subsequent anchorage to, focal adhesion complexes [5, 7]. Cycles of attachment at the cell front, release at the rear, and traction in between, are mediated by adhesion complexes and are required to generate the force necessary for translocation [7, 22]. There are several types of adhesions depending on their location with respect to the leading edge and the assemblies of actin that they interact with (**Figure 1.2**): (1) the nascent adhesion is a small, dot-like, short-lived adhesion found in the lamellipodium that forms directly behind the leading edge [5, 23, 24]. These adhesions exhibit either a very transient existence, with turnover occurring within approximately 60 seconds of formation [5, 7, 9, 24]. These adhesions are enriched with αVβ3 integrin and contain only a subset of known focal adhesion proteins such as vinculin and talin [23]. (2) Focal complexes are found slightly further back from the leading edge at the lamellipodium-lamellum interface, are larger in size and can persist to form focal adhesions [5, 24]. (3) Focal adhesions however, are large, elongated adhesive structures that form at the end of ventral actin stress fibres and can be found at both the leading and trailing edge of migrating cells [5, 14, 25]. To date, upwards of 150 structural and signaling proteins have been identified to reside within the focal adhesion including paxillin, vinculin, talin, the focal adhesion kinase (FAK) and integrins [23, 24, 26]. Lastly, (4) fibrillar adhesions, which are characterized by a highly elongated structure and latency, are involved in the reorganization of ECM, specifically fibronectin matrix assembly, and are not often found in rapidly migrating cells [5, 22, 23].

Adhesion and contraction are interdependent and reliant upon the development of tension in the actomyosin complex. Disruption of the formation or maintenance of stress fibres

<u>Figure 1.1</u>: ***Schematic representation of the anatomy of a migrating cell.*** **(A)** Side view of a migrating cell illustrating the peripheral and dorsal ruffle, lamellipodium, and lamellum. Please note that peripheral and dorsal ruffles are distinct structures with peripheral ruffles assembling at the leading edge, while dorsal ruffles or 'actin ribbons' form on the dorsal surface of the cell. Although both types are ruffles are associated with migration, only dorsal ruffles are also capable of regulating the internalization of receptors and macropinocytosis. **(B-D)** Side views of lamellipodia, ruffles, filopodia and lamellae. The leading edge is rich in actin filaments [27], whereas lamellar filaments (red) are assembled and concentrated behind the lamellipodium. Figure adapted from Chhabra and Higgs (2007) [28].

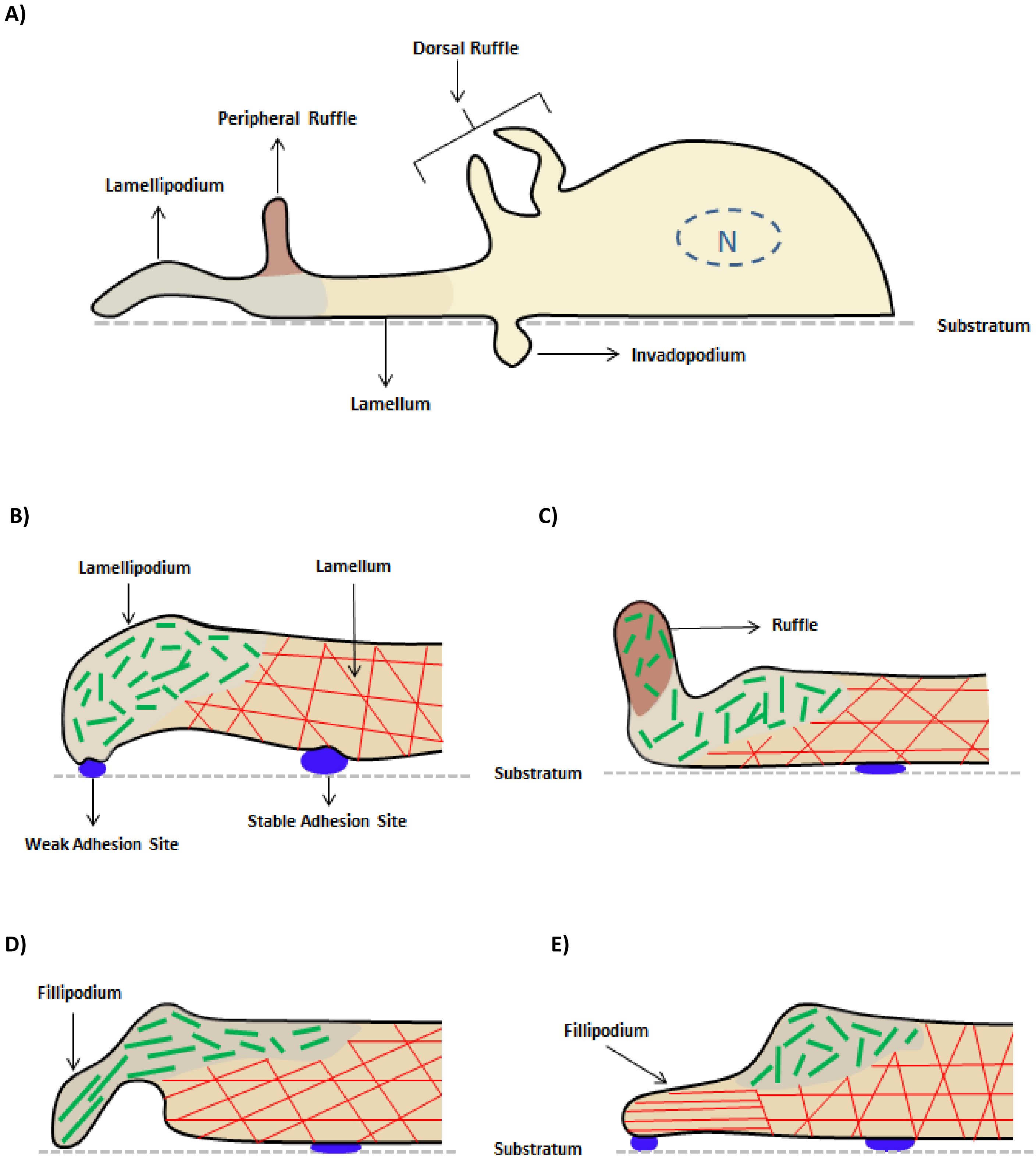
A)
Dorsal Ruffle
Peripheral Ruffle
Lamellipodium
N
Substratum
Invadopodium
Lamellum
B)
Lamellipodium
Lamellum
Weak Adhesion Site
Stable Adhesion Site
C)
Ruffle
Substratum
D)
Fillipodium
E)
Fillipodium
Substratum

by inhibitors of actin polymerization or actomyosin contractility leads to the dissolution of focal adhesions [29, 30]. Conversely, increases in cellular contractility have been shown to induce the simultaneous growth of both focal adhesions and the attached actin stress fibres [30]. Tension within the cell however, has been shown to be mediated by the clustering of the heterodimeric, transmembrane family of proteins known as integrins [23, 31]. Activation of integrins is modulated by an allosteric conformational switch that accompanies the binding of the extracellular domain of the integrin receptor to its ligand [5, 23]. This in turn, catalyzes the recruitment of cytoskeletal proteins into adhesive complexes that function to link integrins to the actin cytoskeleton, inducing the reorganization and polymerization of actin stress fibres [23, 32]. Consequently, sustained tension triggers increased clustering of integrins, converting nascent or focal complexes into stable, mature focal adhesions [23].

In a non-motile cell, the continuous contraction of ventral stress fibres in a myosin II-dependent manner is in equilibrium with adhesion strength, resulting in stable actin bundles that maintain constant length and therefore, shape under tension [5, 14]. However, in migrating cells, there exists a polarization of tensile forces with the leading edge exhibiting strong yet transient tension, whereas forces at the rear are weaker and more stable [33]. This decreased stress fibre-mediated tension at the rear results in the rapid disassembly of focal adhesions which, subsequently induces the retraction of the trailing edge allowing the cell to move forward [23, 33].

Focal adhesion disassembly, or cellular release, of nascent adhesions at the leading edge occurs predominantly at the lamellum-lamellipodium interface as a consequence of actin depolymerisation and reorganization [5]. However at the trailing edge, the dynamic instability

<u>Figure 1.2</u>: *Adhesive structures of the migrating cell*. Sustained membrane protrusion and adhesion formation are interdependent and are required for cell migration. The formation of nascent adhesions in the lamellipodium and/or filopodia is followed by their disassembly or maturation to focal complexes within the region of the transition zone. Adhesion maturation is coupled with the formation of actin filament cross-bridges and bundles, with sustained actin polymerization leading to the generation of the contractile force required that stabilizes the focal contacts into focal adhesions. Please note that the absence of fibrillar adhesions is indicative of a highly motile cell. Figure adapted from Parsons *et al.* (2010) [5].

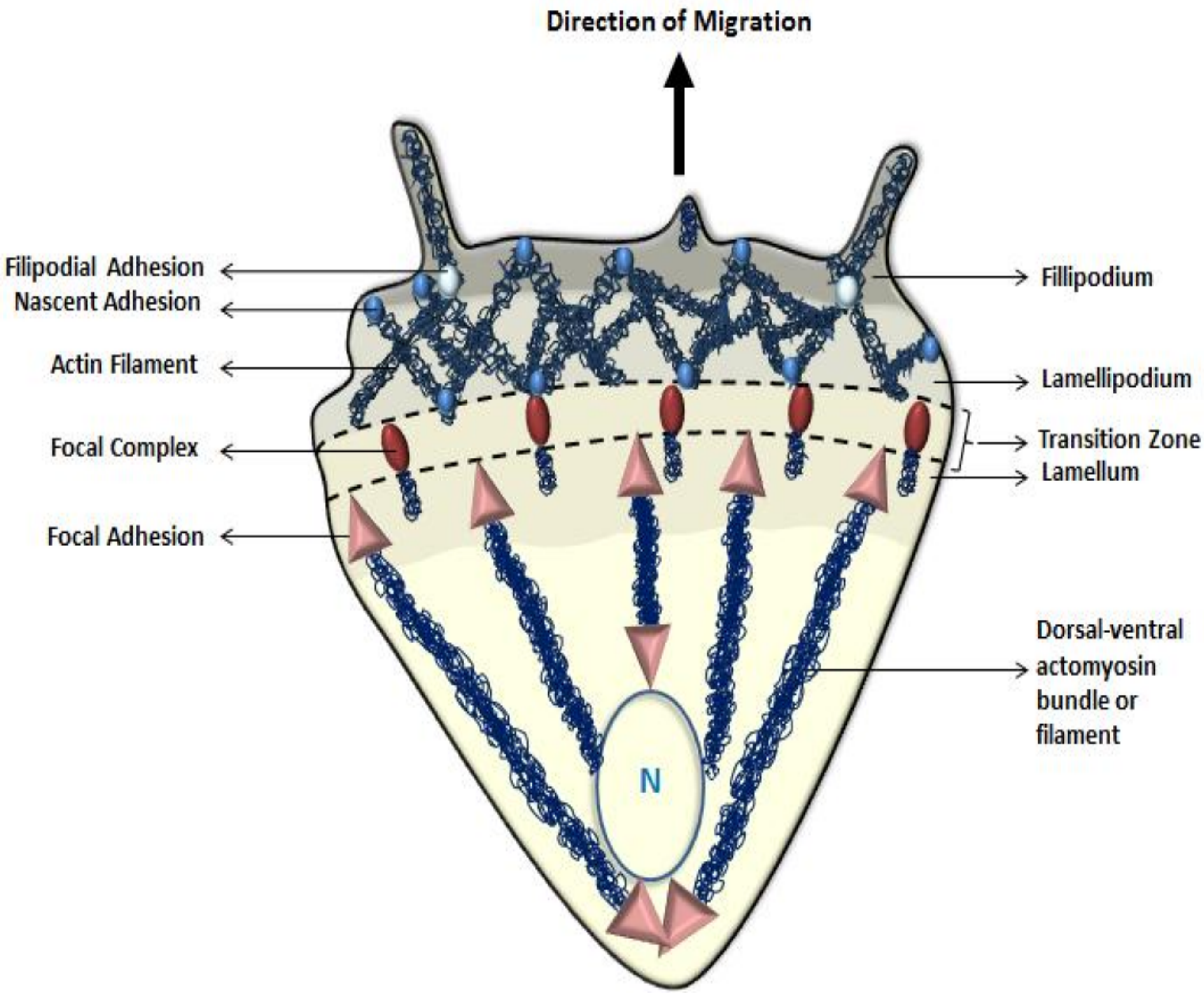
Direction of Migration
Filipodial Adhesion
Nascent Adhesion
Actin Filament
Focal Complex
Focal Adhesion
Fillipodium
Lamellipodium
Transition Zone
Lamellum
Dorsal-ventral actomyosin bundle or filament
N

of microtubules regulates the maintenance or dissolution of focal adhesions [19, 21, 34]. For example, nocodazole-induced microtubule depolymerisation leads to an increase in the number and size of focal adhesions at both the leading and trailing edge, anchoring the cell to the ECM to the point where it becomes immobilized [19]. Rescue of microtubule growth following catastrophe shows a resurgence in targeting events of focal adhesions by microtubule plus ends, resulting in focal adhesion dissolution and cell migration [2, 19, 20]. Microtubule plus ends have been shown to be differentially regulated depending on their subcellular location within the migrating cell. Frequent stabilization and catastrophe of the microtubule plus end has been observed with targeting to larger, mature focal adhesions within the cell body, while at the leading edge, microtubules persist in growth [10, 19, 35]. Although no difference exists between the microtubule growth rates of the leading versus the trailing edge, a difference in dynamic instability has been shown to be 2 to 13 fold higher at the rear of the cell [19]. This, taken in combination with a diminished frequency of catastrophe and a higher duration of pauses observed at the leading edge, suggests that focal adhesion turnover and consequently, cell migration is subject to microtubule polarization and dynamics [19].

Moving Toward Metastasis:

Tumor invasion and metastasis requires the migration of neoplastic cells from the primary tumor mass to distant secondary sites of colonization [7, 36]. As such, an accumulation of evidence correlates an invasive and metastatic state with the dysregulation of signals involved in cell migration [5, 7, 9, 15, 19, 35, 37]. For example, interactions between αvβ3, α5β1 and α6β4 and receptor tyrosine kinases (RTKs) such as ErbB2 and EGFR have been shown to facilitate the proliferation and migration of tumor cells independently of positional constraints in breast cancer [38, 39]. Additionally, aberrant trafficking of integrins to the leading edge has been documented to activate the matrix-degrading proteases such as matrix metalloproteinases (MMPs) and plasmin, required for degradation of the ECM and subsequent cell invasion [38, 40]. Moreover, stimulation of cells with the growth factor heregulin (HRG), has been shown to affect the expression and serine phosphorylation status of the focal adhesion protein paxillin, resulting in both the induction of morphological changes in cell shape as well as the stimulation of cell scattering in the breast cancer epithelial cell line, MCF-7 [41-43]. Paxillin has also been implicated in contributing to tumor invasiveness and metastasis in breast cancer, non-small cell lung cancer, prostate cancer and osteosarcomas [41-43]. Lastly, over-expression of FAK has been documented in invasive and metastatic breast, colon, thyroid and prostate cancers [44, 45]. Specifically, FAK overexpression is postulated to increase cell migration and survival under anchorage-independent conditions [44, 45].

The Focal Adhesion as a Signaling Nexus

Although critically important in providing the traction required for force generation in cellular translocation, focal adhesions are also recognized as being dynamic hubs that coordinate both inside-out and outside-in signal transduction. In this capacity, focal adhesion signaling has been implicated in the regulation of cellular processes such as cell migration, proliferation, differentiation, survival and gene expression, [24, 44, 46].

Signal transduction however, initiates with integrins: currently, 24 individual integrin heterodimers, each consisting of an α and β subunit, have been identified in the human genome [24, 44]. This extensive complement of transmembrane, glycoproteins confers cells with the ability to not only interact with various extracellular environments with a high degree of specificity but to transduce the nature of the environment to which it is attached throughout the cell [5, 47]. Binding of the extracellular domain of integrins to ligands such as fibronectin and collagen, induces a conformational change in the receptor, exposing the relatively short, cytoplasmic tail to intracellular binding partners and triggers integrin clustering [5, 44, 47, 48]. This aggregation of integrins in turn, recruits and activates signaling molecules FAK, Src and components of the Ras/MAPK pathway, as well as scaffolding proteins such as paxillin, vinculin and talin, resulting in the formation of focal adhesion complexes [40, 46]. However, integrins are lacking in both catalytic activity and the ability to bind the actin cytoskeleton directly [24, 46]. Therefore, the focal adhesion complex provides an interface through which extracellular signals can be amplified, and the cytoskeleton reorganized [24, 46].

The focal adhesion complex is defined as the sum of the interactions of more than 150 diverse, signaling, scaffolding and cytoskeletal proteins and their corresponding downstream signaling cascades [22, 47]. The composition of focal adhesions has been shown to vary over time depending on its acquired level of maturity. For example, focal complexes, which are integral to the formation of lamellipodial and filopodial extensions, have been shown to express relatively low to non-existent levels of proteins that are more prevalent in stable adhesions such as paxillin and zyxin, respectively [48-50]. However, the heterogeneity of the adhesion complex does not end with differential protein composition and localization. To a large degree, the signaling plasticity inherent to these structures can be seen as a bi-product of temporally-induced phosphorylated isoforms, or phospho-isoforms, of focal adhesion proteins [51, 52]. For example, FAK activation following integrin binding to the extracellular matrix, induces its auto-phosphorylation at Tyr(Y)397, creating Src-homology-2 (SH2) sites for binding partners Src, PI3K, Grb7 and phospholipase-Cγ [51]. Subsequent Src-mediated phosphorylation of FAK at Y576/Y577/Y861/Y925 further increases its catalytic activity, propagating downstream signaling cascades [51-54].

Phosphorylation

Protein Kinases:

Phosphorylation plays a major role in propagating the transduction of extracellular stimuli in a sensitive, selective and temporally ordered manner [49, 55]. This in turn, functions to activate a diverse cascade of signaling pathways which ultimately culminate in the regulation of global cellular processes [49, 55-57]. Consequently, phosphorylation is recognized to be the most wide-spread, post-translational modification regulating both prokaryotic and eukaryotic cells [49, 55].

Phosphorylation is a reversible and therefore, economical process for the cell: the dynamic interconversion between differentially phosphorylated and dephosphorylated forms of the same protein has the potential to increase the number of possible signaling outcomes without increasing the number of proteins required [58, 59]. For example, phosphorylation of the MAPKs Erk1/2 by MEK results in signaling conducive to cell proliferation, survival and adhesion, whereas their dephosphorylation by MAPK phosphatases (MKPs) like MKP-1, has been shown to induce apoptosis [57]. Consequently, this biphasic cycle of protein phosphorylation/dephosphorylation has been shown to have the ability to modify virtually every aspect of protein function including increasing or decreasing biological activity of proteins, stabilizing or identifying proteins for degradation, facilitating or inhibiting protein translocation between subcellular compartments, as well as inducing or disturbing the formation of protein-protein interactions [49, 55, 57]. This therefore, necessitates a high degree of substrate-kinase specificity in order to maintain signaling fidelity [49]. As such, substrate-kinase specificity has been shown to be regulated through a variety of mechanisms, most notably (1) the structure of the catalytic cleft of the kinase, (2) the sequence flanking the phosphorylation site within the substrate, (3) the intracellular localization of the both the kinase and the substrate as well as (4) the presence of scaffolding/adaptor proteins [49, 60].

Kinase-Substrate Specificity:

The first step toward substrate specificity involves the conformation of the kinase active site, primarily its depth, hydrophobicity, and charge to determine whether the kinase recognizes serine/threonine or tyrosine residues on a target substrate [49, 60]. Although serine/threonine kinases that phosphorylate tyrosine residues have been documented in yeast, human serine/threonine kinases are shown to predominantly phosphorylate substrates on serine/threonine residues and tyrosine kinases, on tyrosine residues [49, 61]. However, the targeting of a specific residue within a substrate is not solely determined by the preference of the kinase for serine/threonine or tyrosine residues. In fact, the active site of the kinase requires a short span of approximately 4 amino acids on either side of the would-be phosphorylation site that is complimentary in charge, hydrophobic interaction and hydrogen bonding [49]. This consensus, or substrate recognition sequence, represents yet another level of substrate specificity and has become a means through which different families of kinases are classified [62]. For example, the consensus sequence of the CMGC kinase family member, cyclin-dependent kinase 2 (CDK2) which corresponds to S/T*-P-X-K/R (where * indicates the phosphorylation site and X denotes any amino acid), dictates that CDK2 substrates must contain a basic residue at the P+3 position to accommodate a phospho-Thr residue within the kinase (Thr160) [49, 63, 64].

Irrespective of compatibility, proximity requirements dictate that kinases and substrates must translocate to the same location within the cell in order for phosphorylation to occur [49, 65]. Specifically, the localization of a kinase to a distinct subcellular compartment or structure enhances specificity by limiting the number and type of substrates that it has access to [49, 65]. Additionally, it is not always the active form of the kinase that is translocated to a specific region of the cell. The generation of differentially activated forms of a given kinase that are location dependent, increases the stringency of substrate selection to correspond not only to a given location, but a given location in which the kinase is active [49, 65]. Moreover, the localization and activation of protein kinases may require the involvement of an intermediate scaffolding/adaptor protein [49]. For example, although targeting of FAK to focal adhesions does not absolutely require an association with paxillin, its phosphorylation by Src at Y576/577 and consequently Y925, does [66, 67].

Discovery of a Novel Kinase

Structure of the Ste20-like kinase, SLK:

Classified as a novel germinal center kinase (GCK-V), the human Sterile20-like kinase (SLK) is ubiquitously expressed in adult tissues and cell lines and has been shown to share extensive sequence homology with the lymphocyte oriented kinase (LOK; 74%) as well as the *Xenopus* polo-like kinase kinase 1 (xPLKK1; 72%) [68-71]. SLK is defined by a sequence of 1202 amino acids, with a predicted molecular mass of 147 kDa which in actual fact, translates to an electrophoretic mobility of 220 kDa on SDS-PAGE [70]. Structurally, SLK is a serine-threonine kinase that contains an N-terminal kinase domain with the archetypal Ste20 consensus motif in kinase subdomain VIII (TPYWMAPE), a central coiled-coil domain and a C-terminal AT1-46 homology (ATH) domain (**Figure 1.3**) [70]. Although there is no known function of the central coiled-coil domain, it has been shown to contain potential SH3 binding sites and a putative caspase 3 cleavage site (DTQD) at positions 735 and 436, respectively [72-74]. The ATH domain however, exhibits a high degree of homology to the ATH1-46 protein of unknown function, and has also been found within both LOK and xPLKK1, suggesting that it may represent a novel motif [75]. In fact, recent studies have shown the ATH domain to be a region within SLK that mediates protein-protein interactions, both with itself to form SLK homodimers, as well as with binding partners such as the LIM domain binding proteins, LDB1 and LDB2 [76, 77].

Involvement in Signaling and Migration:

Recent studies have shown that SLK localizes to the leading edge of migrating cells with vinculin and paxillin as well as with the LIM domain binding proteins, LDB1 and LDB2 following scratch-wounding of a confluent monolayer of fibroblasts [69, 76, 78]. This localization has been shown to occur in response to both the induction of wound-healing as well as the activation of the receptor tyrosine kinase ErbB2 [69, 79]. The initiation of migration signaling has also been documented to induce SLK kinase activity in a cyclical manner: levels of SLK autophosphorylation, which serve as a measure of its kinase activity, have been observed to steadily increase, reaching maximum levels at 60 minutes post stimulation of migration [69]. *In vivo*, overexpression assays using a kinase-inactive form of SLK as well as knockdown of the endogenous kinase, have been shown to negatively regulate both focal adhesion turnover and cell migration [69]. Conversely, disruption of the stoichiometry of the SLK kinase regulators LDB1 and LDB2 via over-expression or knockdown, has been shown to result in an increase in SLK kinase activity and the induction of focal adhesion disassembly and cell migration [76].

Initial characterization had shown that SLK overexpression results in actin fibre dissolution in a Rac-1 dependent manner and apoptosis [70, 75, 78]. Subsequent studies of the cytoskeleton revealed that SLK could co-immuoprecipitate with tubulin, and that induction of microtubule catastrophe via nocodazole treatment would result in the redistribution of SLK with unpolymerized α-tubulin to large, mature focal adhesion complexes [78]. SLK has also been shown to localize with polymerized microtubules under normal adhesion and spreading conditions [78]. Interestingly, SLK demonstrates a dramatic decrease in kinase activity under these adhesion-stabilizing conditions, suggesting a role for activated SLK in the regulation of dynamic focal adhesions [69]. In contrast to its ability to remodel actin, overexpression of SLK

<u>Figure 1.3</u>: ***The structure of the Ste20-like kinase, SLK.*** SLK is characterized by its three functional domains, an N-terminal Ste20 consensus-containing (TPYWMAPE) kinase domain, a central coiled-coil region and a C-terminal ATH domain. The signature kinase motif Gly-X-X-Gly is located within subdomain I of the kinase domain. Despite a predicted molecular mass of 147 kDa, SLK has an electrophoretic mobility of a 220kDa protein on SDS-PAGE.

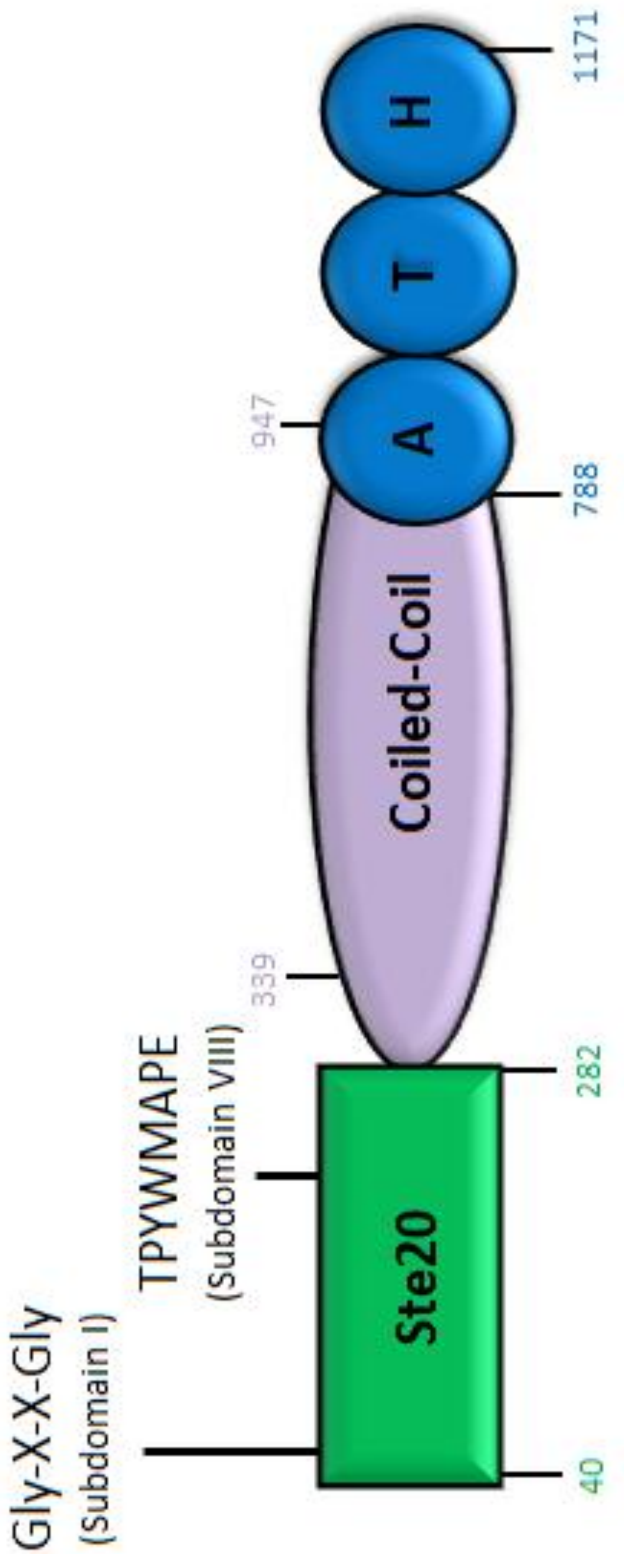
Gly-X-X-Gly
(Subdomain I)
TPYWMAPE
(Subdomain VIII)
Ste20
40
282
339
Coiled-Coil
788
947
A
T
H
1171

does not affect the organization of the microtubule network: SLK has been shown to regulate both microtubule radial array orientation and golgi polarization during interphase, as well as cell cycle progression through G2/M, without affecting microtubule stability [78, 80, 81].

A current hypothesis governing microtubule dynamics involves the delivery of adhesion-destabilizing/relaxation signals to focal adhesions to induce their turnover [10, 21]. Since the localization of SLK to focal adhesions with microtubules has been shown to induce focal adhesion turnover, SLK is believed to regulate efficient cell migration by modulating focal adhesion dynamics [78, 82]. However, despite the compelling correlative data, the exact mechanism by which SLK contributes to focal adhesion turnover has yet to be elucidated.

SLK Auto-Phosphorylation and Substrates:

Recent determination of the SLK kinase domain crystal structure has shown that it assumes a homodimer configuration to facilitate trans-phosphorylation within the consensus sequence, X-X-X-Y-X-T*-ϕ-R/K-X-X-X necessary for auto-activation of the kinase [77]. However, in accordance with the derived dissociation constants of this structure, additional associations appear to be required to achieve efficient dimerization [77]. Interestingly, SLK has been shown to contain dimerization domains adjacent to the kinase region, where Storbeck et al. (2009) demonstrated LDB1/2-SLK binding [76, 77]. Further investigation into this trans-homodimerization has led to the discovery of two novel SLK phosphorylation sites namely S189 and T183, in which T183 was identified as an important site for SLK autophosphorylation [77]. It is important to note that the addition of a phosphate moiety to a kinase not only functions to activate the kinase, but to stabilize the catalytic domain of the kinase in a conformation suitable for substrate binding. As such, autophosphorylation consensus motifs are normally not substrate consensus sites [77]. However, SLK is lacking a known substrate consensus site as a direct result of the fact that a natural substrate for SLK has yet to be identified.

Paxillin

Paxillin first gained widespread interest in 1990 when it was shown not only to localize to integrin-rich sites of focal adhesions, but to also be a novel binding partner for the focal adhesion and actin-binding protein, vinculin [66, 83]. The name paxillin, derived from the latin *'paxillus'* meaning small stake or peg, was chosen to describe this protein in accordance with its ability to tether proteins like vinculin, to the membrane at focal adhesions [66, 84]. Paxillin was later cloned from an avian cDNA library, but has since been isolated from human, mouse, frog, zebrafish, fly, slime mould and yeast [85]. Paxillin is highly conserved between species with approximately 90% and 95% homology between chicken and human, and mouse and human cDNAs (NCBI BLAST accession #AAC50104 and NP_035353), respectively [66]. In terms of overall genomic organization, the human paxillin gene is comprised of 11 exons located on chromosome 12q24.2, and encodes for a protein that is 557 amino acids in length [66, 83, 85, 86]. Paxillin is classified as a molecular adaptor/scaffold protein by virtue of the multitude of protein-protein interactions it mediates via a number of unique structural motifs and overall protein conformation **(Figure 1.4)** [66].

<u>Figure 1.4</u>: *The structure of the focal adhesion protein, paxillin.* α-Paxillin (shown) is highly conserved between species and represents the most ubiquitously expressed isoform of the protein. The expression profile of β and γ splice variants however, is limited in comparison, being found predominantly in cancerous and monocytic cells. These β and γ isoforms represent transcriptional variants and differ from α-paxillin by virtue of an additional exon of 34 and 48 amino acids at positions 277 and 278, respectively. This is in contrast to the translational splice variant, δ-paxillin, which is the product of an alternative translation initiation site 132 amino acids downstream of the ATG that codes for α-paxillin. Unlike the C-terminus of the protein, the N-terminus of paxillin reveals limited structural information besides the presence of a proline-rich region spanning amino acids 48-57 (PPPVPPPP). In humans, the function of α-paxillin is defined by 557 amino acids with a predicted mass of 60 kDa which translates to a 68-75 kDa protein when resolved using SDS-PAGE. Figure adapted from Turner (2000) [85].

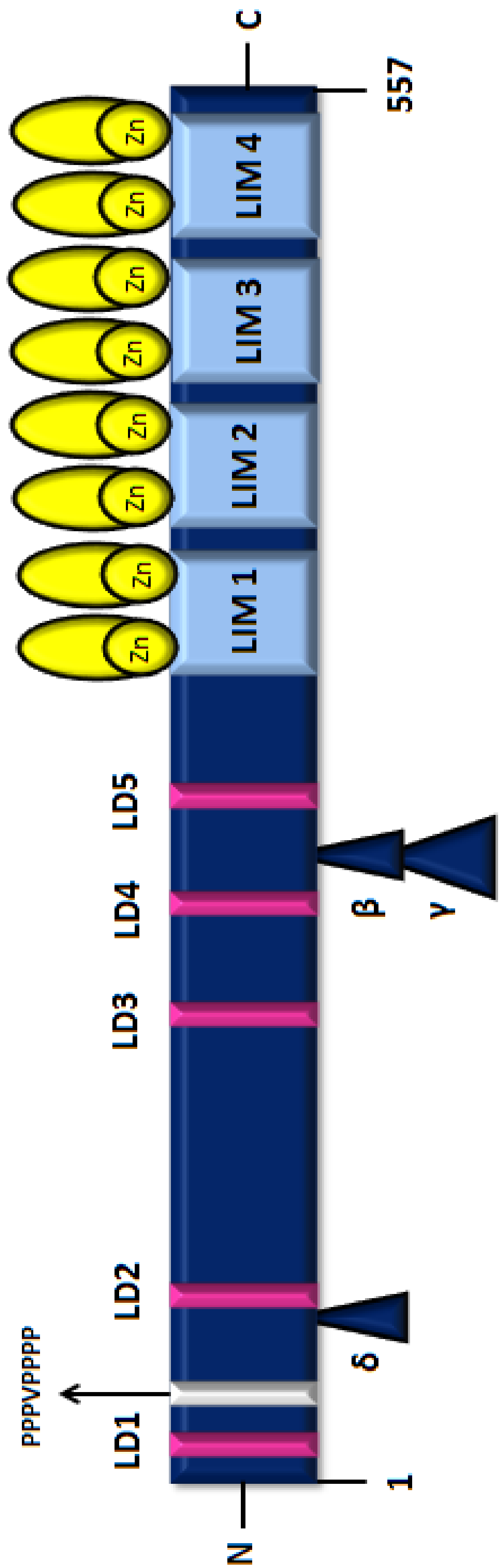

C
557
LIM 4
LIM 3
LIM 2
LIM 1
Zn
LD5
LD4
LD3
LD2
LD1
β
γ
δ
PPPVPPPP
1
N

The Paxillin Superfamily

The paxillin superfamily consists of four paxillin isoforms (paxillin α, β, γ and δ) and two paxillin homologues (leupaxin and Hic-5)[66, 86]. α-Paxillin (68 kDa), the principal and ubiquitously expressed isoform of paxillin, differs from the other two alternatively-spliced transcripts, paxillin β and γ by virtue of an additional exon of 34 and 48 amino acids inserted between lysine 277 and phenylalanine 278, respectively [86]. These insertions have been shown to alter the ability of these paxillin isoforms to interact with known binding partners of α-paxillin [86]. For example, when compared to α-paxillin, β-paxillin exhibits a reduced binding affinity for vinculin, but an equivalent affinity for FAK; the inverse has been shown to be true for γ-paxillin [87]. Additionally, β and γ-paxillin exhibit a more restricted expression profile in comparison to α-paxillin, being expressed primarily in cancer and monocytic cells, respectively [87, 88]. The expression of the fourth paxillin isoform however, δ-paxillin (46 kDa), is enriched in epithelial cells while absent in mesenchymal cells [66, 86-88]. The δ-paxillin isoform is unique in comparison to the α and β transcriptional variants in that it is the result of an alternative translation initiation site located 132 amino acids downstream of the α-paxillin start codon [88]. This internally translated paxillin isoform differs structurally in its N-terminal domain, lacking the proline-rich and SH2-binding site containing LD1 motif found in α-paxillin [88]. Functionally speaking, there is evidence to suggest that this truncated isoform of paxillin acts antagonistically to the function of the wildtype, full-length α-paxillin (hereafter referred to as paxillin), to limit the inappropriate trans-differentiation and cell migration that is required for epithelial cell invasion [66, 86, 87].

The paxillin homologue leupaxin, a 45 kDa protein with ≈ 37% homology to paxillin, was originally characterized as a multi-functional adaptor protein expressed only in hematopoietic cells [87, 89-91]. However, leupaxin, like both Hic-5 and paxillin, has been recently shown to be expressed in a subset of human prostate cancers, accumulating in the nucleus to potentiate androgen receptor (AR) transactivation in a ligand-dependent manner [87, 92, 93]. Whereas the expression profile of leupaxin is exceedingly limited, the expression of Hic-5 (Hydrogen Peroxide-Inducible Clone-5), also known as ARA55 (Androgen receptor Activator 55) has been shown in platelets, cells of mesenchymal origin as well as stromal and smooth muscle tissue layers; Hic-5 expression is altogether absent in epithelial cells [66, 87, 94]. Hic-5, a 55 kDa protein that is ≈ 57% homologous to paxillin, was originally identified as a TGF-β and hydrogen peroxide-inducible gene in the mouse osteoblastic cell line MC3T3 [66, 88, 94]. Although Hic-5 has been shown to have a similar function to paxillin, there is a growing amount of evidence that suggests a role for Hic-5 as a natural antagonist of paxillin by virtue of its ability to ablate paxillin signaling via competition of shared LD binding partners PTP-PEST and FAK, and suppression of downstream paxillin tyrosine phosphorylation [88]. Despite the potential overlap in function inherent to members of the paxillin superfamily, the resulting embryonic lethality of a mouse lacking the paxillin gene (E7.5-E8.5), but still expressing both leupaxin and Hic-5, suggests that neither of these homologues are viable substitutes for paxillin [95, 96].

Irrespective of their cell-type-specific expression profiles, all members of the paxillin superfamily are classified as group III LIM domain proteins which, by definition stipulates that this family of proteins is predominantly found in the cytoplasm interacting with cytoskeletal proteins [87, 90-92, 95]. However, they have also been shown to shuttle into the nucleus and act as transcriptional co-activators of androgen and glucocorticoid receptor signaling cascades [66]. The multi-domain structure of paxillin is required for its localization to sites of focal adhesions as well as its regulated nucleocytoplasmic shuttling. Although paxillin family members lack true nuclear export sequences (NES), the individual motifs of the LD domain, have been shown to act as both de facto NES as well as protein recognition motifs [97]. Specifically, a core NES paxillin signal that regulates nuclear export has been identified within the LD4 motif and corresponds to the phosphorylation status of S272 [66, 98]. Conversely, the C-terminal LIM domain, specifically LIM3 in cooperation with LIM2 has been shown to mediate the discrete subcellular targeting of the protein to both the actin cytoskeleton and focal adhesions; the LIM domain is also believed to be required for localization of paxillin to the nucleus [66, 90].

Paxillin Structure and Function*:*

The N-terminus (amino acids 1-325) of paxillin is defined by the most extensively characterized of its two structural domains, the LD domain [99]. The LD domain consists of five separate motifs that share sequence homology in their binding domain [66]. This sequence homology translates into a leucine and aspartic acid-rich consensus sequence, LDXLLXXL, after which this domain was named [66]. This sequence has been found repeated four times within the N-terminus of the paxillin protein, defining LD motifs 1, 2, 4 and 5 [66, 100, 101]. The fifth LD domain, denoted by LD3 and encoded by the highly divergent exon 5, was later proposed by Tong et al. in 1997 [66]. This domain was originally considered degenerate and disregarded due to a lack of sequence homology in the LD consensus motif but has since been reincorporated into the nomenclature [66]. All members of the paxillin superfamily contain 4-5 of these LD motifs: the LD1 motif, encoded by exons 1 and 2, is missing in paxillin δ and Hic-5, whereas LD2, encoded by exon 4, is missing in leupaxin [66]. Interestingly, LD3 is conserved only among orthologs, while LD4 and 5, encoded by exons 6 and 7 respectively, are conserved across species and paralogs **(Figure 1.5)** [85, 86, 102].

At first glance, the amino terminus of paxillin reveals relatively little structural information besides the presence of a short, proline-rich region spanning amino acids 48-57, suggesting the presence of a potential SH3-docking motif, as well as several tyrosine phosphorylation sites important for integrin-mediated signaling and the formation of potential SH2 binding sites [66, 86, 102, 103]. However, structural modeling programs predict the LD motifs to fold into an amphipathic, α-helical structure with each of the leucine residues being oriented to one side of the helix, forming a hydrophobic interface for binding partners [66]. Individual paxillin LD motifs are evenly distributed throughout the N-terminus and are flanked by proline and glycine-rich regions (≈ 25%); this is believed to contribute to the overall folding, presentation, regulation and function of each of these discrete protein interaction motifs [66, 86, 102]. Comparison of LD motifs both between species and paxillin family members have shown that sequence, in addition to the core consensus motif, is also conserved [66, 86, 102]. This sequence conservation is also reflected in the complement of proteins that each motif is capable of interacting with and is believed to provide the specificity required for the interaction of the LD motifs with various paxillin-interacting proteins [66, 86, 102]. In particular, LD1 has been shown to mediate interactions with actopaxin, the integrin-linked kinase (ILK), vinculin and the papillomavirus protein E6 [66, 86, 102, 104]. LD2 has also been shown to bind to vinculin, but like LD4, also binds FAK and the protein-tyrosine kinase 2-beta (PYK2). Like LD1, LD4 can also interact with actopaxin, but is unique in its binding to the paxillin-linked kinase (PLK), the Arf-GAPs p95PKL/GIT2/GIT1, clathrin and PTBP1 [66, 86]. LD4 however, is the only LD motif capable of binding β1-integrin, specifically the α4- and α9-subunit cytoplasmic tails [66, 86]. Interestingly, there are no known binding partners for LD5, or the 'degenerate' LD3 motif [102].

The C-terminus of paxillin however, is defined by the presence of the LIM (Lin-11, Isl-1, Mec-3) domain which is typified by four unique motifs that are also organized in tandem (LIM1-4) [95, 105, 106]. These motifs are structurally characterized by cysteine/histidine-based double zinc fingers of approximately 60 amino acids [66, 95, 106]. Characterization of these structures shows each zinc finger to be comprised of two antiparallel β-sheets separated by a tight turn and ending in a short α-helix; zinc finger doublets have been shown to interact with one another by virtue of hydrophobic interactions [66, 95]. As is the case with most LIM-containing proteins, the LIM domains of paxillin have been shown to mediate protein-protein interactions, facilitating dimerization with other LIM domains, zinc fingers, tyrosine-tight NPXY (Asn-Pro-X-Tyr) motifs and non-tyrosine-based LIM interaction domains [85]. Accordingly, several paxillin LIM-domain binding partners have been identified, such as the tyrosine phosphatase-PEST (PTP-PEST) and the non-receptor tyrosine kinase Csk (C-terminal Src kinase), both of which function to regulate paxillin subcellular targeting and consequently, focal adhesion architecture [66, 85]. The paxillin LIM domain has also been shown to bind α, and the less abundant, γ-tubulin [51, 107]. These interactions, combined with the ability of the LD domain to bind

<u>**Table 1**</u>**.** ***The paxillin LD domain is conserved among homologues.*** LD motifs from human paxillin as well as murine Hic-5 and leupaxin. Please note that there exists 100% homology in protein sequence between all 5 paxillin LD domains of humans and mice (not shown). Despite sequence homology (yellow), each of the two paxillin homologues is lacking one of the five LD domains found within paxillin, namely LD3 for Hic-5 and LD2 for leupaxin. Figure adapted from Schaller (2001) [86].

Table 1. Alignment of Paxillin Family LD Motifs

Paxillin LD1:	M	D	D	L	D	A	L	L	A	D	L	E	S
Paxillin LD2:	L	S	E	L	D	R	L	L	L	E	L	N	A
Paxillin LD3:	E	S	L	L	D	E	L	E	S	S	V	P	S
Paxillin LD4:	T	R	E	L	D	E	L	M	A	S	L	S	D
Paxillin LD5:	G	S	Q	L	D	S	M	L	G	S	L	Q	S
Hic-5 LD1:	M	E	D	L	D	A	L	L	S	D	L	E	T
Hic-5 LD2:	L	C	E	L	D	R	L	L	Q	E	L	N	A
Hic-5 LD3:													
Hic-5 LD4:	T	Q	E	L	D	R	L	M	A	S	L	S	D
Hic-5 LD5:	K	G	S	L	D	T	M	L	G	L	L	Q	S
Leupaxin LD1:	M	E	E	L	D	A	L	L	E	E	L	E	R
Leupaxin LD2:													
Leupaxin LD3:	E	T	N	L	D	E	T	S	E	I	L	S	T
Leupaxin LD4:	A	A	Q	L	D	E	L	M	A	H	L	T	E
Leupaxin LD5:	K	A	S	L	D	S	M	L	G	G	L	E	Q

several actin-binding proteins such as actopaxin, vinculin and talin suggests that paxillin is capable of mediating cross-talk between the two filament systems [51, 107]. This apparent co-operation between the two structural domains of paxillin can also be seen in the localization and activation of the non-receptor tyrosine kinase, FAK. Failure of FAK to bind paxillin has been shown to result in decreased FAK focal adhesion localization and tyrosine phosphorylation [51, 52, 66, 108]. Characterization of the paxillin-FAK interaction shows that it is the C-terminal focal adhesion targeting domain of FAK, specifically the paxillin binding sequences 1 and 2 (PBS 1 and 2) within this domain, that are capable of binding both the second and the fourth LD motifs of paxillin with equal affinity [51, 108]. Together, the differential phosphorylation of the paxillin LIM motifs 2 and 3, is believed to facilitate the subcellular localization of FAK to focal adhesions [51, 108].

Although paxillin binding is not absolutely necessary for FAK subcellular localization, it is recognized as being the major mechanism by which FAK is not only targeted to sites of focal adhesions, but presented to kinases like Src for full activation [30, 51, 67]. However, without paxillin binding, FAK cannot be phosphorylated at Y576/Y577 and consequently Y925, which negatively regulates cell migration [66, 67]. Conversely, paxillin-mediated focal adhesion disassembly and cell migration, which requires paxillin tyrosine phosphorylation by both FAK and Src, cannot occur without the binding of paxillin to activated FAK (Y925) [66, 109].

Paxillin Phosphorylation:

Initially characterized as an adhesion protein exhibiting a significant increase in tyrosine phosphorylation upon v-src expression, paxillin has since been shown to be extensively phosphorylated by a variety of kinases on serine, threonine and tyrosine residues in response to cell adhesion and/or exposure to a variety of soluble growth factors and cytokines [66, 86].

Paxillin Tyrosine Phosphorylation:

Paxillin tyrosine phosphorylation was initially shown to be induced by integrin-dependent cell adhesion to extracellular matrix proteins but has since been shown to be the consequence of a multitude of diverse signaling events [66, 85, 86]. For example, stimulation of cells with growth factor and cytokine ligands such as epidermal growth factor (EGF), insulin-like growth factor I (IGF-I), monocyte chemoattractant protein I (MCP-1), platelet-derived growth factor, stem cell factor (SCF), and vascular endothelial growth factor (VEGF), have all been shown to induce tyrosine phosphorylation of paxillin [66, 86]. Additional stimuli include, but are not limited to, agonists of many 7-pass transmembrane serpentine family receptors such as acetylcholine, epinephrine, angiotensin II, lysophosphatidic acid and other sphingosine metabolites [66]. Moreover, signalling through immunomodulators such as tumor necrosis factor-α, formyl-methionyl-leucyl-phenylalanine, IgE, T-cell receptor or complement, as well as exposure to the toxic by-products of viral and bacterial infection can also result in paxillin tyrosine phosphorylation [66, 86]. Lastly, cellular stress, in particular membrane depolarization, hypertonicity, physical stretch and shear stress can also be attributed with the induction of paxillin tyrosine phosphorylation [86, 110].

Although paxillin tyrosine phosphorylation is induced by a variety of stimuli, its regulation has been shown to be mediated by specific tyrosine kinases [86]. FAK, and the related protein, CAKβ/Pyk2/CadTK/RAFTK, have not only been shown to physically interact and co-localize with paxillin *in vivo*, but the activation and/or overexpression of these tyrosine kinases has been implicated in an increased proportion of tyrosine phosphorylated paxillin [86, 111, 112]. Specifically, studies have shown that the relative levels of paxillin Y31 and Y118 phosphorylation are reduced in FAK -/- MEFs in comparison to wildtype FAK +/+, with additional studies demonstrating complete inhibition of paxillin tyrosine phosphorylation via overexpression of dominant negative FAK; inflated levels of paxillin tyrosine phosphorylation in the FAK -/- is believed to be the result of the compensatory expression of CAKβ in these cells [83, 86, 109]. Additionally, Src and Src family kinases have also been shown to be candidate kinases for paxillin phosphorylation: as previously mentioned, paxillin was first identified as a tyrosine phosphorylated protein in v-src transformed fibroblasts [86]. Subsequent studies have shown that cells with ablated Csk, the major regulatory kinase of Src, exhibit enhanced Src family kinase activity and consequently, elevated tyrosine phosphorylation of target substrates such as paxillin [86, 113]. Furthermore, SYF cells, fibroblasts genetically engineered to be deficient in the functionally-redundant Src family kinases Src, Yes and Fyn, show a significant reduction in adhesion-dependent tyrosine phosphorylation of paxillin [66].

The primary function of paxillin tyrosine phosphorylation has been described to be the generation of functional SH2-binding domains for signaling proteins [17]. The inducible nature of these protein-interaction domains confers paxillin with an additional level of regulation with respect to the spatial and temporal associations it makes with SH2-containing binding partners like the adaptor protein Crk [66]. Crk has been shown to bind directly to a SH2 site generated by pY31 and pY118 of paxillin which in turn, recruits the guanine nucleotide exchange factor DOCK180 and affects the overall state of cellular polarization and migration through the activation of the Rho GTPase, Rac1 [66, 86, 108, 114, 115]. Other SH2-containing proteins that have been identified to bind directly to tyrosine phosphorylated paxillin include: the p85 subunit of PI3K with pY31, pY40 and pY118 and p120RasGAP with pY31 and PY118 [66, 86, 116]. The Src-inactivating Csk tyrosine kinase and the Src family kinase Lck, have also been shown to bind via SH2 domain to tyrosine phosphorylated paxillin. Csk, like Crk, has been shown to bind paxillin by virtue of the SH2 domain generated by Y31 and Y118 phosphorylation [32]. Although the exact binding site for Lck is unknown, it presumed to involve a minor tyrosine phosphorylation site, Y40 which lies within a stretch of sequence that resembles a high-affinity Src SH2 binding site [32].

Paxillin Serine/Threonine Phosphorylation:

Adhesion of fibroblasts to fibronectin has not only been shown to induce tyrosine phosphorylation of paxillin, but serine phosphorylation as well [32, 86]. Whereas tyrosine phosphorylation of paxillin by FAK/Src is well documented, much less is known of the consequences of paxillin serine phosphorylation or the kinases that are involved [32, 47, 66, 86, 117]. Like tyrosine phosphorylation, paxillin serine/threonine phosphorylation is induced by a variety of stimuli: for example, cellular activation via integrin ligation has been documented to result in phosphorylation of S188/190 [47]. The significance of this phosphorylation is related to an observed decrease in proteasomal-dependent degradation of paxillin under normal conditions when compared to cells over-expressing a S188/190 phospho-mutant [47]. Additionally, cells expressing this mutant paxillin exhibit a defect in spreading and protrusive abilities and migrate more actively [66, 85, 86, 117]. Collectively, this would suggest that paxillin serine phosphorylation regulates the degradation status of the protein, which in turn, is important in the modulation of paxillin-dependent membrane dynamics affecting cell motility. Paxillin serine/threonine phosphorylation has also been shown to be stimulated by growth factors such as angiotensin II, activin A, TGF-β, EGF, heregulin and interleukin [47, 117, 118]. Specifically, paxillin serine phosphorylation following heregulin stimulation of the non-invasive breast cancer cell line, MCF-7 has been shown to redistribute paxillin from focal adhesions to perinuclear cytoplasmic areas; this atypical localization is believed to destabilize focal adhesions, resulting in increased cell scattering and migration [66].

In addition to being induced by the tumor promoter PMA, muscle contraction and virus infection, an increase in paxillin serine/threonine phosphorylation has also been observed at the onset of mitosis [119]. Studies involving nocodazole-arrested mitotic cells typically show a significant decrease in the amount of total paxillin protein that can be immunoblotted in comparison to non-mitotic nocodazole treated or exponentially growing cells [119]. This, combined with the observation that mitotic paxillin is phosphorylated primarily on serine residues, suggests that serine phosphorylation of paxillin may be required to target the protein for degradation during mitosis, facilitating the focal adhesion turnover and cytoskeletal rearrangements necessary for cytokinesis [99, 105].

Although a search for paxillin phosphorylation in PubMed yields in excess of 1000 publications on the subject, most of the kinases that are responsible for the various phosphoisoforms of paxillin have yet to be identified; this is especially true when it comes to paxillin serine/threonine phosphorylation. For example, the combination of adhesion and angiotensin II stimulation has been shown to result in the phosphorylation of paxillin LIM2

T396/401 and LIM3 S455/479, which is believed to target paxillin to sites of focal adhesions [99]. Although LIM2 has been shown to associate and co-immunoprecipitate with a kinase that can phosphorylate threonines 396/401 in human cells and LIM3 to bind a detergent-insoluble kinase that can phosphorylate serines 455/479, when tested, these kinases were immune to inhibition by a variety of broad-spectrum serine/threonine kinase inhibitors, suggesting that the identity of these kinases are novel in nature [66, 86, 120]. Despite this however, several candidate serine/threonine kinases have been identified for paxillin including: protein kinase C, MAPK, JNK, ERK1/2, the p21-activated protein kinase PAK3 and the integrin-linked kinase, ILK [121, 122]. However, with the advent of more sophisticated analytical techniques, specifically the use of phosphatase inhibitors in combination with the enrichment of phosphopeptides with immobilized metal affinity chromatography (IMAC) and subsequent analysis by mass spectrometry, comes a myriad of novel paxillin phosphorylation sites. For example, paxillin S91, 98, 108 and 382 and threonines 295 and 540, as well as S112, 173, 217, 259 and 501 have been found by these methods to be phosphorylated *in vivo* and have been identified as putative PKC and PKA substrates, respectively [121]. Additionally, GSK3 is predicted to phosphorylate paxillin S85, 90, 94, 106, 108, 126 and 227, while S173 is a putative site for Akt phosphorylation. It is important to note however, that these sites, as well as the kinases that are predicted to phosphorylate them, require further investigation to confirm their actual contribution to the overall phosphorylation landscape of paxillin.

<u>Thesis Hypothesis and Objectives</u>:

The purpose of this thesis was to investigate the involvement of SLK signaling in the regulation of focal adhesion dynamics and cell migration. Our working hypothesis is that SLK-mediated phosphorylation of focal adhesion protein(s) results in focal adhesion disassembly and cell migration. Previously published reports have shown that a knockdown of SLK results in impaired focal adhesion turnover and a decrease in cell migration. As such, our first objective was to identify a functional substrate for SLK that is involved in regulating adhesion dynamics. The observation that SLK interacts directly with LDB1/2 and that LDB1/2 are also capable of interacting with the focal adhesion protein paxillin, prompted us to test the phosphorylation status of paxillin by SLK. Since previous reports have also shown paxillin and SLK to co-localize to the membrane ruffle in migrating cells, it was not all together surprising that subsequent kinase assays showed SLK to phosphorylate paxillin *in vitro*. Through the combined use of amino-terminal truncations and site directed mutagenesis, I have identified the site of SLK-mediated paxillin phosphorylation to be S250.

Our second objective was then to determine the physiological relevance of this phosphorylation event on cell migration *in vivo*. Analyses of adhesion, spreading and focal adhesion turnover in cells overexpressing a dominant negative paxillin mutant, S250T, were used to assess the impact of this phosphorylation event on migration.

Lastly, our final objective focused on elucidating the possible mechanism(s) through which SLK-mediated phosphorylation of paxillin induces adhesion turnover and cell migration. Additionally, within the scope of this objective I propose to define a role for this phosphorylation event in the context of breast cancer metastasis. By using a wide variety of biochemical, molecular and cellular approaches, I have demonstrated a critical role for SLK-mediated phosphorylation of paxillin in cell migration through the regulation of adhesion dynamics. Because these studies will outline a potential mechanism through which adhesion turnover leads to migration, it is my contention that the results of this thesis may represent the starting point for the identification of a novel, potentially useful prognostic indicator of breast cancer metastasis.

Chapter 2:

Materials and Methods

2.1- Antibodies and Reagents

Paxillin, FAK and phospho-FAKY397 were purchased from BD transduction laboratories and used at dilutions ranging from 1:1000 to 1:5000 (Mississauga, ON, Canada). Other antibodies used in these studies were γ-tubulin (Sigma-Aldrich, Oakville, Ontario, Canada), Myc (Sigma-Aldrich; 9E10 mouse ascites), HA (Sigma-Aldrich; 12CA5 mouse ascites), GFP (Santa Cruz Biotechnology, Santa Cruz, California, USA), ubiquitin (Abgent Inc., San Diego, California, USA) and DAPI (nucleic acid stain; Invitrogen, Carlsbad, California, USA). Anti-SLK and phospho-paxillinS250 antibodies were custom made by Dr. Toshi Myazaki (Medical & Biological Laboratories, Co., Ltd., Nagoya, Japan).

2.2- Cell Culture and Related Experiments

2.2.1- Cell Lines:

HEK293 (also referred to as 293) and MEF3T3 were purchased from the American Type Culture Collection and Clontech Laboratories, respectively. All cell lines were maintained at 37°C and 5% CO_2 in Dulbecco's modified Eagle Medium (DMEM) supplemented with 10% fetal bovine serum (FBS), 2 mM L-glutamine, 50 µg/ml penicillin and 50 µg/ml streptomycin.

2.2.2- Plasmids and Transient Transfections/Infections:

Paxillin cDNA encoding full length human paxillin4 (accession # U14588) was kindly provided by Dr. Victor Small (Vienna, Austria). Human-paxillin-4 cDNA (h-paxillin-4; accession #U14588) was amplified by PCR with complimentary oligonucleotides containing 5' *BglII* and 3' *EcoRI* restriction sites. The PCR products were subcloned into *BamHI*/*EcoRI*-digested pGex (Promega), pCAN-HA (Clontech), pCAN-Myc (Clonetech) and GFP vectors (Clontech).

Transient transfections in HEK293 cells were performed with 5 µg of plasmid DNA per 10 cm plate of cells using Lipofectamine/Plus transfection reagents as per the manufacturer's instructions (Invitrogen).

Infections of MEF3T3 were performed using SLK-directed short-hairpin RNA sequence expressed in an adenoviral vector at an MOI of 10. Infections in 10 cm plates took place in 1 mL of serum-free DMEM for 1.5 h at 37°C and 5% CO_2, with plates being agitated every 15 minutes to ensure media coverage. Plates were then topped up to 10 ml with DMEM with 10% FBS and left at 37°C and 5% CO_2 for 48 h prior to being collected and used in subsequent experiments.

2.2.3- <u>Generation of Mouse Embryonic Fibroblasts (MEF) and Stable Cell Lines</u>:

MEFs were isolated from 13.5-day postcoitum FVB embryos and maintained according to the protocol outlined by Todaro and Green (1963), until spontaneous immortalization was achieved [27]. Immortalized cells were transiently transfected with 4 ug of Myc-PaxillinS250T, Myc-Paxillin WT and Myc-Vector Cntrl respectively, and selected with 30 µg/ml hygromycin for 10 days; cells were subsequently maintained in 15 µg/ml hygromycin.

2.2.4- Immunofluorescence:

Cells were plated onto fibronectin-coated (10 μg/ml) coverslips and incubated overnight at 37°C prior to being fixed with 4% paraformaldehyde (PFA). Following permeablization using 0.3% Triton X in 1X Stockholm PBS (StoPBS; 4 mM Na_2HPO_4, 2 mM NaH_2PO_4, 140 mM NaCl, 3 mM KCl), cells were washed three times in 1X StoPBS and blocked in 1X StoPBS containing 5% goat serum for 20 minutes. Fresh blocking solution containing primary antibody was added and incubated at room temperature for 1 h or overnight at 4°C. Primary antibodies were detected using anti-mouse and/or anti-goat secondaries that were conjugated to either fluorescein isothiocyanate (FITC; Alexa Fluor 488, Invitrogen) or tetramethyl rhodamine isothiocyanate (TRITC; Alexa Fluor 594, Invitrogen). Slides were visualized with a Zeiss LSM5 laser-scanning confocal microscope and photographed using LSM5 Pascal software and a Sony Corporation HB050 digital camera. A minimum of 3 independent experiments were conducted, with representative images being shown.

2.2.5- Replating Assay:

Transiently transfected MEF3T3 cells with GFP-Paxillin, GFP-PaxillinS250T and GFP vector control were grown to confluence and removed using 1X citric saline (1% potassium chloride (w/v), 0.44% sodium citrate (w/v)). Cells were collected by centrifugation at 1000 r.p.m., resuspended in DMEM with 10% FBS for 20 minutes at 37°C. 1 X 10^6 cells were seeded onto uncoated 6-well plates containing DMEM and 10% fetal bovine serum and allowed to attach at 37°C and 5% CO_2 for 5, 10 or 20 minutes. Cells were washed once with 1X phosphate buffered saline (PBS) and collected using 2 ml of 1X trypsin-EDTA. The trypsin/cell suspension mixture was then divided into two separate samples, each consisting of 1 ml, for cell counting via trypan blue dye exclusion with a Beckman Coulter, Inc. Vi-CELL cell counter and GFP content analysis by flow cytometry. The cell counts for the initial number of cells plated as well as the number of cells that adhered were normalized to percent GFP content. Percent adhesion was then calculated by averaging the normalized counts of 3 replicates for each time point, in three independent experiments.

2.2.6- Transwell and Wound-Healing Migration Assays:

Stably transfected cell lines were serum-starved overnight in DMEM with 1% BSA prior to use in migration assays. For transwell Boyden chamber migration assays, serum-starved cells were seeded at a density of 5 X 10^4 cells per transwell (pore size, 0.8 µm; Fisher, Ottawa, Ontario, Canada) migration chamber in 10% FBS DMEM. Migration chambers were precoated with 10 µg/ml fibronectin for one hour prior to plating. Cells were allowed to migrate for 6 h toward 10% FBS DMEM in the bottom chamber. Cells remaining on the upper side of the filter were removed and cells that migrated through to the underside of the filter were fixed in 4% paraformaldehyde (PFA) and stained with 0.5 µg/ml DAPI (4,6-diamidino-2-phenylindole; Sigma). Membranes were then removed from transwells and mounted onto slides where DAPI-stained nuclei were visualized (10x) and counted from four random fields of view using a Zeiss Axiocam digital camera. For each cell line, three independent experiments were performed in triplicate.

Wound healing experiments were also conducted using Myc-expressing stable cell lines. Cells were seeded at a density of 3 x 10^5 cells per well in a 24-well, fibronectin-coated plate and grown overnight at 37°C with 5% CO_2 to confluency. Artificial wounds of similar width and length were introduced in the confluent monolayer using a micropipette tip. Resultant wounds were visualized using phase contrast microscopy and photographed using a Zeiss Axiocam digital camera. For each wound, five pre-determined and independent points were photographed at 0 and 10 h to measure the distance between converging wound fronts. Measurements made using ImageJ software were averaged among 4 independent experiments to calculate the percent wound closure.

2.2.7- <u>GFP Sorting, Cell Spreading and Live Imaging Microscopy</u>:

MEF3T3 were transfected with GFP-fusion proteins GFP-Paxillin, GFP-PaxillinS250T and GFP alone. 1-2 X 10^7 cells/ml were collected the next day and sorted for GFP content. For cell spreading, 1 X 10^4 GFP-positive cells were plated onto fibronectin-coated dishes and allowed to spread for 2 h at 37°C and 5% CO_2. Phase contrast and fluorescent images (488 nm) were collected every 30 minutes using a Zeiss Colibri LED microscope. Eight different frames of view were photographed using AxioVision software for each cell type and time point. Cell spreading was assessed by measuring the surface area of >10 isolated cells per field of view using ImageJ software.

Live cell imaging was performed on 1-5 X 10^4 GFP-positive cells that were plated onto fibronectin-coated dishes and allowed to spread for 12 h at 37°C and 5% CO_2 prior to imaging.

Throughout the imaging process, cells were maintained at 37°C and 5% CO_2 using a heated stage and gas hook-up. Fluorescent images were captured at a frequency of one image/minute for 10 minutes at 488 nm using a Zeiss Colibri LED microscope and AxioVision software. The area of at least 20 focal adhesions per cell type was measured over time using ImageJ software. Dissociation constants were then calculated as previously described by Webb et al. (2004) [76, 123]. Briefly, the ratio of the area of the focal adhesion as observed from the GFP fluorescence at T=0 and T=X was determined. Plotting of the natural log of this quotient ($\ln[I_0/I_t]$) over time and subsequent calculation of the slope was used to obtain the value for K*diss*(min^{-1}). Means of the K*diss* and standard errors of the means of more than 20 adhesions were calculated.

2.3- Protein Analysis

2.3.1- Synthesis of Glutathione S-Transferase (GST)-Paxillin Deletion Fusion Proteins:

Selected regions of h-paxillin-4 cDNA (accession #U14588) were amplified by PCR with complimentary oligonucleotides containing 5' *BglII* and 3' *EcoRI* restrictions sites. The PCR products were subcloned into *BamHI*/*EcoRI*-digested pGex4T-2 (Promega). Verification of the correct reading frame was achieved by sequencing with deletion-specific custom primers (Nanuq- McGill University and Genome Quebec Innovation Center, Montreal, Québec, Canada). Protein synthesis was verified via SDS-Page and coomassie staining.

Point mutations were made using and according to the protocol from Stratagene's (Agilent; Santa Clara, California, USA) 'QuikChange XL Site-Directed Mutagenesis Kit' using GST-tagged paxillin cDNA as the template. Briefly, primers were designed to exploit a single nucleotide substitution to change a serine residue to a glycine, alanine and/or threonine residue. Please note that serine(s) were mutated to an A or G according to whichever mutation could be achieved by making a single nucleotide change. A single, as opposed to a double nucleotide substitution, has a much higher success rate of incorporation [124]. The resulting PCR products were then incubated with *Dpn I* endonuclease to select for the newly synthesized mutated DNA, transformed into ultra-competent cells and verified for the mutated DNA sequence and protein production as described above. Myc-tagged paxillin cDNA in a hygromycin vector was also used as template to make point mutants for use in the generation of stable cell lines.

2.3.2- Purified Recombinant GST-Fusion Protein Preparations:

Overnight cultures of glutathione-S-transferase (GST)-tagged fusion protein were grown from bacterial DH5α, RP or RIL stocks in 3 ml of Luria-Bertani broth (LB) containing 50 µg/ml ampicillin in a 37°C shaker. Diluted cultures (1 in 10) were allowed to grow the next day for an additional hour prior to a 2 h induction with 1 mM isopropyl-beta-D-thiogalactopyranoside (IPTG; Sigma). Following induction, bacteria were collected by centrifugation at 4000 *g*, lysed in RIPA buffer (50 mM Tris-HCl (pH 7.4), 150 mM NaCl, 1 mM EDTA, 1% TritonX-100, 0.5% sodium deoxycholate, 0.1% SDS, 1% Nonidet P-40) with protease inhibitors (2 mM DTT, 10 µg/ml leupeptin, 10 µg/ml pepstatin, 10 µg/ml aprotinin, 1 mM phenylmethylsulphonylfluoride (PMSF) and 100 µM benzamidine), sonicated and left on ice for fifteen minutes. Protein lysates were cleared by centrifugation (10 minutes at 14,000 *g*) and transferred to glutathione sepharose beads (GE Healthcare Life Sciences) for 30 minutes at room temperature. Beads were recovered by pulse centrifugation at maximum speed and washed 4X in NETN ((20 mM

Tris-HCl pH 8.0, 1 mM EDTA, 200 mM NaCl, 0.5% Noniodet P-40) buffer prior to being used in other assays.

2.3.3- <u>Thrombin Protease Cleavage</u>:

To cleave the GST moiety from the fusion proteins, recombinant, purified GST-protein on beads was inverted with 5 u/µl of thrombin protease (Amersham) in 30 µl of 1X PBS overnight at room temperature. Purified, recombinant protein without GST was collected from the supernatant by centrifugation at 14,000 *g* for 10 minutes.

2.3.4- <u>Native PAGE</u>:

Polyacrylamide gels were made and run in the absence of SDS as per the protocol outlined by Walker (2002) [125].

2.3.5- <u>*In Vitro*-Direct Binding Assays</u>:

In vitro translated proteins were generated using the TNT quick coupled *in vitro* transcription/translation kit (Promega) as per the manufacturer's instructions. Translated proteins were incubated with purified, recombinant GST-protein on beads in 1X PBS and inverted for 30 minutes at room temperature. Beads were collected by pulse centrifugation at maximum speed, washed 3X in NETN buffer and eluted with the addition of 4X SDS sample buffer. Proteins were resolved by SDS-PAGE, stained with Coomassie brilliant blue (Sigma), destained in a solution of 30% methanol and 10% glacial acetic acid, and dried to visualize the

GST-fusion proteins. Autoradiography was used to visualize *in vitro* protein translation and to evaluate binding to GST-fusion proteins.

2.3.6- <u>Western Blotting</u>:

Cells were washed once with cold PBS before being scraped down and collected by centrifugation at 5000 g for 3 minutes. Cell pellets were lysed in RIPA buffer containing 50 mM Tris-HCl (pH 7.4), 150 mM NaCl, 1 mM EDTA, 1% TritonX-100, 0.5% sodium deoxycholate, 0.1% SDS, 1% Nonidet P-40. Protein lysates were cleared by centrifugation at 10,000 g for 5 minutes and quantitated via Bradford Assay at 595 nm (BIORAD; Mississauga, Ontario, Canada). Equal amounts of protein (20-40 µg) were resolved on an 8-12% acrylamide gel then transferred to PVDF (polyvinylidene difluoride) membrane. Membranes were blocked and probed with the indicated antibodies in the presence of 5% BSA or milk powder at 4°C in 1X TBST (50 mM Tris pH 7.4, 150 mM NaCl, 0.1% Tween 20). Proteins were visualized following the addition of horseradish peroxidase-coupled secondary antibody, chemiluminescence (Perkin-Elmer, Waltham, MA, USA), and exposure to X-ray film. A minimum of 3 independent experiments were conducted, with representative images being shown.

Ubiquitin Immunoblotting:

Proteins transferred to PVDF membranes were sandwiched between Whatman papers wetted in ddH_20 and placed in a Pyrex glass container prior to being autoclaved for 30 minutes in the liquid cycle. Following this cycle, the water was removed and the blot with the Whatman papers still present was autoclaved again, this time for 15 minutes on a dry cycle.

Immunoblotting then proceeded as previously described with blocking in 5% BSA and the addition of a polyclonal anti-ubiquitin antibody (Abgent; San Diego, California, USA).

2.3.7- <u>Immunoprecipitation</u>:

For immunoprecipitation, 200-400 µg of protein lysate was used in combination with 2 µg of SLK antibody in the presence of 20 µl of protein A sepharose beads (GE Health Care, Piscataway, NJ, USA) and inverted for 2 h at 4°C. Immune complexes were collected by pulse centrifugation at maximum speed and washed 4 times in NETN buffer (20 mM Tris-HCl pH 8.0, 1 mM EDTA, 200 mM NaCl, 0.5% Noniodet P-40).

2.3.8- <u>*In vitro* Kinase Assays</u>:

In vitro kinase assays were performed as previously described in [70] on SLK immunoprecipitations obtained from scratch-wounded cell lysates. Scratched plates were obtained by removing approximately 50% of the cells from a confluent, 10 cm dish by scratching with a p20 micropipette tip. Scratched monolayers were then incubated for the indicated time prior to collection. In the case of the *in vitro* kinase assays where purified recombinant GST protein is added, the recombinant protein on glutathione S-transferase beads is mixed in with the immunoprecipitated SLK on protein A sepharose prior to the first wash in NETN buffer. The kinase reaction was stopped by the addition of 4X SDS sample buffer and resolved using 4-20% acylamide gels (depending on the size of the other proteins in the assay) and SDS-PAGE. Gels were either stained with coomassie brilliant blue and dried, or transferred to PVDF prior to exposure to X-ray film at -80°C for autoradiography. Transferred membranes were then subjected to Western blot analysis.

<u>Non-Radioactive (Cold) Kinase Assays</u>:

Non-radioactive kinase assays were performed as described above except that 10 mM unlabelled ATP was substituted for γ-^{32}ATP.

2.3.9- <u>Phosphoamino Acid Analysis</u>:

Partial amino acid hydrolysis of [^{32}P]-labelled phosphorylated protein was achieved by excising metabolically labeled proteins from PVDF membranes post kinase assay and incubating the section of membrane at 100°C in 6 M HCL for 1h. Samples were then lyophilized before phospho-standards (phospho-serine, threonine and tyrosine) were added (1 mg/ml). Phosphoamino acids were separated using 2-D thin layer electrophoresis (TLC) plates and electrophoresis as seen in Duclos et al (1991) [126]. P-Ser and P-Thr were separated from P-Tyr in pH 3.5 buffer containing acetic acid, pyridine and H_20 (50: 5: 945 (v/v/v)), followed by a separation of P-Ser and P-Thr in pH 1.9 buffer containing formic acid, acetic acid and water (50: 156: 1794 (v/v/v)). Phosphoamino acids were then detected via ninhydrin staining and autoradiography.

2.3.10- <u>Tryptic Peptide Mapping of Immobilized Proteins</u>:

Kinase assays were transferred to nitrocellulose membranes and exposed to X-ray film. [^{32}P]-labelled proteins were cut from the membrane and incubated for 30 minutes at 37°C with polyvinylpyrrolidine (PVP). The membrane was washed extensively in ddH_2O (5 X 1 ml) then incubated at 37°C with 10 µg TPCK-trypsin (Sigma) for 2 h in 200 µl ammonium bicarbonate (NH_4HCO_3) buffer (pH 8). An additional 10 µg of TPCK-trypsin was added for 2 more hours prior to eluting of the peptides. Lyophilized peptides were resuspended in 5 µl of electrophoresis buffer (acetic acid/ formic acid/water 15/5/80) and spotted onto TLC plates. Phosphopeptides were resolved using 2D electrophoresis (20 minutes at 1.0 kV). Autoradiography at -80°C for 3 days was used to visualize the phosphorylated peptides.

2.4- <u>Immunohistochemistry</u>:

Paraffin-embedded human tissues (HuFPT130) and tissue microarrays (BRC961) [127] were purchased from US Biomax (Rockville, Maryland, USA). Tissues were processed as described by Luise and Nuciforo (2006) [128]. Briefly, tissues were de-paraffinized in xylene and re-hydrated using a graded series of ethanol (1 X 3 minutes). Antigen retrieval using citrate buffer (0.1 M citric acid and 10mM sodium citrate, pH 6) and quenching of endogenous peroxidases using 3% H_2O_2 was also performed. Tissues were blocked in 10% BSA for 30 minutes prior to the addition of primary antibody. Serial dilutions were used to determine optimal primary antibody concentration of total paxillin and phospho-S250 antibodies. Tissues were then incubated in primary antibody at 4°C overnight. Biotinylated secondary antibody (Dako, Burlington, Ontario, Canada) and DAB (Vector Laboratories, Burlington, Ontario, Canada) were used to develop tissue sections. Counterstaining with hematoxylin and subsequent dehydration of the samples was performed prior to mounting.

<u>Chapter 3</u>:

In vitro phosphorylation of paxillin by SLK

<u>Paxillin is a substrate for SLK *in vitro*</u>:

SLK phosphorylates paxillin in vitro

Kinase specificity for, and subsequent phosphorylation of a substrate is dependent upon proximity, requiring both elements to be present at the same subcellular compartment/structure at the same time [49]. We have previously shown that SLK is required for efficient focal adhesion turnover [78]. Furthermore, we have determined that SLK is capable of localizing with paxillin **(Figure 3.1)**, a focal adhesion protein that has also been implicated in the regulation of adhesion turnover, to the leading edge and membrane ruffle of migrating cells [78, 99, 107, 120]. Since SLK is required for fusion in C2C12, a process whereby coordinated migration signaling is required for the alignment and formation of myoblasts into myotubes, we tested for, and observed that SLK is capable of co-localizing with paxillin in differentiating myoblasts **(Figure 3.1)** [129, 130].

Interestingly, paxillin has been shown to become serine phosphorylated in response to a variety of stimuli including adhesion to fibronectin and migration [47, 66, 122]. To investigate whether paxillin is phosphorylated by SLK *in vitro*, endogenous, SLK was immunoprecipitated from scratch-wounded monolayers of MEF3T3 and incubated with purified, recombinant GST-paxillin protein in the presence of ^{32}P-γ-ATP. The presence of the GST-fusion protein was confirmed by Coomassie stain. Subsequent autoradiography of the dried gel shows that SLK phosphorylates paxillin *in vitro* **(Figure 3.2 (A))**.

A large-scale analysis of paxillin phospho-peptides using mass spectrometry in 2006 by Webb et al., revealed in excess of 40 unique, potential paxillin phosphorylation sites at

<u>Figure 3.1</u>: *SLK and paxillin co-localize to membrane ruffles and the leading edge of migrating cells.* Confocal microscopy (63X) of subconfluent and confluent-scratched MEF3T3 fibroblasts and subconfluent C2C12 myoblasts on fibronectin and collagen-coated coverslips, respectively. For the scratch-wound panel, a single wound was introduced using a micropipette tip prior to incubation for 1 h at 37°C and subsequent fixation. Endogenous SLK and paxillin were visualized using SLK and paxillin antibodies coupled with Alexa Flor 594 nm (red) and 488 nm [27], respectively.

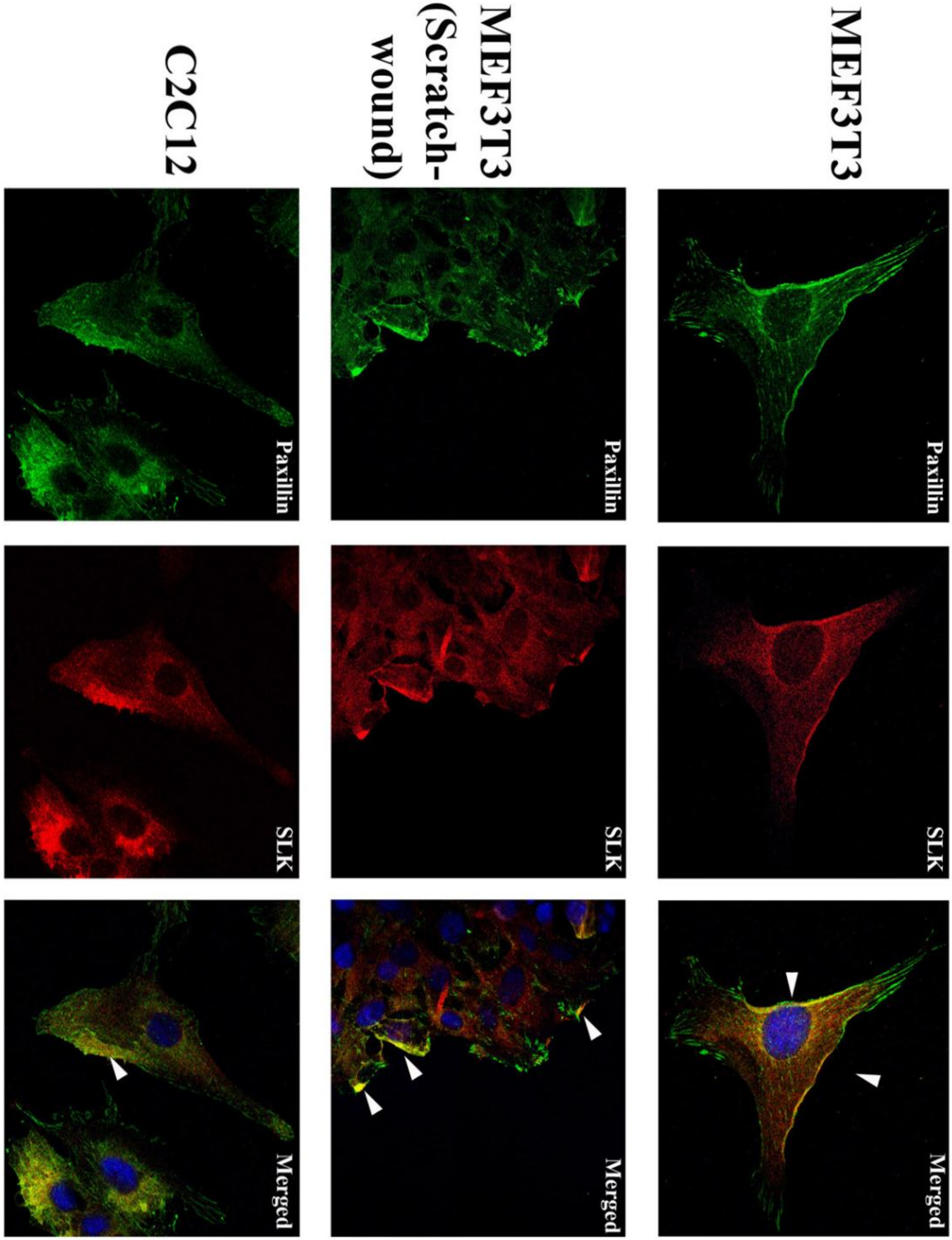
MEF3T3
MEF3T3 (Scratch-wound)
C2C12
Paxillin
SLK
Merged
Paxillin
SLK
Merged
Paxillin
SLK
Merged

<u>Figure 3.2</u>: *SLK phosphorylates paxillin on a serine residue, in vitro*. (A) Endogenous SLK was immunoprecipitated (IP) from scratch-wounded MEF3T3 using anti-SLK antibody and subjected to an *in vitro* kinase assay. Purified, recombinant GST-paxillin and GST-vector protein was added to the respective SLK IPs prior to the addition of ^{32}P-γ-ATP. Samples were incubated in kinase buffer for 30 minutes at 30°C prior to SDS-PAGE. Coomassie stain and autoradiography (AUTORAD) were used to visualize protein content and kinase signal, respectively. **(B)** Phospho-amino acid analysis of *in vitro* SLK-phosphorylated, GST-paxillin (pGST-paxillin). Separated phospho-serine, threonine and tyrosine residues were visualized by exposing the TLC plate to X-ray film for 3 days at -80°C. **(C)** Tryptic digest of *in vitro* SLK-phosphorylated, thrombin cleaved, GST-paxillin. Phosphorylated paxillin fragments were resolved in two dimensions and visualized by exposing the TLC plate to X-ray film for 5 days at -80°C.

A)

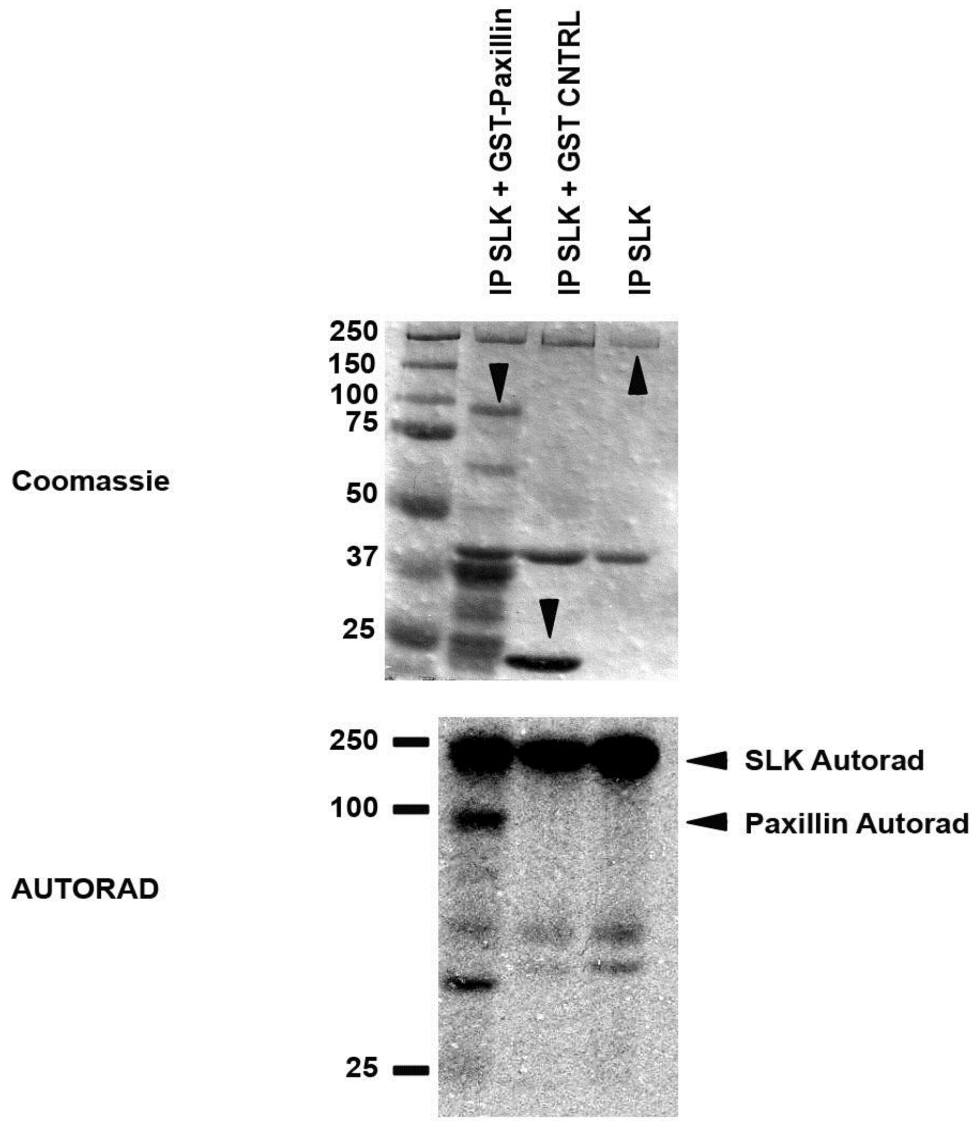
IP SLK + GST-Paxillin
IP SLK + GST CNTRL
IP SLK
250
150
100
75
Coomassie
50
37
25
250
100
SLK Autorad
Paxillin Autorad
AUTORAD
25

B)

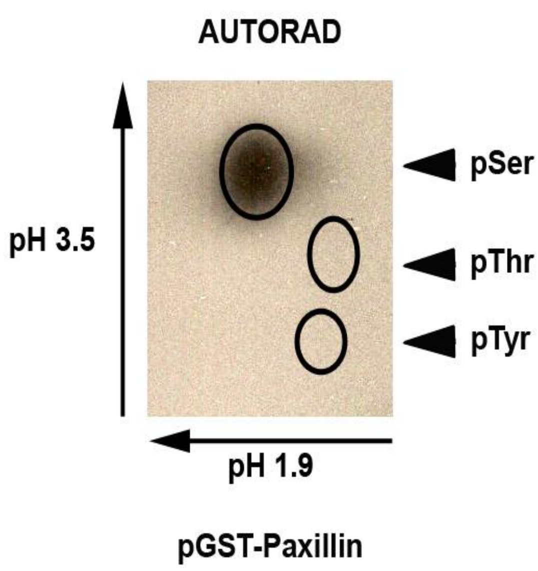
AUTORAD
pSer
pH 3.5
pThr
pTyr
pH 1.9
pGST-Paxillin

C)

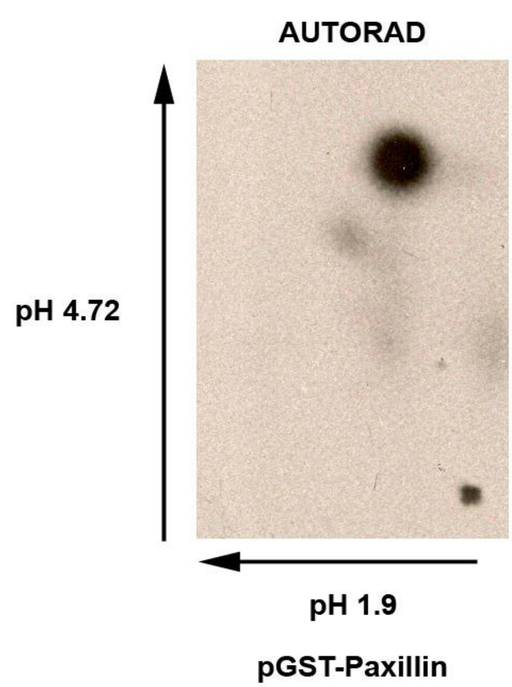
AUTORAD
pH 4.72
pH 1.9
pGST-Paxillin

<u>Figure 3.3</u>: ***Predicted sites of serine/threonine phosphorylation as determined by NetPhos2.0 software (http://www.cbs.dtu.dk/services/NetPhos/)*** **[131].** Human paxillin 4 protein sequence, NCBI accession #14588, was inputed into the NetPhos 2.0 server to predict potential sites of serine and threonine (S/T) phosphorylation within the protein; tyrosine residues were not selected for prediction. **(A)** Schematic representation of predicted S/T sites within human paxillin. Please note that the blue horizontal line found at the 50% confidence statistic of the vertical axis, represents the threshold of phosphorylation delineation. **(B)** Predicted paxillin S/T phosphorylation sites that overcome the threshold statistic. Sites of note include: S95, 103, 126, 216, 219, 230, 250, 258, 288, 298, 499, all of which overcome 90% < confidence interval for phosphorylation; the closest candidate threonine is T89 at 88.6%.

A)

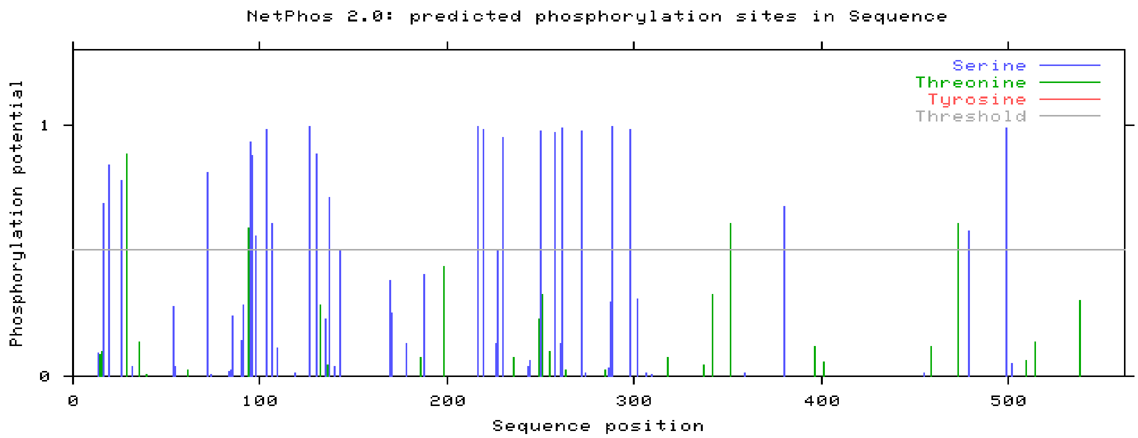

B)

Phosphorylation sites predicted: Ser: 25 Thr: 4

Serine predictions

Name	Pos	Context	Score	Pred
Sequence	13	ADLESTTSH	0.091	.
Sequence	16	ESTTSHISK	0.688	*S*
Sequence	19	TSHISKRPV	0.841	*S*
Sequence	26	PVFLSEETP	0.781	*S*
Sequence	32	ETPYSYPTG	0.038	.
Sequence	54	PPPPSSEAL	0.277	.
Sequence	55	PPPSSEALN	0.034	.
Sequence	72	QWQPSGSRF	0.807	*S*
Sequence	74	QPSGSRFIH	0.006	.
Sequence	83	QQPQSSSPV	0.021	.
Sequence	84	QPQSSSPVY	0.025	.
Sequence	85	PQSSSPVYG	0.241	.
Sequence	90	PVYGSSAKT	0.141	.
Sequence	91	VYGSSAKTS	0.285	.
Sequence	95	SAKTSSVSN	0.933	*S*
Sequence	96	AKTSSVSNP	0.879	*S*
Sequence	98	TSSVSNPQD	0.560	*S*
Sequence	103	NPQDSVGSP	0.982	*S*
Sequence	106	DSVGSPCSR	0.605	*S*
Sequence	109	GSPCSRVGE	0.112	.
Sequence	119	EHVYSFPNK	0.012	.
Sequence	126	NKQKSAEPS	0.995	*S*
Sequence	130	SAEPSPTVM	0.885	*S*
Sequence	135	PTVMSTSLG	0.227	.
Sequence	137	VMSTSLGSN	0.710	*S*
Sequence	140	TSLGSNLSE	0.034	.
Sequence	143	GSNLSELDR	0.496	.
Sequence	169	DEANSSPPL	0.379	.
Sequence	170	EANSSPPLP	0.253	.
Sequence	178	PGALSPLYG	0.127	.
Sequence	188	PETNSPLGG	0.403	.
Sequence	216	DVRPSVESL	0.996	*S*
Sequence	219	PSVESLLDE	0.981	*S*
Sequence	226	DELESSVPS	0.131	.
Sequence	227	ELESSVPSP	0.503	*S*
Sequence	230	SSVPSPVPA	0.952	*S*
Sequence	243	QGEMSSPQR	0.036	.
Sequence	244	GEMSSPQRV	0.060	.
Sequence	250	QRVTSTQQQ	0.975	*S*
Sequence	258	QTRISASSA	0.966	*S*
Sequence	260	RISASSATR	0.127	.
Sequence	261	ISASSATRE	0.986	*S*
Sequence	272	ELMASLSDF	0.977	*S*
Sequence	274	MASLSDFKF	0.010	.
Sequence	286	GKTGSSSPP	0.029	.
Sequence	287	KTGSSSPPG	0.297	.
Sequence	288	TGSSSPPGG	0.991	*S*
Sequence	298	PKPGSQLDS	0.981	*S*
Sequence	302	SQLDSMLGS	0.309	.
Sequence	306	SMLGSLQSD	0.010	.
Sequence	309	GSLQSDLNK	0.005	.
Sequence	359	EEIGSRNFF	0.013	.
Sequence	380	HNLFSPRCY	0.673	*S*
Sequence	455	ENYISALNT	0.014	.
Sequence	479	FVNGSFFEH	0.577	*S*
Sequence	499	ERRGSLCSG	0.989	*S*
Sequence	502	GSLCSGCQK	0.052	.

Threonine predictions

Name	Pos	Context	Score	Pred
Sequence	14	DLESTTSHI	0.086	.
Sequence	15	LESTTSHIS	0.098	.
Sequence	29	LSEETPYSY	0.886	*T*
Sequence	35	YSYPTGNHT	0.136	.
Sequence	39	TGNHTYQEI	0.009	.
Sequence	61	ALNGTILDP	0.025	.
Sequence	94	SSAKTSSVS	0.589	*T*
Sequence	132	EPSPTVMST	0.282	.
Sequence	136	TVMSTSLGS	0.044	.
Sequence	186	GVPETNSPL	0.073	.
Sequence	198	AGPLTKEKP	0.433	.
Sequence	236	VPAITVNQG	0.074	.
Sequence	249	PQRVTSTQQ	0.225	.
Sequence	251	RVTSTQQQT	0.327	.
Sequence	255	TQQQTRISA	0.101	.
Sequence	263	ASSATRELD	0.027	.
Sequence	284	AQGKTGSSS	0.027	.
Sequence	318	LGVATVAKG	0.074	.
Sequence	337	GQVVTAMGK	0.043	.
Sequence	342	AMGKTWHPE	0.323	.
Sequence	351	HFVCTHCQE	0.609	*T*
Sequence	396	DKVVTALDR	0.116	.
Sequence	401	ALDRTWHPE	0.056	.
Sequence	459	SALNTLWHP	0.119	.
Sequence	473	RECFTPFVN	0.608	*T*
Sequence	509	QKPITGRCI	0.063	.
Sequence	514	GRCITAMAK	0.133	.
Sequence	538	LNKGTFKEQ	0.298	.

serine or threonine residues [121]. Additionally, 29 S/T phosphorylation sites were also predicted via artificial neural network techniques **(Figure 3.3 (A & B))**. Interestingly, not all 29 predicted sites overlap with what was determined by mass spectrometry analysis [121, 131]. These findings, taken together with the fact that SLK has been identified as a serine/threonine kinase, prompted us to investigate whether SLK phosphorylated a serine and/or threonine residue within paxillin. Through the use of phosphoamino-acid analysis **(Figure 3.2 (B)),** we were able to determine that SLK phosphorylates paxillin on a serine residue, exclusively. Moreover, subsequent tryptic mapping **(Figure 3.2 (C))** has revealed that only a single major peptide fragment within paxillin is phosphorylated by SLK. However, this does not exclude the possibility that phosphorylation occurs on multiple serine residues within that peptide fragment.

A sensitive and widely-used method of identifying potential sites of phosphorylation is through the combined use of immobilized metal affinity chromatography (IMAC) and matrix-assisted laser desorption ionization (MALDI) mass spectrometry (MS) on a library of peptide fragments generated by tryptic digestion [132, 133]. Through this approach, phosphopeptides are identified by examining observed peptide masses of the respective tryptic fragments for the added mass of a phosphate group (80 Da) relative to the expected peptide masses [133]. For this study, a non-radioactive kinase assay was conducted using 0.1 mM of unlabelled ATP in the presence of immunoprecipitated SLK and recombinant GST-paxillin protein [134]. Interestingly, two potential sites were identified within paxillin that are phosphorylated by SLK, specifically serines 272 and 274 **(Appendix A)**. However, subsequent testing using site directed mutagenesis of these sites into alanine residues showed no loss of paxillin phosphorylation in an SLK *in vitro* kinase assay. This suggests that paxillin S272 and/or 274 are not in fact phosphorylated by SLK *in vitro* (**Appendix B**).

SLK <u>is not</u> associated with another kinase that is capable of phosphorylating paxillin in vivo

Previous inquiries via mass spectrometry were conducted on immunoprecipitated SLK to identify potential associating proteins (data not shown; unpublished). Although proteins like tubulin, vimentin and the Rho/Rac guanine nucleotide exchange factor 2 were identified, no kinases were shown to co-immunoprecipitate with SLK (data not shown; unpublished). However, this does not exclude the possibility that SLK could co-immunoprecipitate with other kinases. In fact, since we have shown that SLK activity is modulated depending on the stage of migration, it is possible that SLK is capable of forming transient interactions that are condition-specific with other proteins as well. Consequently, to determine whether paxillin is phosphorylated *in vitro* by SLK and not some other SLK-associated kinase, wildtype (HA-SLK) and kinase dead (HA-K63R) SLK were transiently transfected into 293 cells and immunoprecipitated using an anti-HA(12CA5) antibody. IPs were then incubated with recombinant GST-paxillin in a kinase assay prior to SDS-PAGE. Transferred proteins were visualized on PVDF using a combination of autoradiography and immunoblotting. As seen in **Figure 3.4**, wildtype HA-SLK can phosphorylate paxillin, while the kinase dead, K63R cannot. This suggests that paxillin phosphorylation *in vitro* is a result of SLK activity and not that of an SLK-associating kinase.

<u>Figure 3.4</u>: *Paxillin phosphorylation is not due to an SLK-associated kinase*. Transiently expressed, HA-tagged, wildtype (HA-SLK) and kinase dead (HA-K63R) SLK were immunoprecipitated using beads pre-conjugated with HA (12CA5) antibody in 293 cells. Purified, recombinant GST-paxillin protein was added to the respective IPs and subjected to an *in vitro* kinase assay. Blotting with anti-SLK, GST and HA antibodies was then performed to verify the presence and amount of protein present. Please note that the panel showing HA blotting was a separate gel that was run using 30 µg of whole cell lysate from each of the transfections to validate the presence of transfected proteins.

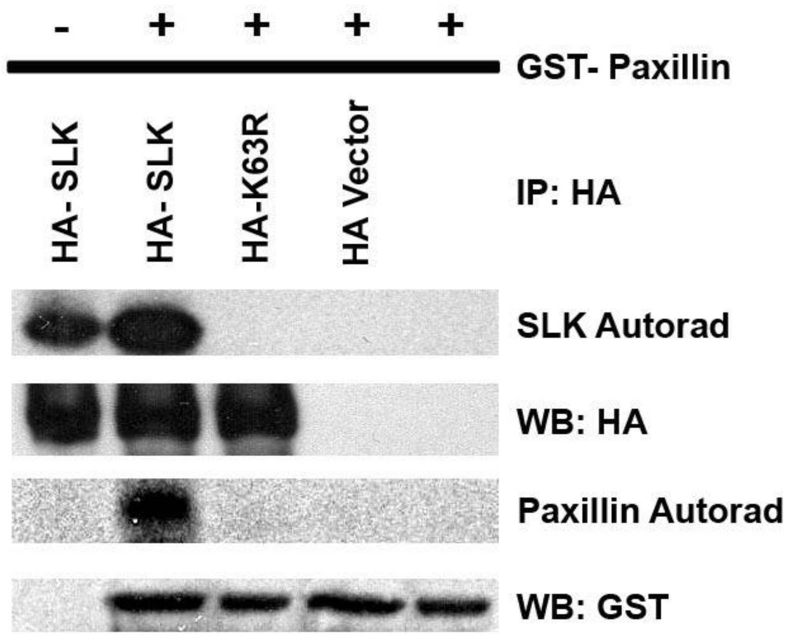

- + + + +
GST- Paxillin
HA- SLK
HA- SLK
HA-K63R
HA Vector
IP: HA
SLK Autorad
WB: HA
Paxillin Autorad
WB: GST

SLK phosphorylates the LD3 domain of paxillin, in vitro

Since mass spectrometry-related approaches failed to yield a site of SLK-mediated, paxillin phosphorylation *in vitro*, chemical cleavage using trypsin (K-X, R-X), cyanogen bromide (M-X) and hydroxylamine (N-G) was used to try to narrow down the region of phosphorylation by generating a peptide fragment map by the process of elimination (data not shown). However, low yield and difficulty reproducing results rendered this approach ineffective. Therefore, the only viable alternative remaining to identify this site(s) of phosphorylation was the creation and testing of a series of deletion constructs **(Figure 3.5)**. Deletions isolating the paxillin LD and LIM domains were tested using an *in vitro* kinase assay with endogenous SLK from MEF3T3 as the source of kinase. From this assay **(Figure 3.6(A))**, we were able to ascertain that SLK phosphorylates the N-terminal LD domain and not the C-terminal LIM domain of paxillin. N-terminal deletions of paxillin within the LD domain were then generated within the context of the full length protein in an effort to maintain as much of the native protein structure as possible. Subsequent *in vitro* kinase assays showed that SLK phosphorylates paxillin within its LD3 domain, specifically within a region of 20 amino acids that contains 3 serine residues, namely S243, S244 and S250 **(Figure 3.6 (B))**.

SLK phosphorylates paxillin at S250

Since N-terminal deletions were successful in narrowing down the site(s) of paxillin phosphorylation to three serine residues within the LD3 domain, each of the three sites was mutated to a non-phosphorylatable residue such as a glycine (G; S243G, S244G) or an alanine

<u>Figure 3.5</u>: ***Protein construct map of domain mutations and N-terminal deletion mutants generated from human paxillin cDNA.*** Deletions were amplified by PCR with complimentary oligonucleotides corresponding to ATGGACGACCTCGACGCCCTG (LD1-5), AAAGGAGTCTGCGGGGCCTGC (LIM1-4), TTGGATGAACTGGAGAGCTCC (Δ660), GCCATCACTGTGAACCAGGGC (Δ699) and CAGCAGACACGCATCTCGGCC (Δ758), and containing 5' *BglII* or 3' *EcoRI* restrictions sites. The PCR products were subcloned into *BamHI*/*EcoRI*-digested pGex4T-2, sequenced and protein-purified to verify the deletion.

Human Paxillin Protein (U14588):

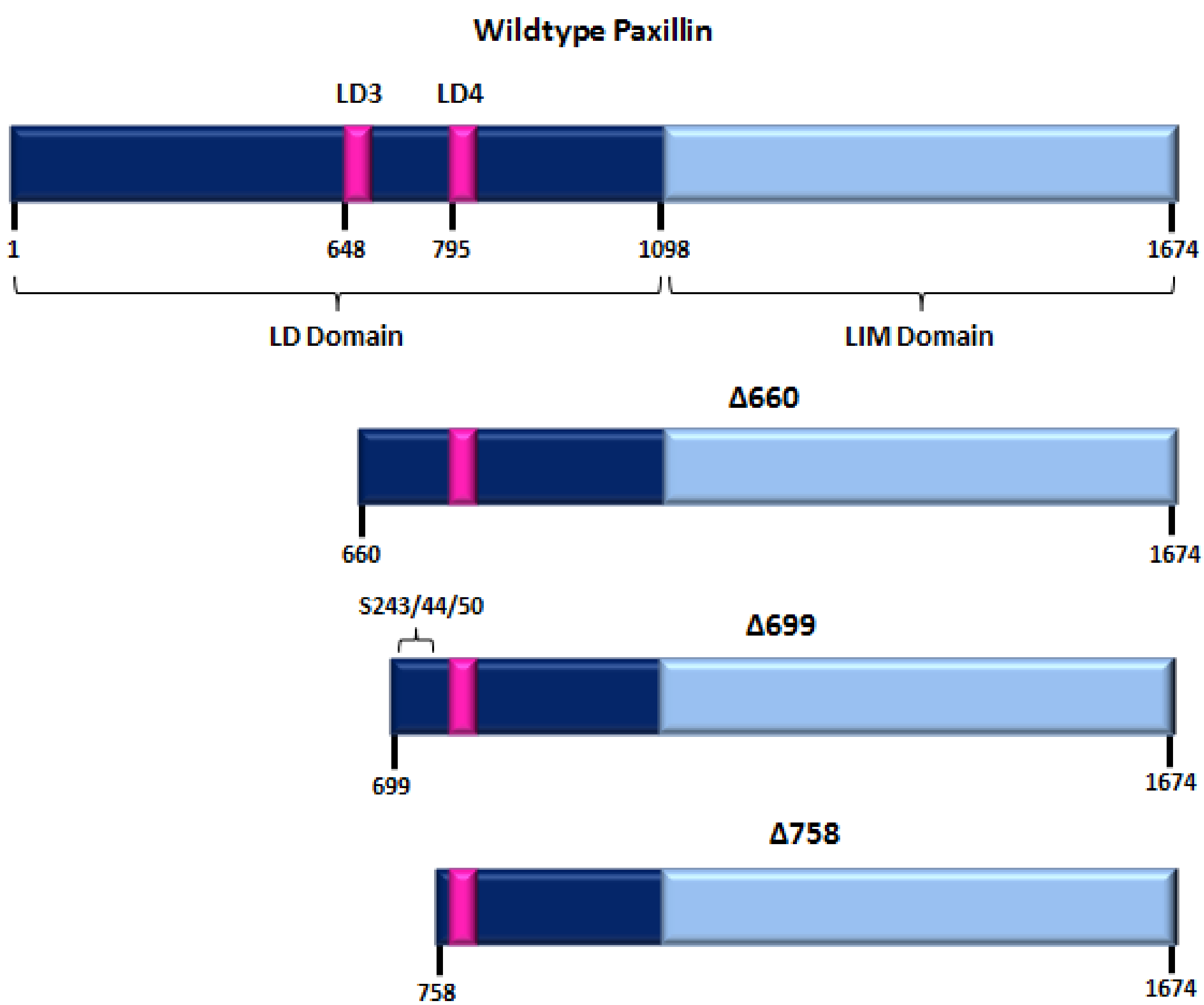

<u>**Figure 3.6**</u>**:** ***SLK phosphorylates paxillin in its LD domain in a region defined by nucleotides 699-758.*** **(A)** Endogenous SLK was immunoprecipitated from scratch-wounded MEF3T3 using anti-SLK antibody and subjected to an *in vitro* kinase assay. Purified, recombinant GST-paxillin domain constructs, GST-LD1-5 (2) and GST-LIM1-4 (3), as well as full length, wildtype protein (3) were added to SLK IPs prior to the addition of radioactive ATP [γ-ATP^{32}]. Samples were incubated in the presence of kinase buffer at 30°C for 30 minutes then subjected to SDS-PAGE; Coomassie stain and autoradiography (AUTORAD) were used to visualize protein content and kinase signal, respectively. **(B)** Same as in **(A)** except: GST-domain constructs were substituted for GST-tagged, N-terminal deletion constructs, GST-Δ660, Δ699 and Δ758, where 660, 699 and 758 are indications of the number of N-terminal nucleotides deleted to generate the respective deletion mutants.

A)

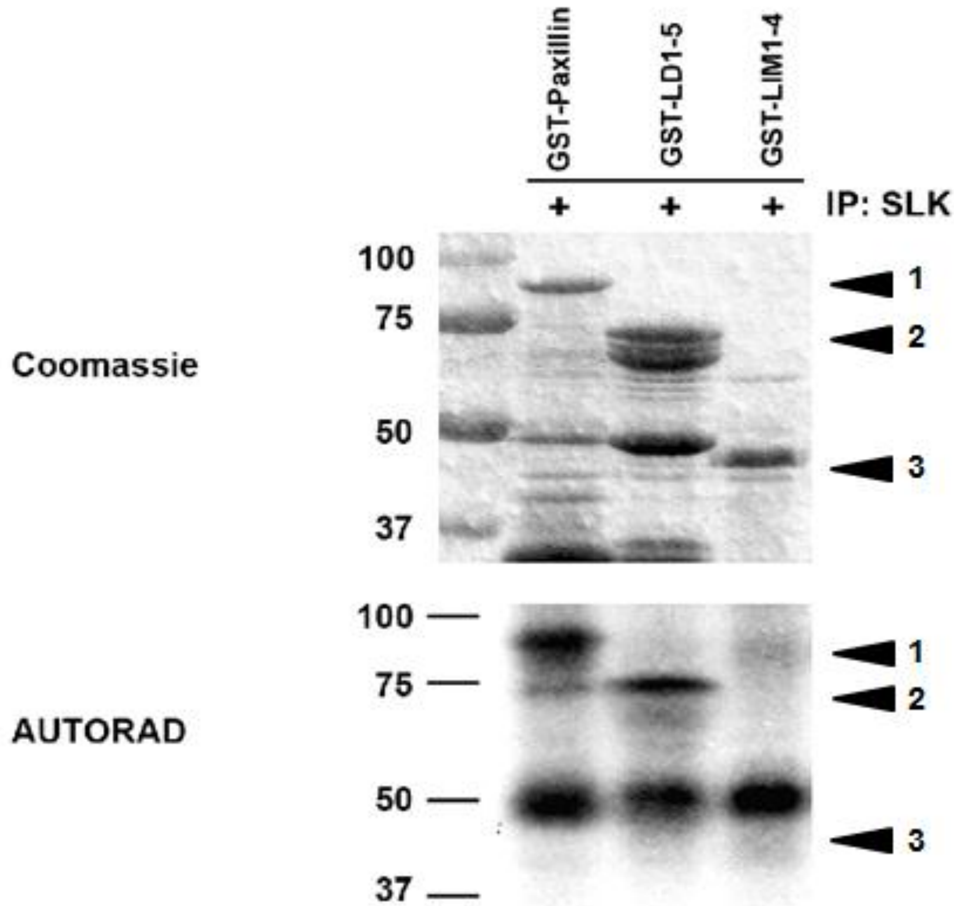
GST-Paxillin
GST-LD1-5
GST-LIM1-4
+ + + IP: SLK
Coomassie
100
75
50
37
1
2
3
AUTORAD
100
75
50
37
1
2
3

B)

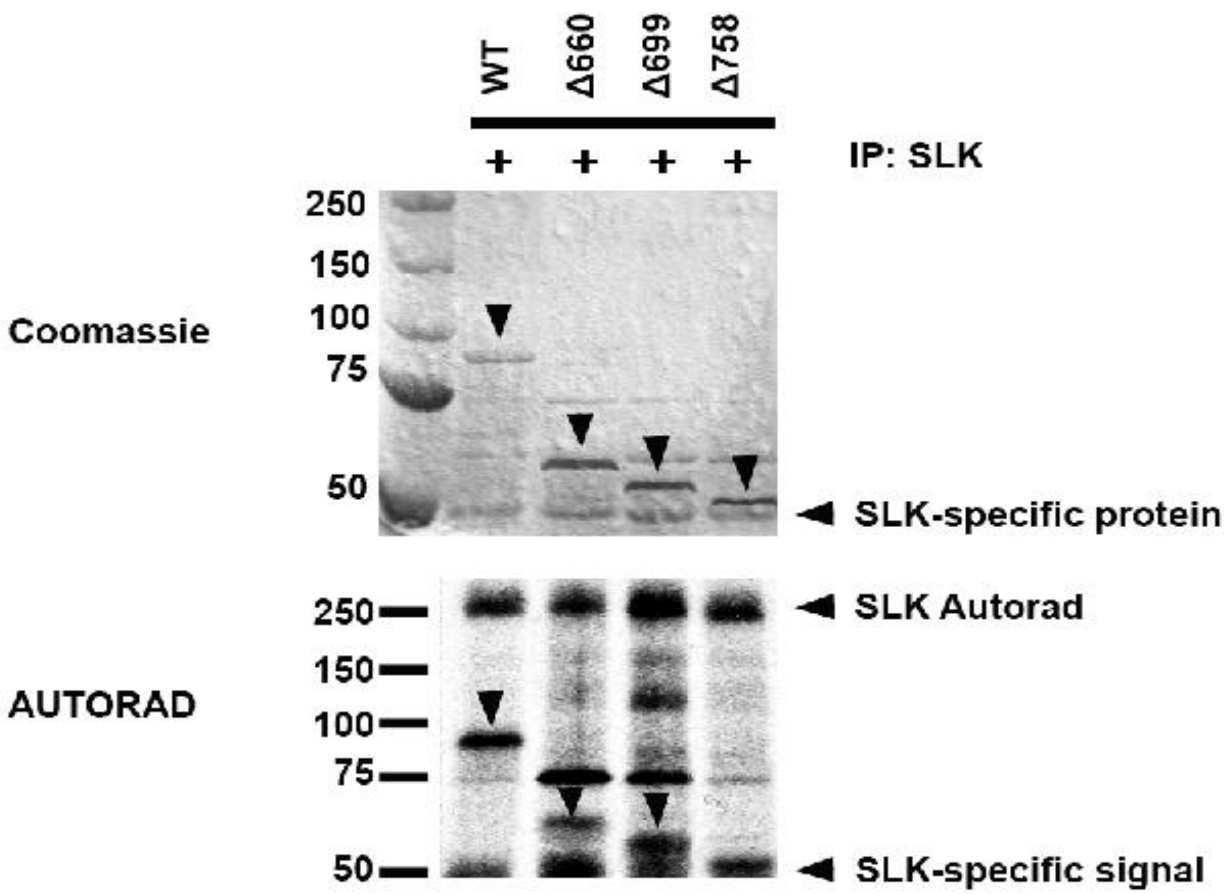
WT
Δ660
Δ699
Δ758
+ + + + IP: SLK
Coomassie
250
150
100
75
50
SLK-specific protein
AUTORAD
250
150
100
75
50
SLK Autorad
SLK-specific signal

(A; S250A). GST-fusion paxillin point mutants were then subjected to an *in vitro* kinase assay with endogenously-activated, SLK immunoprecipitated from MEF3T3. Interestingly, we observed that all three phospho-inactivating mutations resulted in a complete loss of paxillin phosphorylation **(Figure 3.7)**, suggesting that all three sites were important for SLK-mediated paxillin phosphorylation. However, the tryptic digest data **Figure 3.2 (C)** would suggest that a single major paxillin peptide fragment is phosphorylated *in vitro* by SLK. Since S243/44 lie in a different peptide fragment than S250, it is unlikely that SLK is capable of phosphorylating all three sites. One possibility is that the mutations may have altered the conformation of the protein, rendering the phosphorylation site inaccessible or unrecognizable to SLK.

To test this hypothesis, the GST-paxillin point mutants were cleaved off the GST-protein tag using thrombin protease prior to being resolved using native PAGE. Staining of the proteins with Coomassie revealed a change in protein conformation as evidence by the altered mobility of the point mutants in comparison to wildtype paxillin. Consequently, we believe that the loss of SLK-mediated paxillin phosphorylation observed with the mutants S243G, S244G and S250A may in fact, be the result of an atypical paxillin conformation and/or the alteration of the SLK recognition sequence within the paxillin protein.

To circumvent the potential conformational issues that may have arisen from introducing alanine or glycine substitutions, we made new point mutations using a residue that would generate proteins that were more electrophoretically similar to wildtype paxillin. To do this, we chose to mutate serines 243, 244 and 250 to threonine residues. Like serine, threonine

<u>Figure 3.7</u>: ***Mutation of serines 243, 244 and 250 to glycine (243 & 244) or alanine (250), results in a loss of in vitro paxillin phosphorylation by SLK***. Site-directed mutagenesis of S243/44 (AGC) to glycine (GGC) and S250 (TCC) to alanine (GCC) in full length, GST-fusion paxillin. **(A)** *In vitro* kinase assay using the above mutants and scratch-activated SLK immunoprecipitations. Recombinant mutated protein was incubated with SLK IPs for 30 minutes at 30°C in the presence of kinase buffer prior to being resolved on SDS-PAGE, and stained with Coomassie. Paxillin point mutant phosphorylation was assessed by exposing the dried, radioactive gel to X-ray film at -80°C for 2h (AUTORAD). **(B)** Purified, recombinant, thrombin-treated paxillin point mutants resolved on a native (SDS-free) gel using PAGE. The differential protein structure of point mutants versus wildtype paxillin was assessed by visualizing the protein using Coomassie.

A)

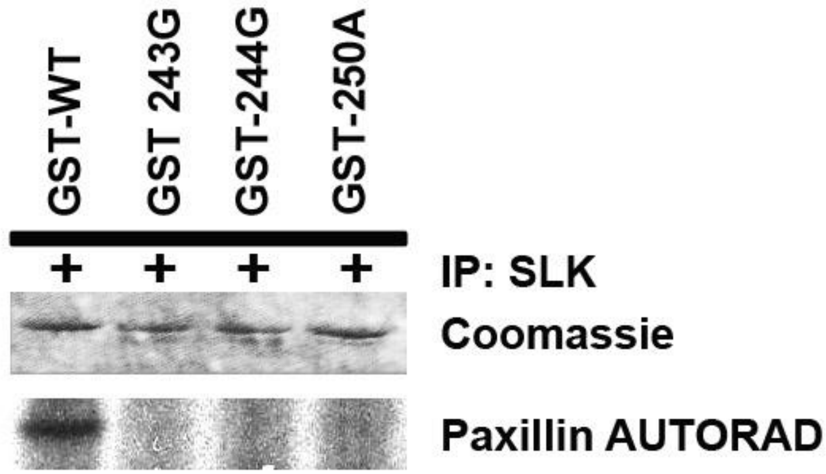
GST-WT
GST 243G
GST-244G
GST-250A
+ + + +
IP: SLK
Coomassie
Paxillin AUTORAD

B)

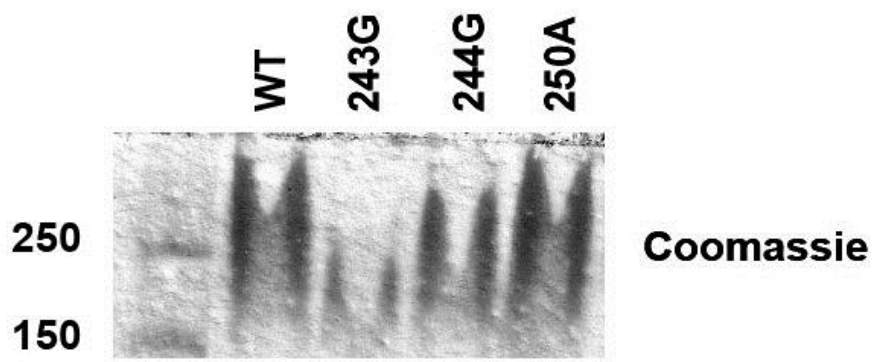
WT
243G
244G
250A
250
150
Coomassie

is classified as a polar, uncharged residue [135]. Although the secondary structure of threonine reveals an additional methylene group not present in the side chain of serine, we believe that a threonine may prove to be a better substitution for serine than alanine or glycine since it too contains an aliphatic hydroxyl group; these similarities suggest that its introduction into the paxillin protein sequence would not disrupt the overall conformation [135, 136]. Serines 243, 244 and 250 within full-length GST-paxillin were mutated to threonine residues using site-directed mutagenesis prior to being subjected to an *in vitro* kinase assay using endogenous SLK from MEF3T3. Despite there being less recombinant protein in the S243T, S244T and S243/44T lanes, these mutations fail to produce a reduction in the phosphorylation status of paxillin **(Figure 3.8(A))**. However, mutant S250T exhibits an almost complete reduction in its phosphorylation suggesting that SLK phosphorylates paxillin exclusively on S250 *in vitro* **(Figure 3.8(A); Appendix C)**.

Since SLK is a serine/threonine kinase it is by definition, capable of phosphorylating serine as well as threonine residues. Although serine/threonine kinases are documented as having a preference for phosphorylating serine over threonine residues, we cannot discount the possibility that SLK phosphorylates one or both of S243/S244 when mutated to a threonine residue [49]. Phospho-amino acid analysis of double mutant GST-paxillin (GST-243/44T) phosphorylated by SLK *in vitro* failed to show threonine phosphorylation, further supporting the observation that SLK phosphorylates paxillin *in vitro* on S250, exclusively **(Figure 3.8 (B))**.

Figure 3.8: ***Paxillin is phosphorylated by SLK on S250.*** Site-directed mutagenesis of S243/44 (AGC) and S250 (TCC) to threonine (ACC and GCC) in full length, GST-fusion paxillin. **(A)** *In vitro* kinase assay using the above mutants and scratch-activated SLK. Recombinant proteins were incubated with SLK IPs for 30 minutes at 30°C in the presence of kinase buffer prior to being resolved on SDS-PAGE, and stained with Coomassie. Paxillin point mutant phosphorylation was assessed by exposing the dried, radioactive gel to X-ray film at -80°C for 2 h (AUTORAD). **(B)** Phospho-amino acid analysis of *in vitro* SLK-phosphorylated, GST-paxillin (pGST-paxillin) and GST-paxillin double serine mutant S243/44T (pGST-243/44T). Phosphorylated paxillin protein was separated by phospho-serine, threonine and tyrosine residues in two dimensions. Exposure of the TLC plate to X-ray film for 3 days at -80°C was used to visualize the radioactive signal from phosphorylated residue(s).

A)

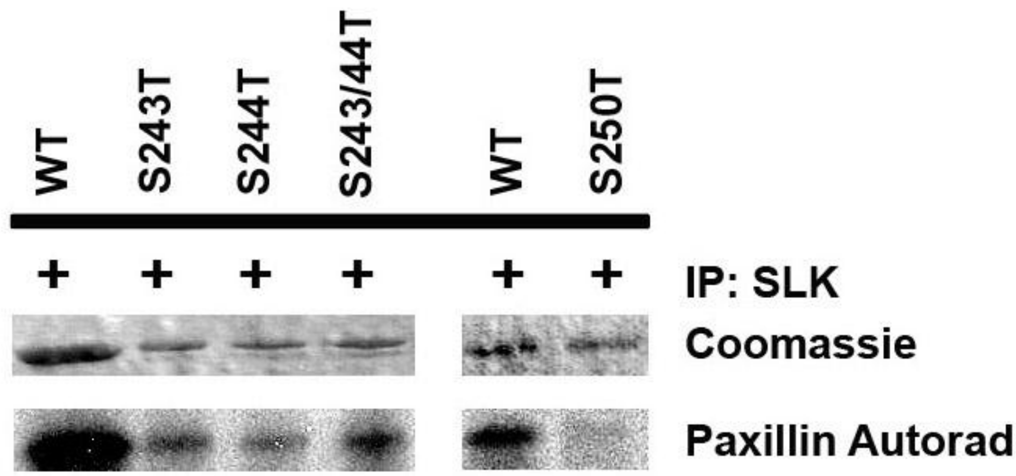
WT
S243T
S244T
S243/44T
WT
S250T
+ + + + + +
IP: SLK
Coomassie
Paxillin Autorad

B)

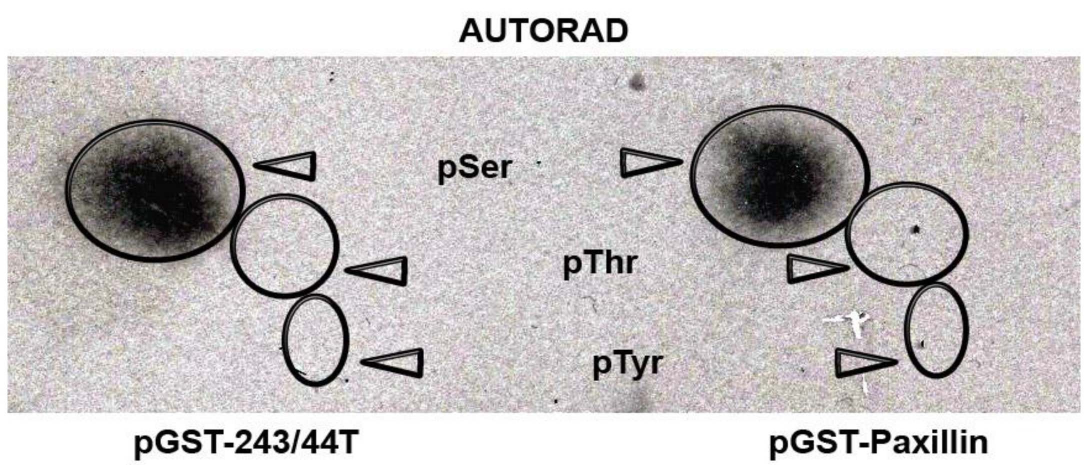
AUTORAD
pSer
pThr
pTyr
pGST-243/44T
pGST-Paxillin

<u>SLK associates with paxillin *in vivo*</u>

To determine whether SLK and paxillin associate *in vivo*, endogenous paxillin and SLK protein was co-immunoprecipitated from MEF3T3 with an anti-SLK antibody, subjected to SDS-PAGE, then immunoblotted with an anti-paxillin antibody. Since previous studies from our lab have shown SLK to be differentially activated in response to the stimulation of migration, lysates were derived from cells collected at different time points post wounding [69, 78]. As shown in **Figure 3.9**, paxillin is capable of co-immunoprecipitating with SLK, and does so preferentially at 90 minutes post-scratching. Association of the two proteins at the point where SLK kinase activity begins to decline may be indicative of a more favourable conformation induced by one or more modification(s), potentially involving a combination of phosphorylation and/or dephosphorylation of the kinase, substrate or both at this point. In fact, a study looking at the crystal structure and autophosphorylation requirements of SLK conducted by Pike *et al.* (2008), suggests that dimers of active kinases may add an additional level of stringency to the substrates that they interact with [77]. Specifically, these activated dimers are believed to function as a sort of specificity filter that discourages low affinity interactions to make way for the high affinity substrate binding that takes place during a phosphorylation event [77]. Consequently, a persistent interaction with paxillin may not be favourable until the kinase activity of SLK has begun to subside. Additionally, this may explain why **Figure 3.9** shows very low levels of paxillin co-immunoprecipitating with SLK at 30 and possibly 60 minutes post scratching: it is possible that we might have been able to capture the high affinity interaction between SLK and paxillin that occurs during phosphorylation. Since phosphorylation is a short-lived event in which the kinase and substrate interact only for the catalytic transfer of a

<u>Figure 3.9</u>: *SLK associates with paxillin in vivo*. SLK IP from MEF3T3 throughout a scratch-wound time course. SLK IPs were either subjected to an *in vitro* kinase assay to evaluate SLK kinase activity or were immunoblotted (IB) for paxillin protein to evaluate an SLK-paxillin association. SLK IB was used to ensure equal amounts of endogenous SLK protein was immunoprecipitated from cells at each of the above time points.

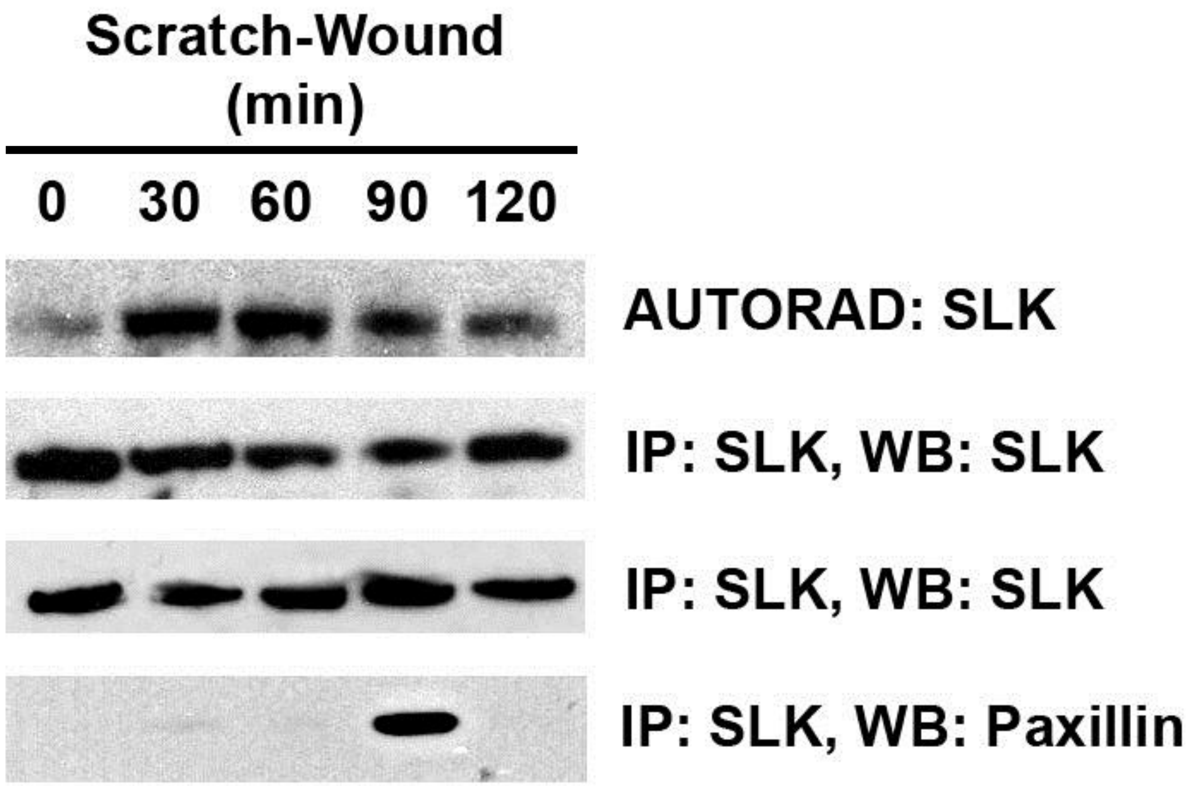
Scratch-Wound
(min)
0
30
60
90
120
AUTORAD: SLK
IP: SLK, WB: SLK
IP: SLK, WB: SLK
IP: SLK, WB: Paxillin

phosphoryl group, it is unlikely that in a heterogeneous population of cells that we would be able to visualize this interaction by Western blot. However, in order to confirm this hypothesis, we must first determine (1) whether SLK is capable of phosphorylating paxillin *in vivo* and if so, (2) at what point during the onset of migration does this phosphorylation at S250 occur.

SLK phosphorylates paxillin *in vivo* on S250

Although we have shown that SLK phosphorylates paxillin *in vitro*, *in vivo* phosphorylation has yet to be described. To determine whether SLK is capable of phosphorylating paxillin *in vivo*, a paxillinS250-specific phospho-antibody was generated against a murine paxillin phosphopeptide corresponding to amino acids 244-255 (CSPQRVTS*SQQQT), where S* is phosphorylated S250). Verification of this antibody has shown it to identify phosphorylated paxillin both *in vitro* and *in vivo* **(Appendix E)**. Cross-reactivity with phosphorylated human paxillin has also been observed **(Figure 5.2)**. Interestingly, *in vivo* knockdown of SLK using shRNA in contact inhibited cells showed a reduction in the amount of paxillin S250 phosphorylation **(Figure 3.10 (A))**. Moreover, upon scratch wounding, there was a dramatic decrease in S250 phosphorylation at 60 minutes in cells treated with the SLK-directed shRNA compared to control treated cells **(Figure 3.10 (A))**. Although the persistence of a basal level of paxillin S250 phosphorylation remains despite SLK knockdown, we contend that the amounts of SLK remaining post sh-infection may be sufficient to elicit this phenomenon. However, we cannot discount the possibility that the incidence of this, albeit reduced level of paxillin S250 phosphorylation, could be attributed to another kinase capable of phosphorylating paxillin on this residue.

<u>**Figure 3.10**</u>**:** ***Paxillin S250 is phosphorylated by additional kinases in MEF3T3***. **(A)** shRNA targeted to the murine SLK sequence was used to infect MEF3T3 with cell lysates being collected when maximum SLK knockdown was achieved (48h post infection). SDS-PAGE and immunoblotting with anti-phospho-S250, anti-paxillin and anti-SLK were used to evaluate levels of paxillin S250 phosphorylation under SLK knockdown conditions. **(B)** Paxillin S250 is differentially phosphorylated post wounding. MEF3T3 cells were scratch-wounded and lysates were collected at the indicated time points. Immunoblotting with total paxillin and phospho-S250 antibodies was used to correlate paxillin phospho-S250 status and migration dynamics.

A)

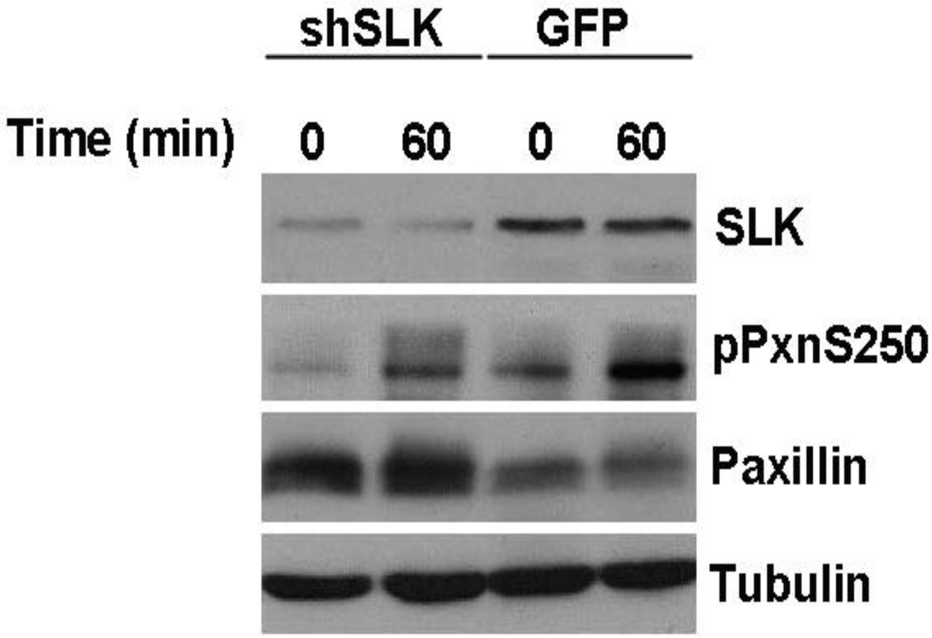
shSLK
GFP
Time (min)
0
60
0
60
SLK
pPxnS250
Paxillin
Tubulin

B)

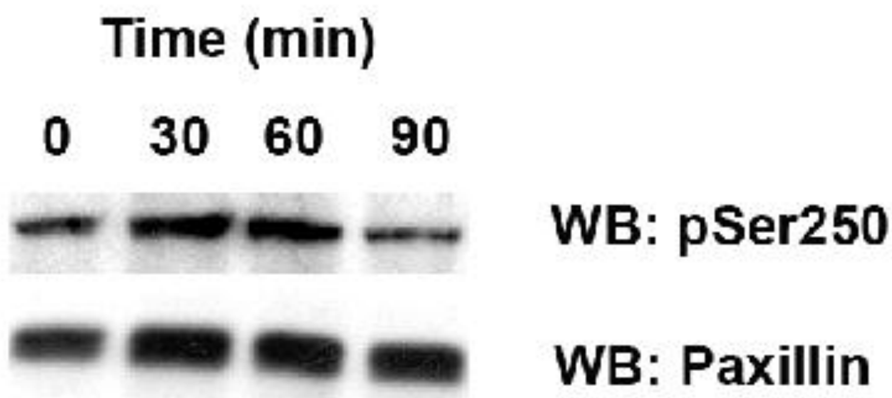
Time (min)
0
30
60
90
WB: pSer250
WB: Paxillin

We next investigated whether paxillin was differentially phosphorylated on S250 upon scratch wounding. Confluent monolayers of MEF3T3 were scratched and left to incubate for 0, 30, 60 and 90 minutes at 37°C, at which time they were collected and subjected to SDS-PAGE. Interestingly, blotting with anti-phospho-S250 revealed that like SLK activity, paxillin S250 levels are increased during migration, with the highest levels of phosphorylation being observed at 30-60 minutes post-wounding **(Figure 3.10 (B))**.

SLK binds paxillin directly *in vitro*

Although **Figure 3.9 (A)** demonstrates that SLK and paxillin are capable of forming a complex *in vivo*, it is unclear whether or not SLK and paxillin are capable of interacting directly. It is not uncommon to find serine/threonine kinases using modular binding partners to target the kinase to specific substrates [49]. Additionally, these modular proteins have been shown to mediate the interaction between kinase and substrate by functioning as a molecular scaffold that recruits both proteins into the same complex, often times increasing the efficiency of phosphorylation [49]. To determine whether SLK interacts with paxillin directly, both full length SLK (HA-SLK) and a constitutively active C-terminal deletion of SLK known as YΔC (amino acids 1-373; HA-YΔC) were *in vitro* translated in the presence of [^{35}S]-methionine and incubated with GST fusion paxillin protein and a GST vector control. SLK and/or YΔC bound to GST-paxillin was detected by autoradiography; the presence of equal amounts of GST protein was assessed by SDS-PAGE and Coomassie staining. As shown by the autoradiography in **Figure 3.11**, the SLK deletion, YΔC appears to bind with a higher affinity to paxillin than the full length kinase. However, the relative over-exposure of the YΔC *in vitro* translation reaction suggests that this

<u>Figure 3.11</u>: *SLK binds directly to paxillin in vitro.* Binding of *in vitro* translated full length SLK and the constitutively active, truncated SLK mutant, YΔC to GST-paxillin. GST-paxillin fusions were incubated with [^{35}S]-labeled SLK and YΔC, washed and resolved by SDS-PAGE. Bound SLK and YΔC were detected by autoradiography (AUTORAD); visualization of GST proteins was achieved through Coomassie staining.

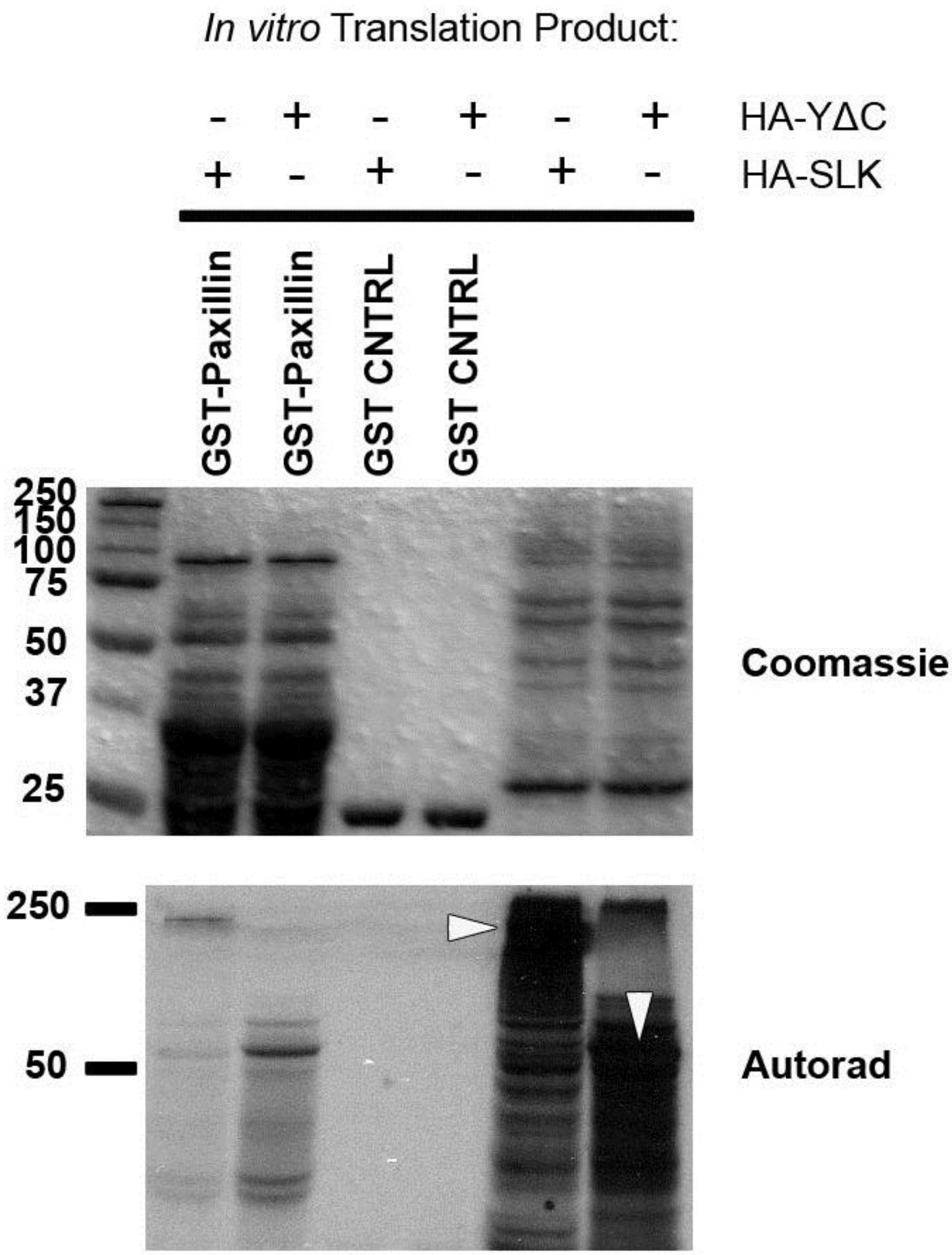
In vitro Translation Product:
- + - + - + HA-YΔC
+ - + - + - HA-SLK
GST-Paxillin
GST-Paxillin
GST CNTRL
GST CNTRL
250
150
100
75
50
37
25
Coomassie
250
50
Autorad

interaction is low affinity; this is even more evident for the interaction between paxillin and the full length kinase. Due to the low affinity binding observed *in vitro*, it appears unlikely that a direct relationship exists between SLK and paxillin *in vivo*. However, weak interactions have been documented as being commonplace in enzyme-substrate interactions [137].

SLK-paxillin interaction may be mediated by the LIM-domain binding proteins, LDB1 and LDB2

We have previously shown SLK kinase activity to be modulated by the presence of the LIM domain binding proteins, LDB1 and LDB2 [76]. Specifically, we have shown LDB1 and LDB2 to bind directly to the carboxy-terminal ATH domain of SLK both *in vitro* and *in vivo*, and to co-localize with SLK in migrating cells [76]. Knock-down and overexpression of either LDB1 or LDB2 has been shown to increase cell motility, suggesting that a fixed stoichiometry of these factors is required for mediating SLK-regulated migration [76]. LDB1 and LDB2 are transcriptional co-regulatory proteins that were identified through their ability to interact with other LIM-domain containing proteins, namely LIM homeodomain transcription factors [138]. However, being a Group II LIM-protein, LDB1 and 2 are also recognized as having a cytoplasmic influence, being capable of forming protein-protein interactions with other LIM-domain, containing proteins outside of the nucleus [95]. Since SLK has been shown to bind LDB1/2 and paxillin to bind SLK, we investigated whether the LDBs may be capable of binding paxillin, a LIM-domain containing protein in its own right [66, 76, 95]. To test this, LDB1 and LDB2 were *in vitro* translated and labeled with [^{35}S]-methionine, incubated with GST-paxillin and washed, prior to being resolved by SDS-PAGE. As is seen in **Figure 3.12**, GST-paxillin does bind to both LDB1 and LDB2 *in vitro*.

Interestingly, this may suggest that the LDBs are required to complex with the kinase and substrate to facilitate phosphorylation.

<u>Figure 3.12</u>: *Paxillin binds directly to the LIM domain binding proteins, LDB1 and LDB2 in vitro.* Binding of *in vitro* translated LDB1 and LDB2 to GST-paxillin. GST-paxillin fusions were incubated with [^{35}S]-labeled LDB1 and LDB2, washed and resolved by SDS-PAGE. Bound LDB1 and LDB2 were detected by autoradiography; visualization of GST proteins was achieved through Coomassie staining.

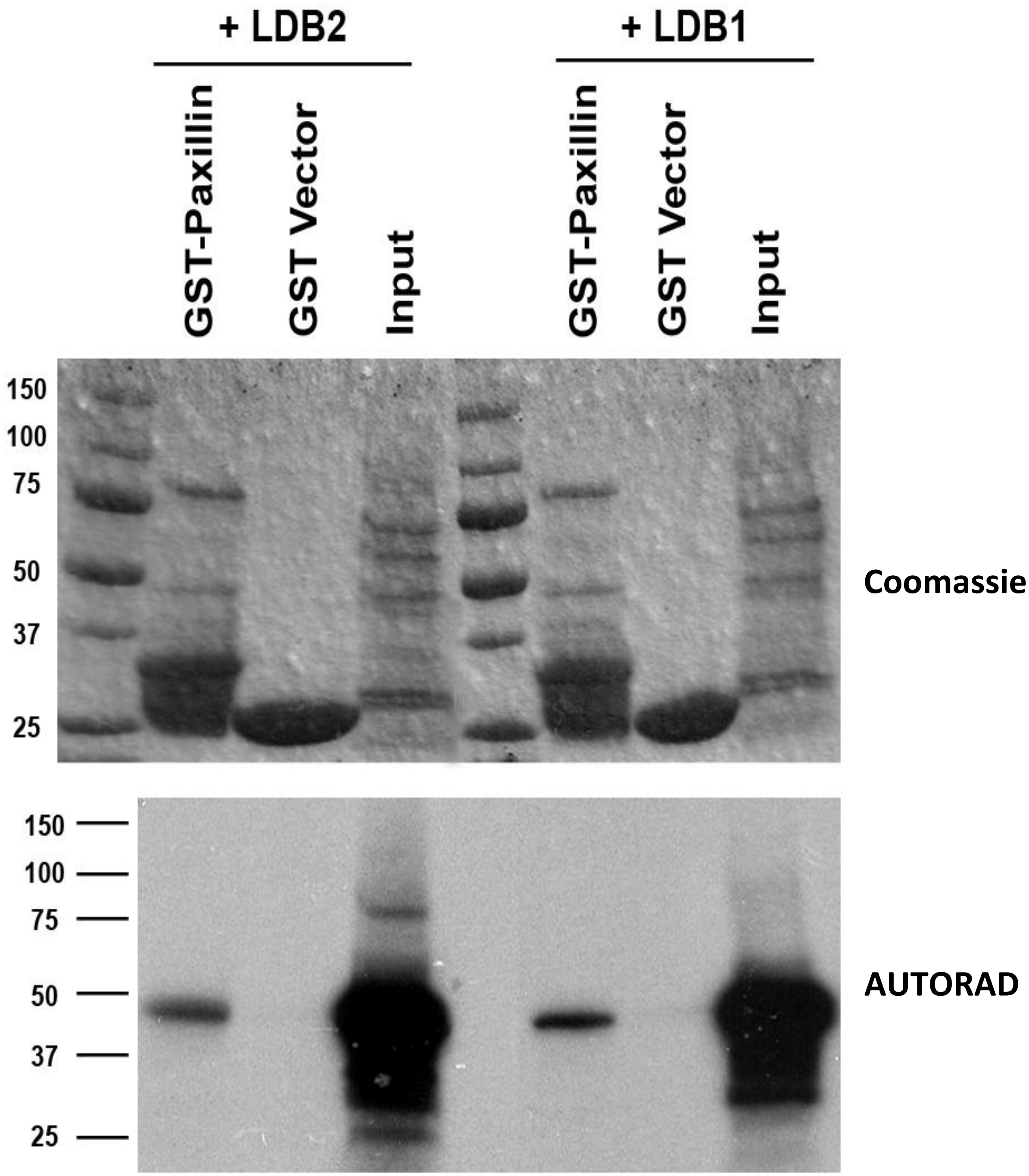

+ LDB2
+ LDB1
GST-Paxillin
GST Vector
Input
GST-Paxillin
GST Vector
Input
150
100
75
50
37
25
Coomassie
150
100
75
50
37
25
AUTORAD

Chapter 4:

Paxillin S250 is required for focal adhesion turnover and efficient cell migration

<u>Paxillin S250 is required for focal adhesion turnover and efficient cell migration</u>:

A role for paxillin in regulating adhesion dynamics has been previously described [110, 139]. Briefly, fibroblasts deficient in paxillin exhibit defects in the cortical cytoskeleton, cell spreading and migration; cell adhesion however, is not affected [96, 107, 123]. Additionally, paxillin-null fibroblasts have been shown to display abnormal focal adhesion architecture and inefficient localization and activation of FAK [107, 123]. The involvement of paxillin in cell spreading and migration is believed to be a direct consequence of its association with, and regulation of, focal adhesions and their dynamics [139]. Differential paxillin phosphorylation within the focal adhesion has been shown to mediate focal adhesion assembly and disassembly [139, 140]. Specifically, serine phosphorylation of the LIM domain of paxillin has been found to temporally target and/or regulate the integration of paxillin into focal adhesions while tyrosine phosphorylated paxillin has been shown to recruit the focal adhesion proteins FAK and Src into the adhesion complex [99, 110, 111]. Actively disassembling adhesions, such as early adhesions and the distal part of late adhesions, are preferential zones of microtubule targeting and catastrophe that have been shown to be enriched in phosphorylated paxillin [22, 30, 110, 140]. Conversely, larger, more mature adhesions such as fibrillar adhesions, exhibit relatively reduced levels of paxillin phosphorylation [22, 30].

Paxillin S250 is not required for adhesion formation

As paxillin-null MEF overexpress the paxillin homologue Hic-5 **(Appendix D)**, which compensates to an extent for the absence of paxillin, we have chosen to overexpress both mutant and wildtype paxillin in fibroblasts that express endogenous levels of paxillin. Although the initial characterization of paxillin-null embryonic stem cells by Wade *et al.* (2002) suggests that paxillin is not required for the formation of adhesions, previous studies conducted by Brown *et al*. (1998) had shown paxillin serine/threonine phosphorylation to be required for adhesion formation in CHO-K1 cells to fibronectin-coated plates [99, 107]. To test whether S250 is required for cell adhesion, GFP-fusion S250T and wildtype paxillin were transiently transfected into MEF cells, plated onto uncoated surfaces and removed for analysis using GFP-sorting and cell count. Normalization of cell counts to the GFP-expressing population of cells revealed no statistically significant difference in the rate of adhesion between cells over-expressing the S250T mutation versus wildtype paxillin **(Figure 4.1)**.

Paxillin S250 is required for cell spreading

Characterization of paxillin-null fibroblasts has shown that the formation of adhesions is possible in the absence of paxillin [96]. However, analysis of the composition of the cytoskeleton in response to fibronectin receptor engagement revealed that paxillin-null cells exhibit a reduction in cortical cortactin levels and consequently, an altered frequency and rate of lamellipodia formation [96]. Accordingly, paxillin deficient cells have been observed to spread and migrate at a reduced rate when compared to wildtype cells [96].

To determine whether S250 is required for cell spreading, MEF cells were transiently transfected with, and sorted for GFP-paxillin, S250T and GFP control vector prior to being plated on fibronectin-coated plates. Phase contrast and fluorescence microscopy was used at 30 minute intervals to capture the extent of spreading of the fibroblasts. Area measurements of

Figure 4.1: ***Paxillin S250 is not required for adhesion of MEF3T3 cells to plastic.*** MEF3T3 were transiently transfected with GFP-fusion proteins, S250T and wildtype paxillin, as well as the GFP vector alone as a positive control. Transfected cells were removed using 1X citric saline and resuspended in DMEM containing 10% BSA for 30 minutes prior to plating in triplicate onto 30 mm plastic dishes. Cells were allowed to adhere for 5, 10 or 20 minutes before the cell suspension was removed and adherent cells were washed once in 1X PBS, collected and counted. Subsequent GFP-sorting via flow cytometry was used to normalize cell counts in terms of adherent, GFP-positive cells. Percent adhesion was determined from normalized cells by dividing GFP adherent counts by the total number of cells plated. The mean and standard error of the mean were calculated from the averaged normalized counts of four independent experiments; subsequent statistical analyses were conducted using the Student's t test ($p < 0.05$).

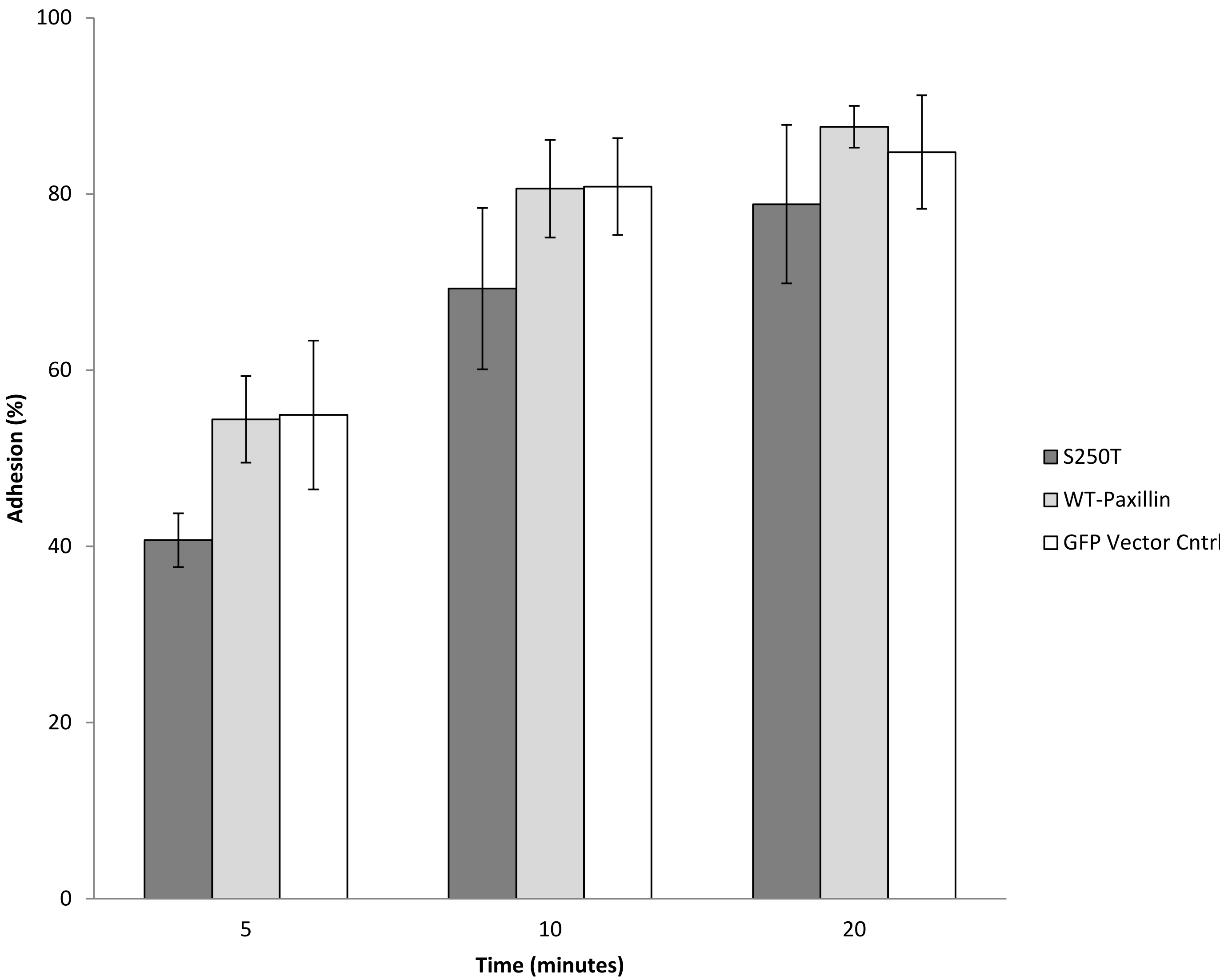
100
80
60
40
20
0
Adhesion (%)
5
10
20
Time (minutes)
S250T
WT-Paxillin
GFP Vector Cntrl

more than 200 cells per time point revealed that a serine to threonine mutation at position 250 in paxillin results in a delay in cell spreading when compared to both wildtype paxillin and the GFP control (**Figure 4.2 (A)**). Phase contrast images of cells at 90 minutes post-plating **(Figure 4.2 (B))**, further illustrate this delay with a higher proportion of unspread cells (bright cells) being found in the cultures overexpressing the S250T mutation.

Paxillin S250 is required for efficient cell migration

More often than not, a deficiency in cell spreading translates into a reduced rate of cell migration. Therefore, we tested whether this spreading defect extended insofar as to impair motility. To investigate the migratory capacity of the paxillin S250T mutant, MEF cells stably expressing Myc-S250T, Myc-paxillin or vector control were subjected to haptotaxis assays in fibronectin-coated Boyden chambers **(Figure 4.3(A))**. Cells were plated onto the upper side of the transwell membrane and allowed to migrate for 6 hours, fixed and stained using DAPI. Positive migration was scored if the nucleus was visible on the underside of the transwell membrane (fibronectin-coated side). As seen in **Figure 4.3 (B)**, almost twice as many cells migrated in the wildtype paxillin cell line when compared to the mutant S250T. Consistent with the cell spreading data **(Figure 4.2)** and Boyden chamber assays **(Figure 4.3 (B))**, **Figure 4.4** shows that the paxillin S250 mutant exhibits a ≈ 30% reduction in migratory rate in a wound-closure assay. Taken together, these results demonstrate that paxillin S250 is required for efficient cell spreading and migration.

Figure 4.2: ***Paxillin S250 is required for cell spreading of MEF on fibronectin.*** MEF were transiently transfected with GFP-fusion proteins, S250T and wildtype paxillin, as well as the GFP vector alone as a positive control. GFP-sorted cells were plated on fibronectin-coated 30 mm plates and visualized by both phase contrast and fluorescence microscopy. **(A)** At least 6 independent fields of view in which more than 200 cells were analyzed using ImageJ software for each time point and are represented as a mean of pixel units^2. Standard error was calculated from the means of each cell type at each time point; a Student's t test was conducted relative to the S250T mutant to evaluate the data (*, $p < 0.05$; **, $p <0.01$; ***, $p < 0.005$). **(B)** Representative phase contrast and corresponding fluorescent (488 nm) field of view photography at 90 minutes post plating. Please note that weakly fluorescing cells are considered to be spread, whereas bright cells are not.

A)

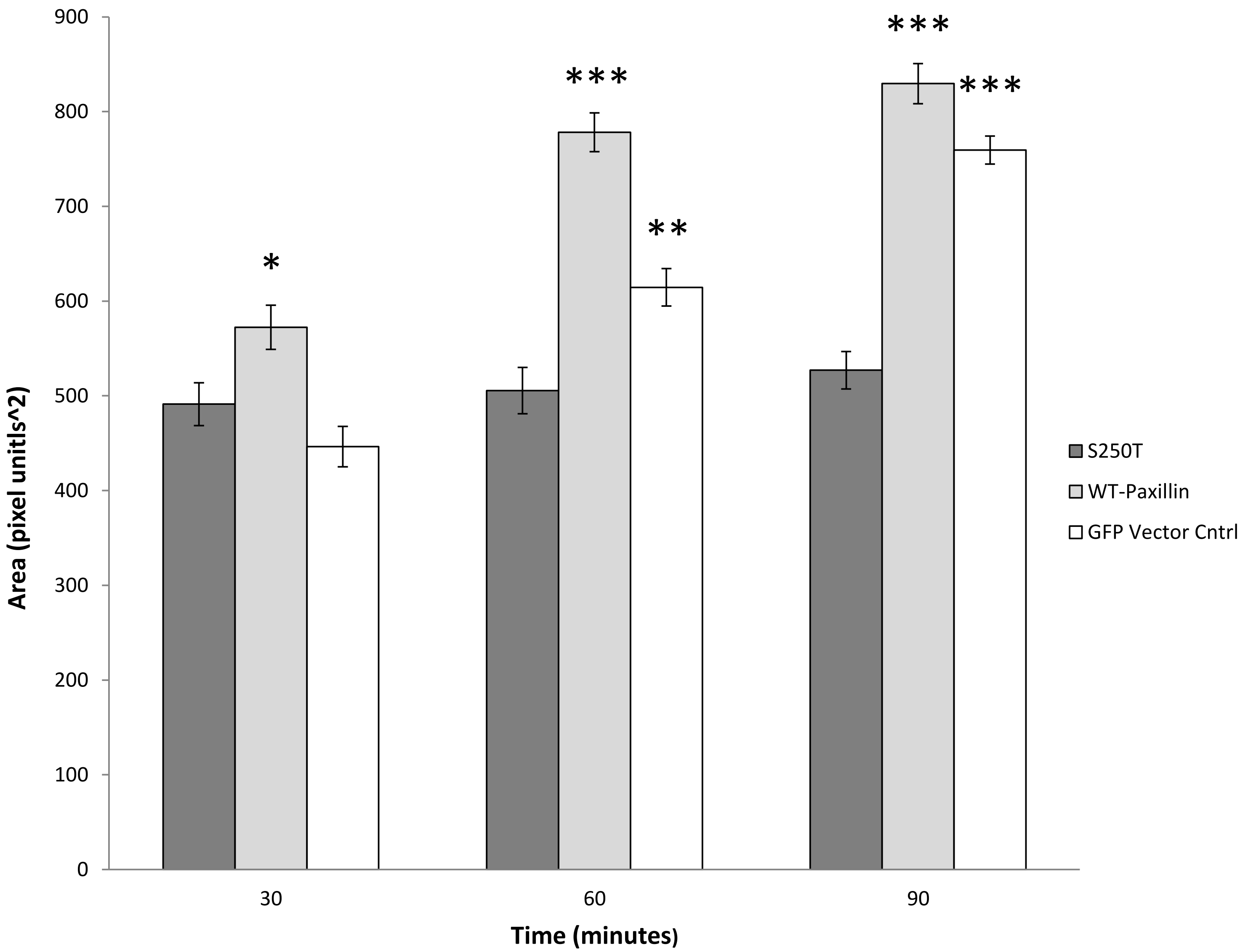

900
800
700
600
500
400
300
200
100
0
Area (pixel unitls^2)
*
***
**
***
***
30
60
90
Time (minutes)
S250T
WT-Paxillin
GFP Vector Cntrl

B)

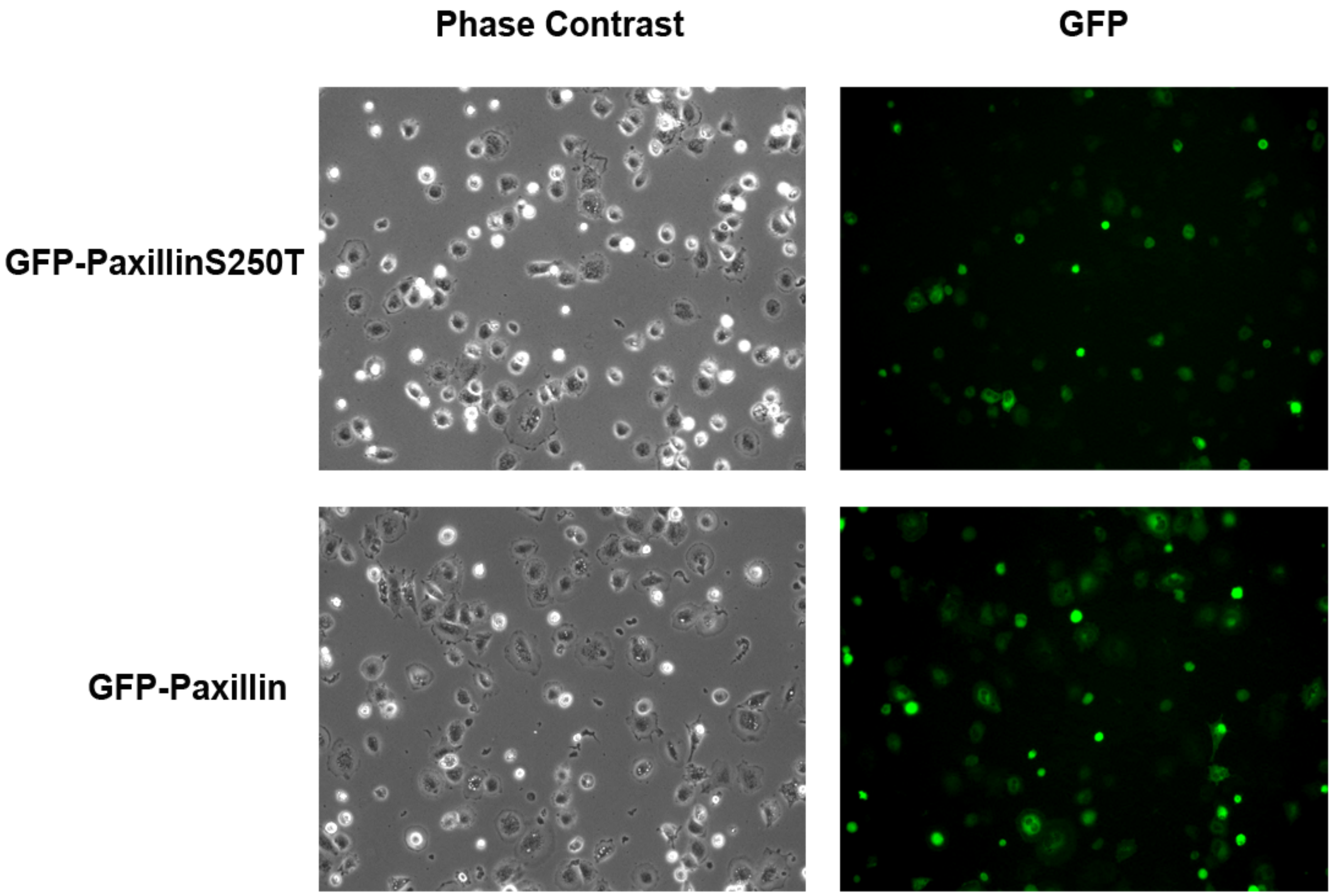

<u>Figure 4.3</u>: *Paxillin S250 is required for fibronectin haptotaxis in a Boyden chamber assay.* (A) Spontaneously immortalized mouse embryonic fibroblasts derived from FVB mice were induced to stably express Myc-PaxillinS250T, Myc-Paxillin and Myc vector control (Cntrl) via hygromycin B selection. **(B)** Stably transfected Myc-PaxillinS250T and Myc-Paxillin MEF were plated onto the upper side of a transwell membrane that had been pre-coated on the underside with 10 μg/ml fibronectin. Cells were allowed to migrate for 6 hours prior to the underside of the membrane being fixed in 4% PFA and stained with DAPI. Subsequent use of fluorescence (350 nm) microscopy allowed for nuclei to be counted using ImageJ software. Means and standard errors of the means of more than 3 independent experiments (3 filters per experiment) were calculated from 5 independent fields of view. Statistical analyses were then conducted using a Student's t test and are displayed relative to the paxillin S250T mutant (*, $p < 0.05$; **, $p < 0.01$; ***, $p < 0.005$).

A)

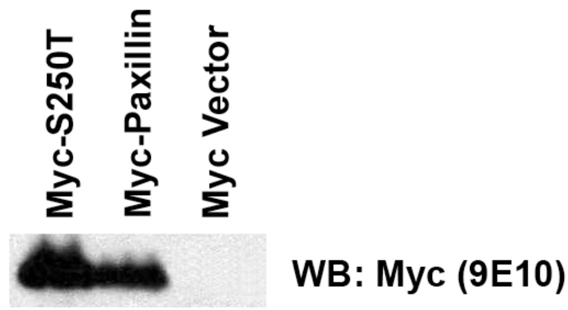
Myc-S250T
Myc-Paxillin
Myc Vector
WB: Myc (9E10)

B)

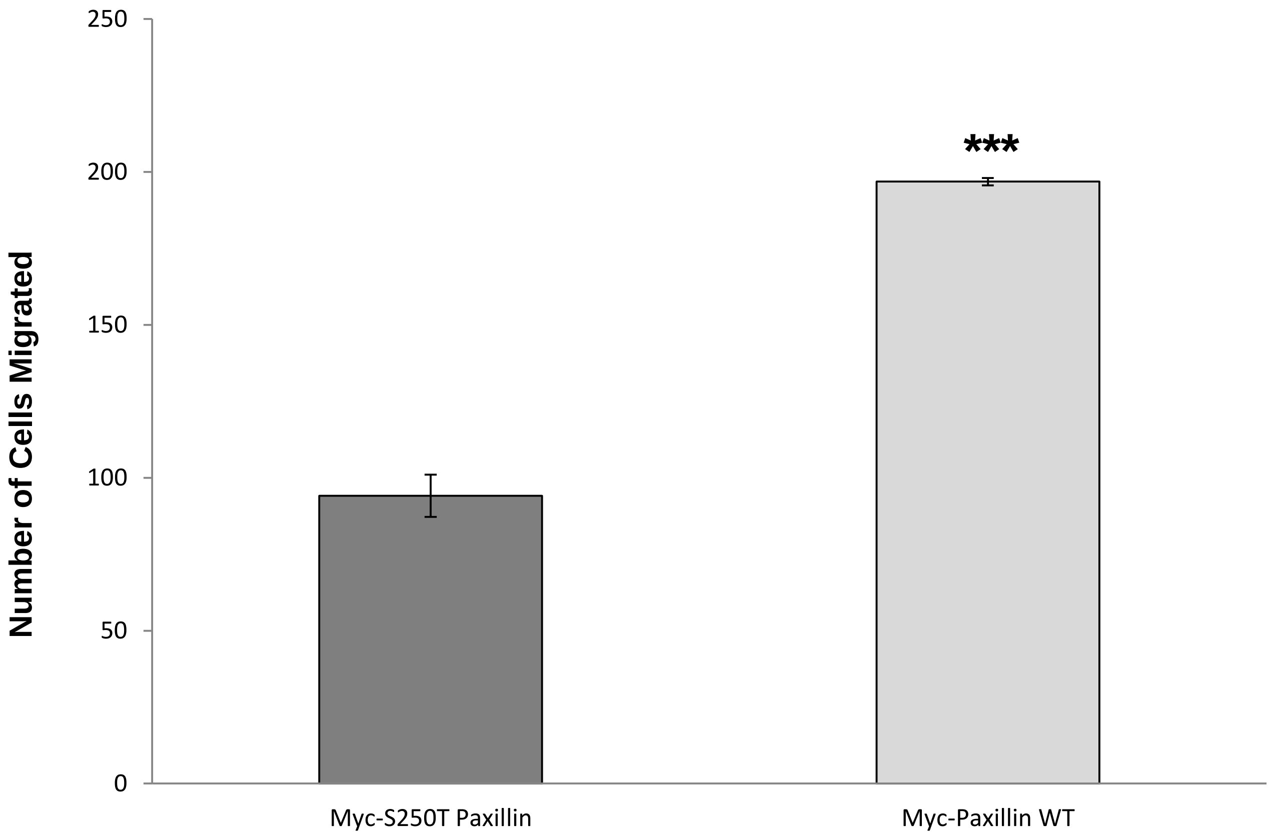
250
200
150
100
50
0
Number of Cells Migrated
***
Myc-S250T Paxillin
Myc-Paxillin WT

<u>Figure 4.4</u>: *Paxillin S250 is required for wound closure in MEF on fibronectin.* Stably transfected Myc-PaxillinS250T and Myc-Paxillin MEF were plated on fibronectin-coated 24-well plates and grown to confluency. Induction of wound closure was induceded by scratching the monolayer with a p200 micropipette tip; this is considered to be T = 0. Phase contrast photography was taken of the artificial wounds at T = 0 and at T = 10 hours. For each wound, three reference points were designated for photographs, from which three measurements of wound size were taken using ImageJ software. This was repeated for at least 8 different wells, with two wounds in each well. The mean and standard error of the mean of each well was calculated by averaging the measurements of both wounds in a given well. Statistical analyses were conducted relative to the S250T mutant using a Student's t test (*, $p < 0.05$; **, $p < 0.01$; ***, $p < 0.005$).

A)

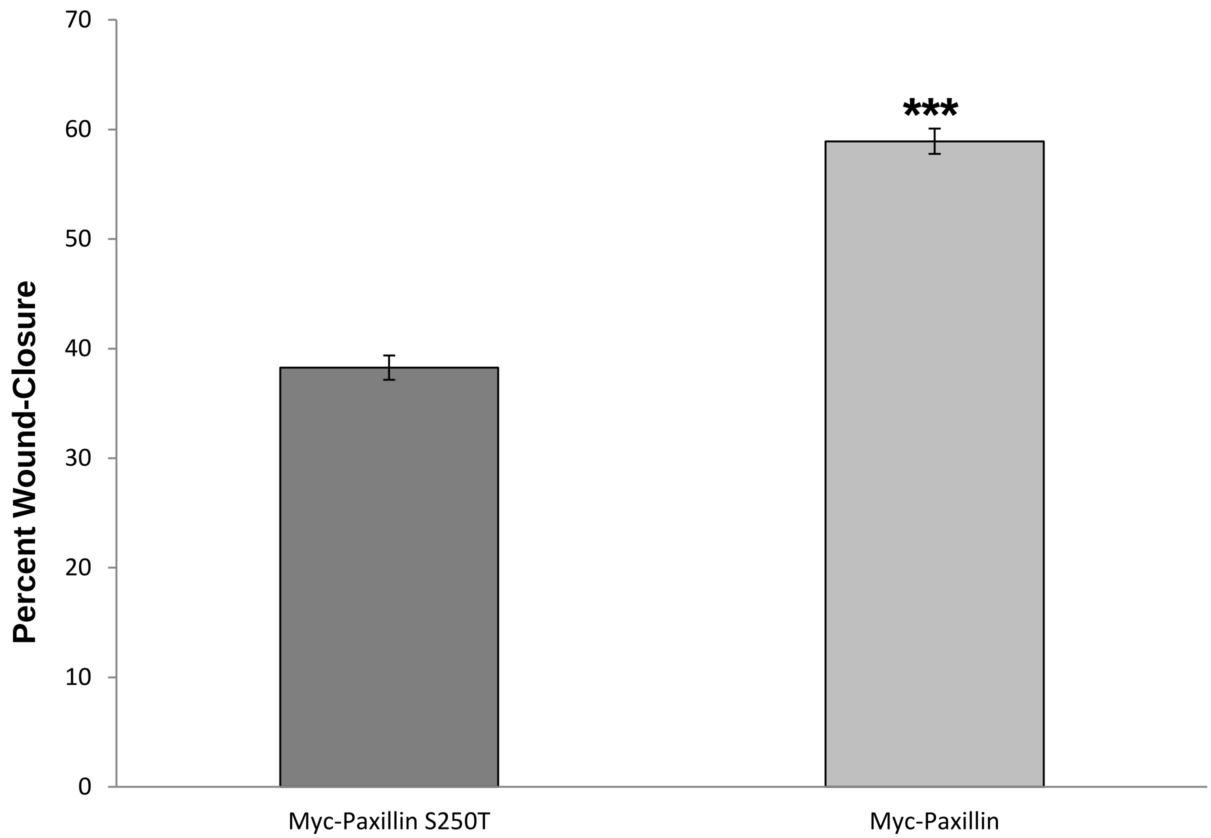
70
60
50
40
30
20
10
0
Percent Wound-Closure
***
Myc-Paxillin S250T
Myc-Paxillin

B)

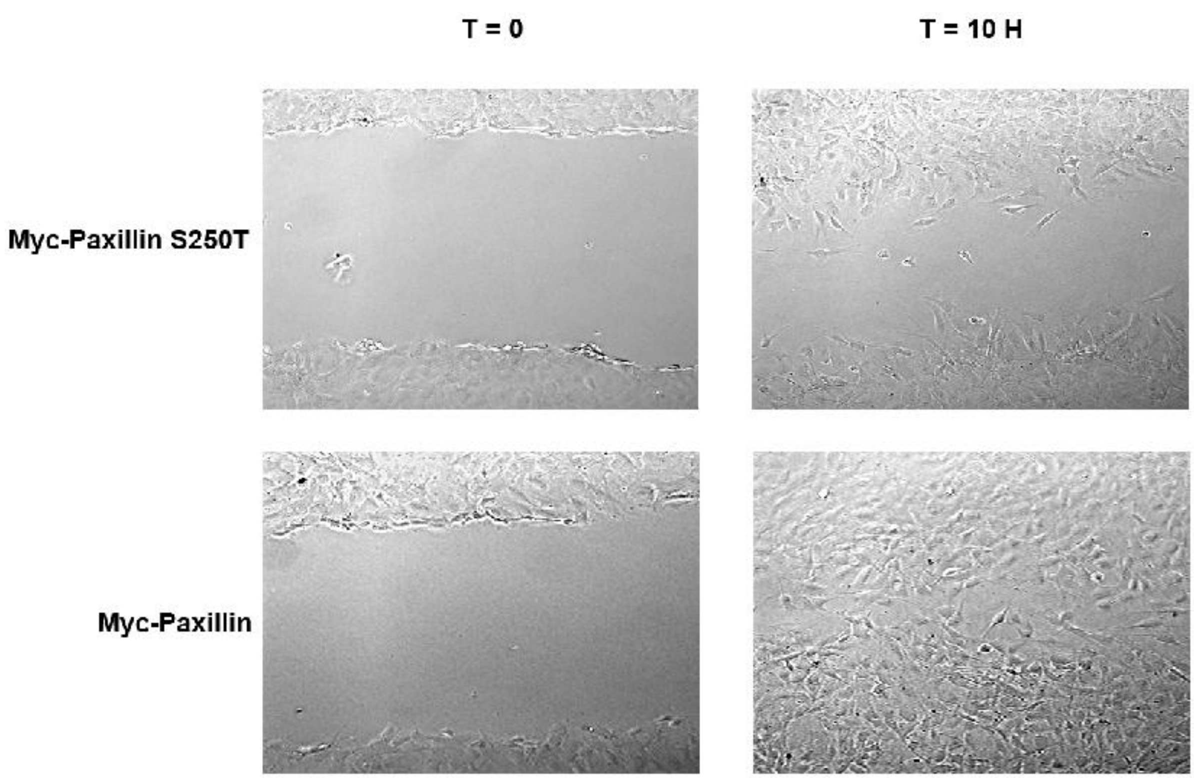
T = 0
T = 10 H
Myc-Paxillin S250T
Myc-Paxillin

Paxillin S250 is required for focal adhesion turnover

Studies in paxillin-null cells overexpressing paxillin lacking the LD4 motif have been shown to reduce focal adhesion disassembly 11-fold when compared to full length, wildtype paxillin [66, 123, 141]. Subsequent studies have revealed that a phospho-inactivating substitution of an alanine at S274 (human; S273 in chicken), which is contained within the LD4 motif, resulted in a similar, albeit less dramatic phenotype, with adhesions persisting for 25% longer than wildtype paxillin in CHO-K1 cells [120].

Since adhesion dynamics play a critical role in the regulation of cell migration, we tested whether paxillin S250 phosphorylation was required for focal adhesion turnover. To investigate this, MEF3T3 were transiently transfected with GFP-paxillin constructs, S250T and wildtype paxillin prior to plating onto a fibronectin-coated dish and live-cell imaging. At least 20 adhesions were examined by fluorescence microscopy for 10 minutes for both wildtype and mutant paxillin [53]. Determination of the adhesion dissociation constant revealed a 5-fold decrease in the rate of adhesion turnover in cells expressing mutant paxillin when compared to wildtype **(Figure 4.5 (A))**. Specifically, adhesions were found to persist over a 9 minute period in the GFP-PaxillinS250T mutant whereas cells expressing wildtype GFP-paxillin exhibit signs of dissociation in as little as 6 minutes **(Figure 4.5 (B))**.

Focal adhesion turnover has been correlated with decreased phospho-FAKY397 immunoreactivity [51, 53]. Conversely, cells enriched with stable adhesions show elevated levels of this FAK phosphoisoform [51, 53]. Therefore, to validate the data seen in **Figure 4.5 (A)** & **(B)**, 293 cells were transiently transfected with Myc-PaxillinS50T, Myc-Paxillin and Myc vector control and subjected to Western blotting for phospho-FAKY397. Our results show that cells expressing Myc-PaxillinS250T display elevated levels of phospho-FAKY397 **(Figure 4.5 (C))**, which is consistent with a reduced rate of turnover. Conversely, cells expressing Myc-Paxillin wildtype, show a comparatively higher amount of FAKY925 phosphorylation to that of the Myc-PaxillinS250T population. Interestingly, previous reports have indicated that an increase in FAKY925 phosphorylation is indicative of an increased rate of turnover [66, 67]. This further supports the live imaging data that cells expressing wildtype paxillin are undergoing a higher rate of turnover than the mutant-expressing cells.

The increased incidence of FAKY925 phosphorylation noted in the wildtype-expressing cells in **Figure 4(C)** and absent in the mutant, suggested that FAKY925 phosphorylation follows phosphorylation of paxillin at S250. To test this hypothesis, MEF3T3 cells were treated with the microtubule-destabilizing agent nocodazole (10 µM) for 3 hours prior to nocodazole washout and collection at the indicated time points. Interestingly, we observed the onset of paxillin S250 phosphorylation at 15 minutes that proceeded through to 45 minutes, whereas FAKY925 phosphorylation was noted at earliest, 30 minutes post wash-out, suggesting that S250 phosphorylation does precede that of FAK at Y925 **(Figure 4(D))**. Additionally, it would appear as though in terms of total paxillin, that higher species of paxillin emerge at 30-45 minutes post nocodazole wash-out. Interestingly, this occurrence had been noted previously in the lab under over-expression conditions (unpublished), and had been determined to represent a ubiquitylated form of the protein; this finding will be expanded on in Chapter 5.

<u>**Figure 4.5**</u>**: *Paxillin S250 regulates focal adhesion disassembly.* (A)** MEF3T3 were transiently transfected with GFP-fusion proteins, S250T and wildtype paxillin prior to being plated onto fibronectin-coated plates. Cells were maintained at 37°C and 5% CO_2 while undergoing phase contrast and fluorescent (488 nm) live-cell imaging microscopy (40X). At least 10 cells from each transfection were photographed at one minute intervals for no less than 10 minutes. The focal adhesion disassociation constant (K*diss*) was calculated as described by Storbeck et al. (2009) [76]. Briefly, the ratio of the area of the focal adhesion as observed from the GFP fluorescence at T=0 and T=X was determined. Plotting of the natural log of this quotient ($\ln[I_0/I_t]$) over time and subsequent calculation of the slope was used to obtain the value for K*diss*(min^{-1}). Means of the K*diss* and standard errors of the means of at least 20 adhesions were calculated from 10 cells. Statistical analyses were then conducted using a Student's t test and are displayed relative to the paxillin S250T mutant (*, $p < 0.05$; **, $p < 0.01$; ***, $p < 0.005$). **(B)** Immunofluorescent microscopy (40X) of transiently transfected GFP-PaxillinS250T and GFP-Paxillin in ME3T3 at intervals of 3 minutes. Arrows point to stable adhesions (GFP-PaxillinS250T) and adhesions that are actively turning over (GFP-Paxillin) **(C)** Western blot of 293 cells transiently overexpressing Myc-fusion proteins, Myc-PaxillinS250T, Myc-Paxillin and Myc vector control (Cntrl). Immunoblotting with phosho-FAKY397, phospho-FAKY925 total FAK, paxillin and Myc show a higher proportion of FAKY397 in cells overexpressing the paxillin S250T mutant and a higher proportion of FAKY925 in cells overexpressing wildtype paxillin. **(D)** Western blot of nocodazole-treated MEF3T3 cells and collection at the indicated time points post wash-out. Immunoblotting with FAKY925, total FAK, PxnS250 and total paxillin indicate paxillin S250 phosphorylation precedes FAK activation at Y925.

A)

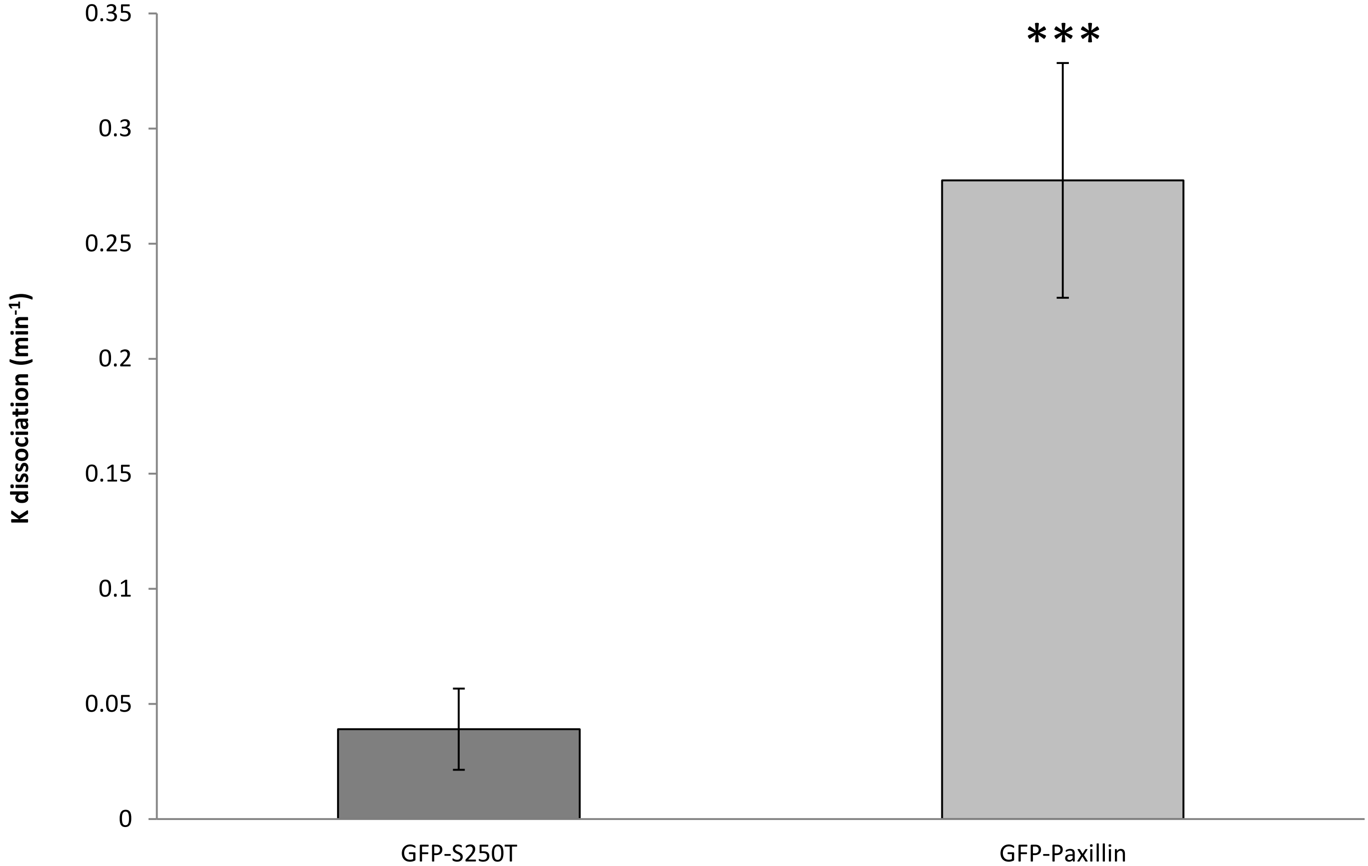

***
0.35
0.3
0.25
0.2
0.15
0.1
0.05
0
K dissociation (min-1)
GFP-S250T
GFP-Paxillin

B)

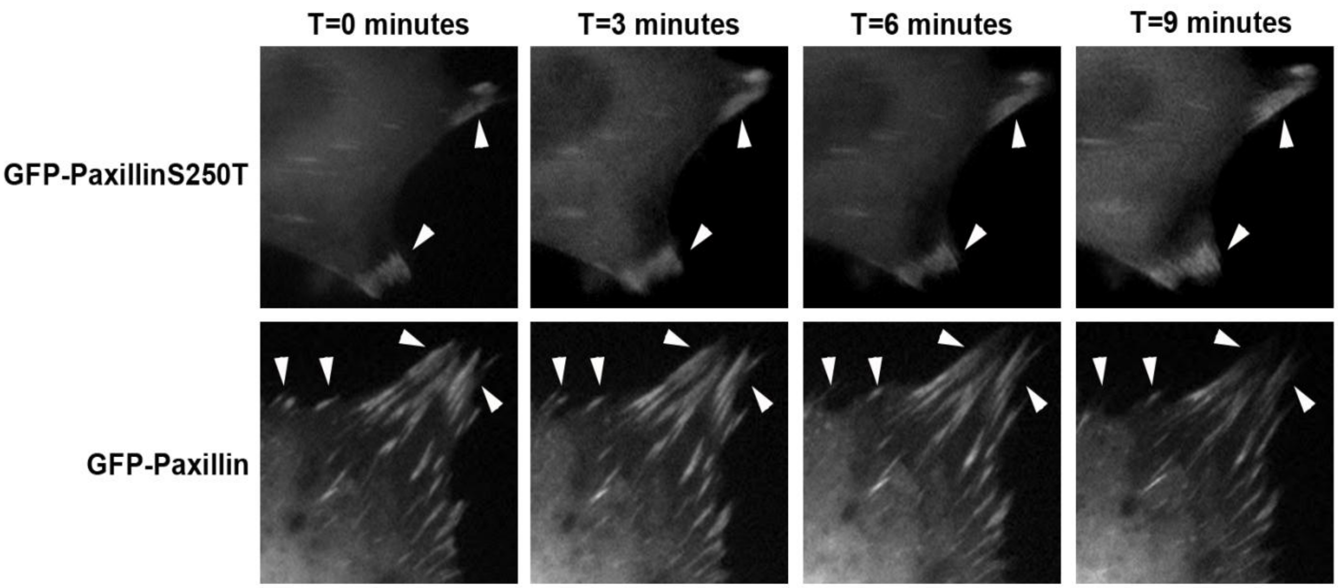
T=0 minutes
T=3 minutes
T=6 minutes
T=9 minutes
GFP-PaxillinS250T
GFP-Paxillin

C)

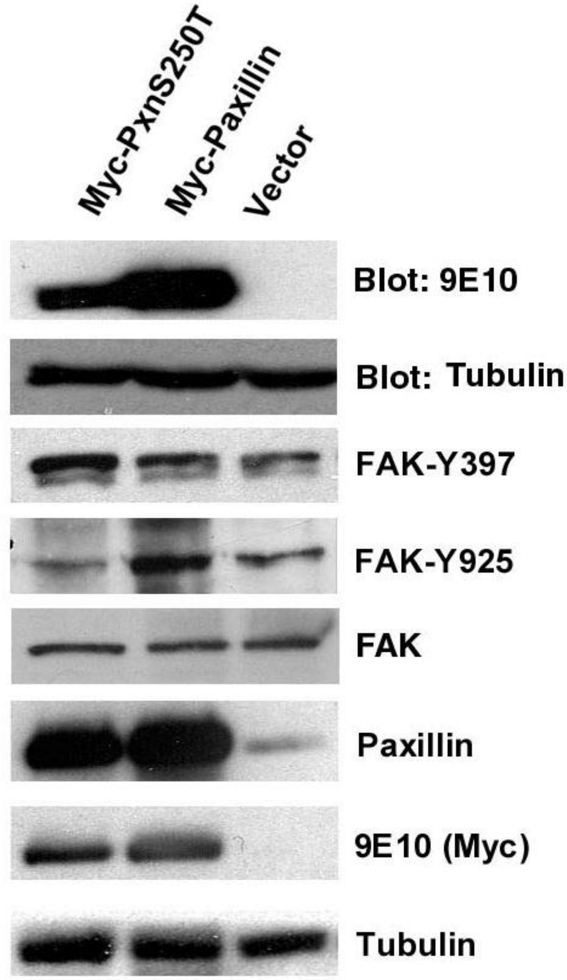
Myc-PxnS250T
Myc-Paxillin
Vector
Blot: 9E10
Blot: Tubulin
FAK-Y397
FAK-Y925
FAK
Paxillin
9E10 (Myc)
Tubulin

D)

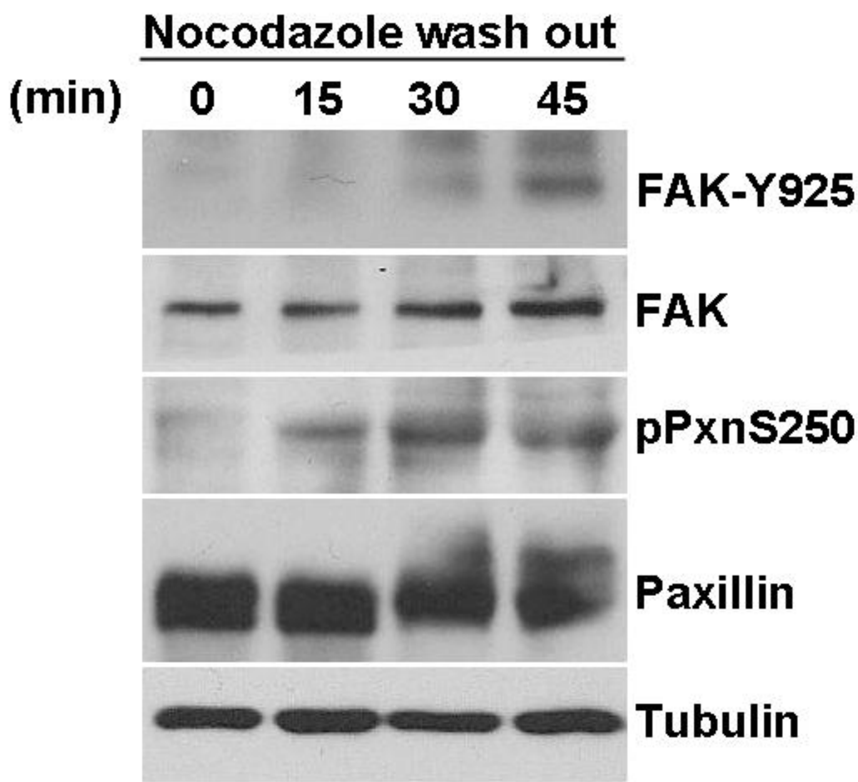
Nocodazole wash out
(min)
0
15
30
45
FAK-Y925
FAK
pPxnS250
Paxillin
Tubulin

Chapter 5:

Paxillin S250 is required for paxillin ubiquitylation and focal adhesion turnover

PaxillinS250T is unable to co-localize to the membrane ruffle with SLK

Since we have been able to establish that a phospho-inactivating mutation of paxillin at S250 is capable of interfering with the rate of focal adhesion turnover and cell migration, its expression will hereafter be used as a de novo dominant negative to investigate the mechanisms governing these processes. As such, it is of interest to investigate this mutant within the context of known protein associations inherent to the wildtype protein.

We have previously shown that paxillin, while being present predominantly at sites of focal adhesions, is capable of co-localizing to the membrane ruffle in a migrating cell with SLK [66, 69]. Therefore, we tested whether mutant S250T paxillin could still co-localize with SLK at membrane ruffles. Interestingly, **Figure 5.1** shows that while GFP-PaxillinS250T is still capable of localizing to focal adhesions, there is a dramatic reduction in the amount that is present at the membrane ruffle with SLK. Furthermore, consistent with the reduced rate of adhesion turnover and migration **(Figures 4.2-4.5**), the observed overexpression of GFP-PaxillinS250T results in an increase in both the number of fibrillar adhesions as well as the size of the focal adhesions themselves (**Figure 5.1**).

Paxillin phospho-S250 co-localizes with actin filaments to adhesions

Although the S250T mutant is found only at adhesions, we have yet to determine where endogenous paxillin phosphorylated at S250 localizes to. Immunofluorescence studies using our phospho-S250 antibody showed the paxillin phospho-isoform to localize with actin fibres to focal adhesions **(Figure 5.2 (A & B))**. It is not all together unexpected that the phospho-S250 isoform of paxillin co-localizes with actin filaments. In fact, a study by Hu and Chien (2007) has

Figure 5.1: ***SLK co-localizes with GFP-paxillin but not GFP-paxillinS250T to the membrane ruffle of migrating cells.*** Confocal immunofluorescent microscopy (63X) of subconfluent MEF3T3 transiently transfected with GFP-fusion proteins, GFP-Paxillin and GFP-PaxillinS250T and plated onto fibronectin-coated coverslips. The strength of the GFP signal was intensified with the addition of GFP primary antibody and subsequent Alexa Flor at 488 nm; SLK was visualized using an SLK antibody and Alexa Flor at 594 nm.

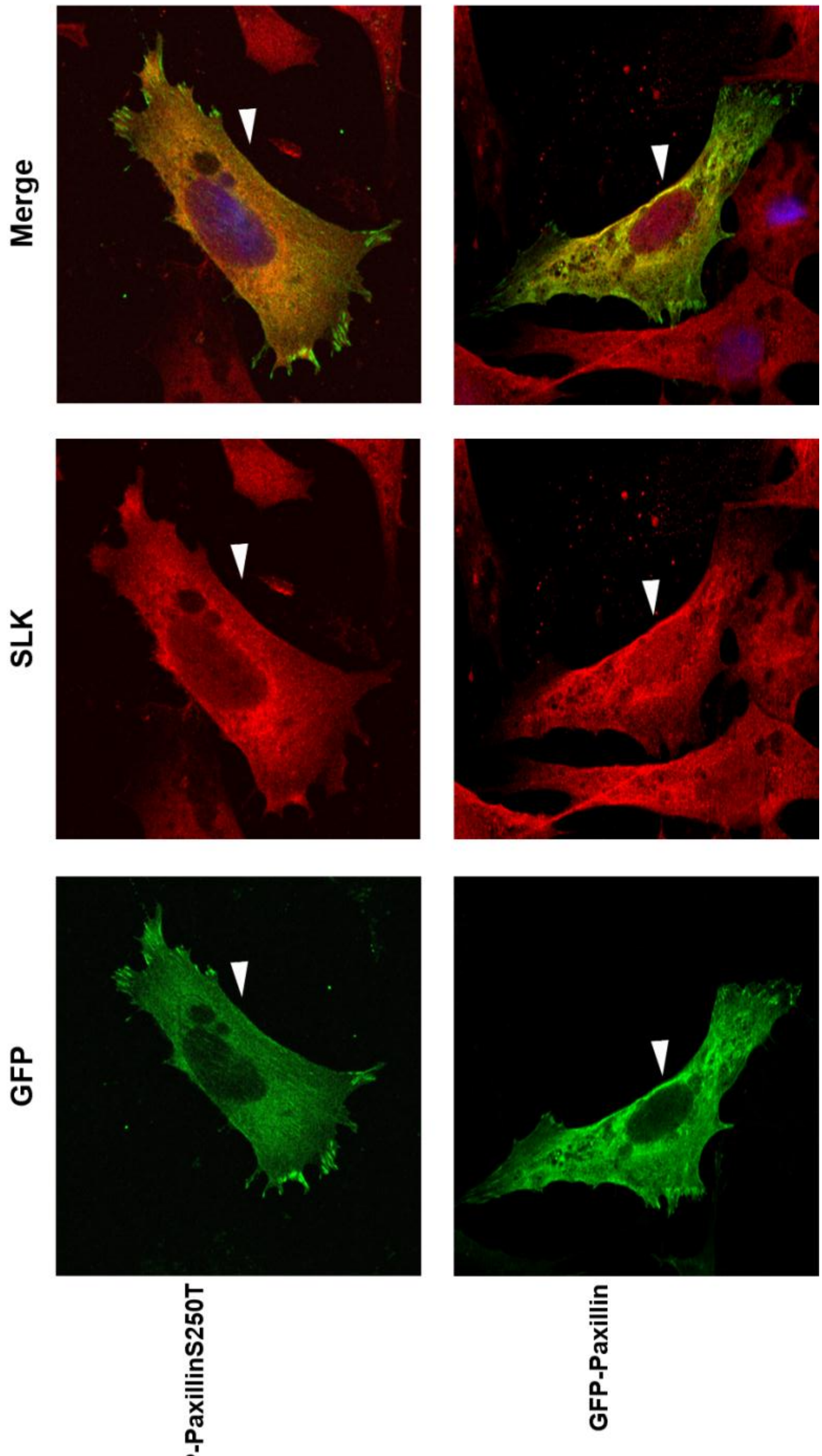
Merge
SLK
GFP
GFP-PaxillinS250T
GFP-Paxillin

<u>**Figure 5.2**</u>: ***The S250 paxillin phospho-isoform co-localizes with actin to adhesions.*** **(A)** Immunofluorescent microscopy (63X) of subconfluent MEF3T3 fibroblasts on fibronectin-coated coverslips. Endogenous paxillin and phospho-paxillin S250 proteins were visualized with the respective primary antibodies and the addition of Alexa Flor 594 nm (red) and 488 nm, respectively. **(B)** Phospho-S250 paxillin co-localizes with actin filaments. Same as in **(A)**, except TRITC was used to visualize actin at 594 nm.

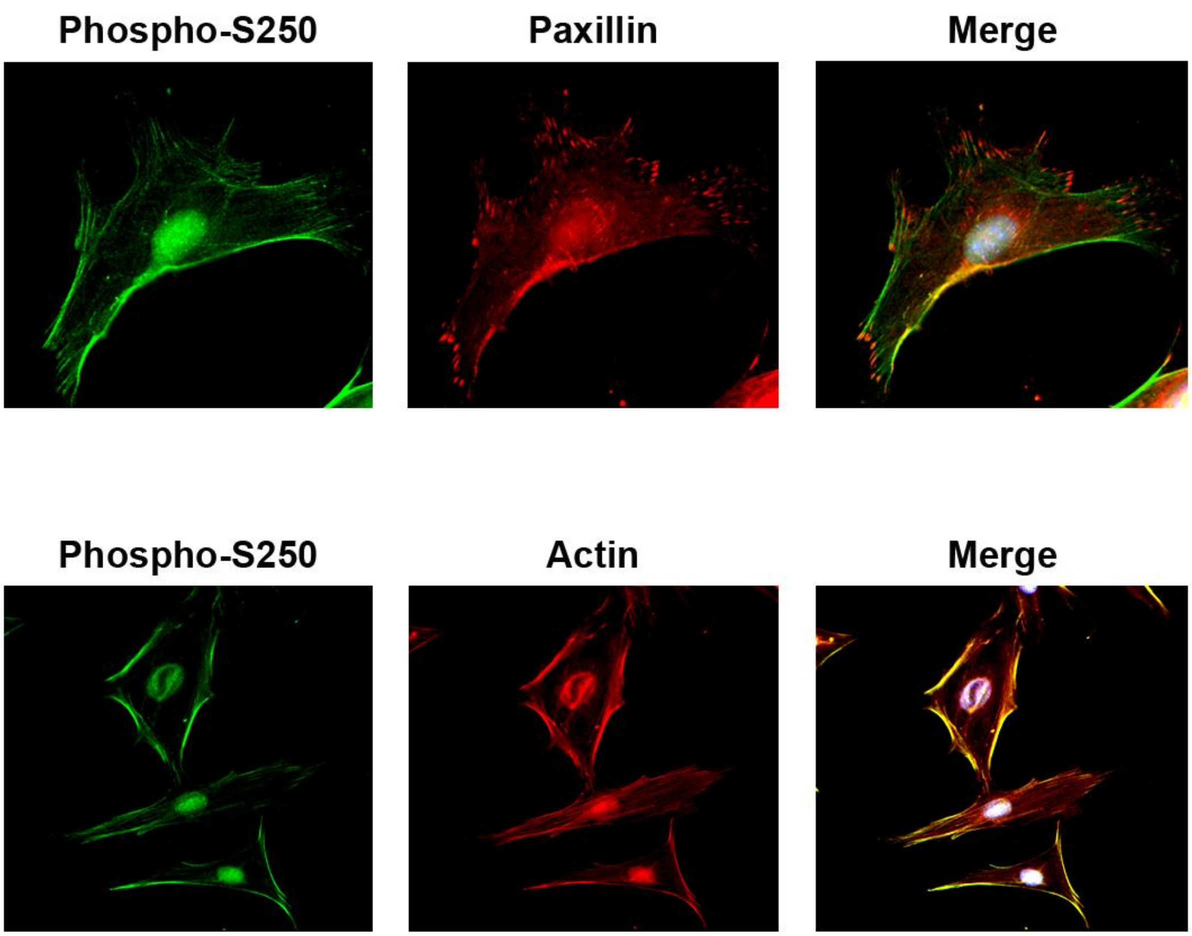
Phospho-S250
Paxillin
Merge
Phospho-S250
Actin
Merge

shown total paxillin to co-localize to actin filaments as fibrous structures in endothelial cells [142]. Specifically, their work suggests that the actin network facilitates the assembly/disassembly of paxillin at focal adhesions by providing the protein with a means of intracellular transportation [142]. Interestingly, the S250 phosphorylated paxillin is not found at focal adhesions with total paxillin. However, we do see co-localization of total and phosphorylated paxillin at the membrane ruffle. The presence of both total and phosphorylated paxillin at the membrane ruffle where we have shown SLK to localize to as well, suggests that SLK phosphorylates paxillin at the membrane ruffle.

Paxillin S250 is required for paxillin-FAK association

Studies involving paxillin null fibroblasts demonstrate that while paxillin is not critically necessary for the localization of FAK to focal adhesions, an interaction between FAK and paxillin is required for the proper activation of the kinase [30, 51, 67]. Specifically, in the absence of this association, FAK is still capable of undergoing Y397 autophosphorylation upon integrin engagement, but shows altered Src-mediated phosphorylation at Y567 and Y577 [66, 67]. This, in turn, prevents subsequent phosphorylation of FAK, in particular Y925, which is necessary for the induction of focal adhesion disassembly [66, 67]. Therefore, an interruption in the interaction between paxillin and FAK may result in the accumulation of mature adhesions and a delay in their turnover because FAK cannot be properly activated. To test whether paxillin S250 is required for the interaction between paxillin and FAK, 293 cells were transfected with the Myc-tagged proteins, Myc-PaxillinS250T, Myc-Paxillin and Myc vector control (Cntrl). Subsequent IP-Western of the protein lysates revealed that FAK is unable to co-IP with the

<u>**Figure 5.3**</u>**:** ***Paxillin S250 is required for paxillin-FAK interaction***. Anti-Myc immunoprecipitation and Western blot of 293 cells transiently overexpressing Myc-fusion proteins, Myc-PaxillinS250T, Myc-Paxillin and Myc vector control (Cntrl). Immunoblotting with total FAK, paxillin and Myc show a requirement for paxillin S250 for paxillin-FAK co-immunoprecipitation to be possible. Please note that the panel showing Myc blotting was a separate gel that was run using 30 μg of whole cell lysate from each of the transfections to validate the presence of transfected proteins.

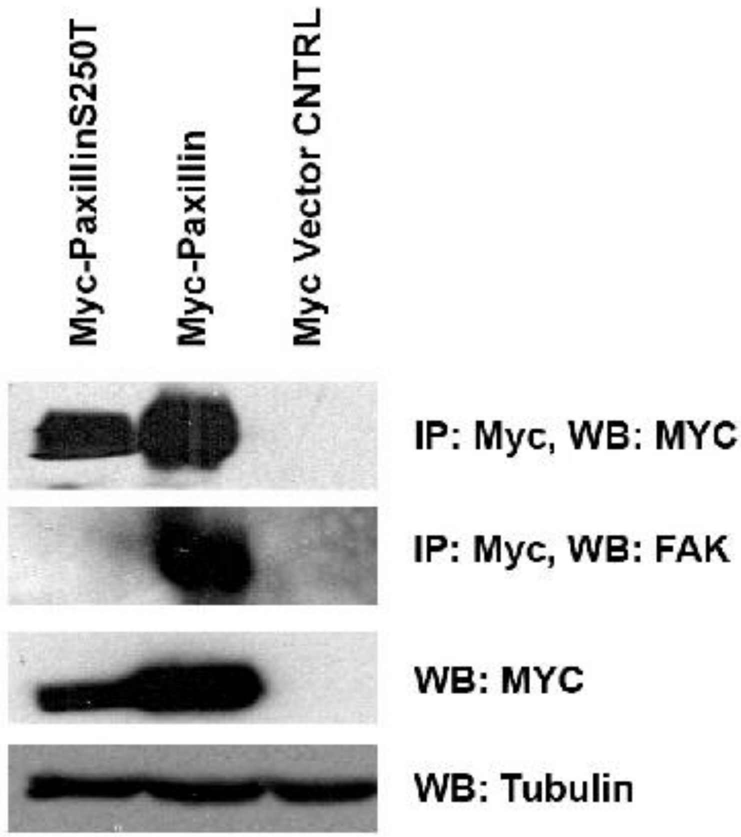
Myc-PaxillinS250T
Myc-Paxillin
Myc Vector CNTRL
IP: Myc, WB: MYC
IP: Myc, WB: FAK
WB: MYC
WB: Tubulin

paxillin S250T mutant (**Figure 5.3**). This suggests that paxillin S250 is required to recruit paxillin to FAK, which in turn, allows for turnover to occur. Supporting this, an accumulation of phospho-FAKY397 was observed in cells expressing mutant paxillin **(Figure 4.5 (C))**. Consequently, this reduction in fully activated FAK may contribute to the delay in focal adhesion turnover and migration that was previously observed (**Figure 4.3-4.5)**.

<u>The redistribution of paxillin between the membrane ruffle and the adhesion involves ubiquitylation and requires paxillin S250</u>

Ubiquitylation is best known for its role in the selective degradation and/or processing of intracellular proteins in eukaryotic cells [143]. In conjunction with a series of enzymes namely, E1, E2 and E3 ligases, ubiquitin is prepared for conjugation to other proteins in an ATP-dependent manner [135, 144]. The conjugation of multiple ubiquitin molecules to a specific protein functions to target the protein for degradation by way of the 26S proteosomal pathway [143]. Consequently, like phosphorylation, ubiquitylation represents another post-translational modification that influences a wide variety of biological processes including, but not limited to gene expression, cellular stress response, antigen presentation, DNA repair, apoptosis, cell cycle and tumorigenesis [143, 145]. However, recent evidence suggests that the impact of ubiquitylation may be more far reaching than the proteasome: a comprehensive review of the subject by Chen *et al*. (2009) argues a non-proteolytic role for ubiquitin in the regulation of protein localization and activation [144, 145].

Previously, we have observed that the transient overexpression of paxillin in 293 cells generated paxillin immunoblots with ‘laddered’ banding patterns that extended insofar as to include protein reactivity >200 kDa in size (unpublished data). This of course, was in dramatic contrast to the expected single band at 68 kDa observed with endogenous paxillin immunoblotting (**Figure 5.4 (A)**). Interestingly, a study by Zied *et al.* (2006) showing endogenous paxillin to be ubiquitylated in the rat bladder carcinoma cell line NBT-II, suggested to us that maybe the presence of the higher molecular weight paxillin in our blots was indicative of a ubiquitylated form of the protein. Since phosphorylation is often times required to alter the conformation of proteins such that they are recognizable to E3 ligases, we tested whether paxillin was ubiquitylated and required S250 phosphorylation [135, 144].

To test this, Myc-PaxillinS250T, Myc-Paxillin and Myc vector control (Cntrl) were transiently transfected into 293 cells and subjected to immunoprecipitation with anti-Myc prior to being resolved on SDS-PAGE. Subsequent immunoblotting with anti-Myc, anti-paxillin and anti-ubiquitin antibodies revealed that the higher molecular weight banding pattern seen in the presence of overexpressed wildtype paxillin was in fact, the result of ubiquitylation (**Figure 5.4 (B)**). Perhaps more interesting however, was the complete absence of ubiquitylated protein in the Myc-PaxillinS250T immunoprecipitation, suggesting that paxillin S250 phosphorylation is required for paxillin ubiquitylation.

To define a function for S250-directed paxillin ubiquitylation, we wanted to determine which E3 ligase is involved in the catalysis of this reaction. A 2003 study by Didier *et al*. gave us a lucrative starting-off point by showing the RING finger-containing E3 ligase, RNF5 to not only ubiquitinate paxillin, but to be responsible for its redistribution from adhesions to the cytoplasm [146]. Blotting of the previous experimental membrane with an anti-RNF5 antibody appears inconclusive as to whether RNF5 is the E3 ligase that is involved in this S250-mediated

Figure 5.4: ***Paxillin S250 is required for ubiquitylation.*** **(A)** Transient overexpression of Myc-fusion proteins Myc-PaxillinS250T, Myc-Paxillin and Myc vector control (Cntrl). **(B)** An equal amount of protein was used for anti-Myc immunoprecipitation prior to SDS- PAGE. Autoclaving of the PVDF membrane prior to ubiquitin immunoblotting was used to further heat-inactivate the membrane-bound ubiquitin to increase immunoreactivity of the protein for the antibody.

A)

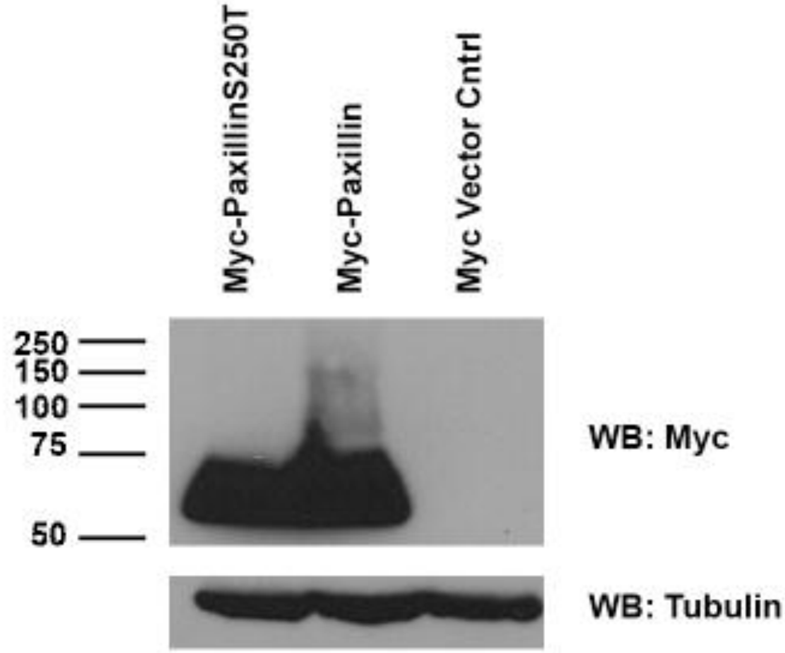
Myc-PaxillinS250T
Myc-Paxillin
Myc Vector Cntrl
250
150
100
75
50
WB: Myc
WB: Tubulin

B)

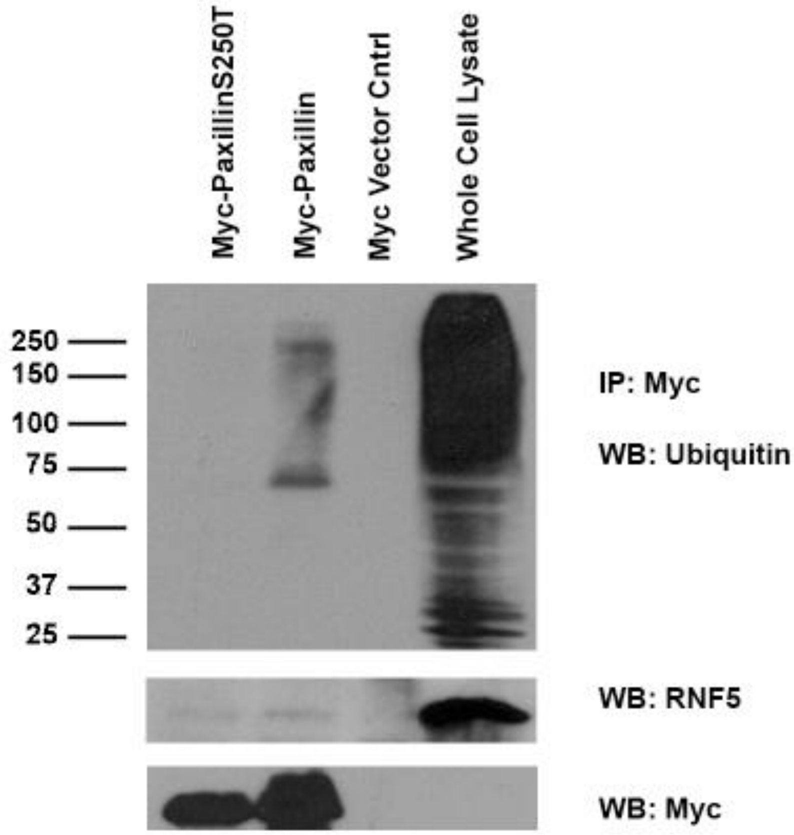
Myc-PaxillinS250T
Myc-Paxillin
Myc Vector Cntrl
Whole Cell Lysate
250
150
100
75
50
37
25
IP: Myc
WB: Ubiquitin
WB: RNF5
WB: Myc

paxillin ubiquitylation and requires further investigation (**Figure 5.4 (B)**).

Paxillin S250 is differentially phosphorylated in breast cancer

The long-term goal of this project is to achieve a better understanding of the mechanisms governing migration dynamics as they apply not only to normal but neoplastic cells. Overexpression of HER2 (ErbB2 (mouse); Neu (rat); HER2 (human), a receptor tyrosine kinase (RTK) that is a member of the epidermal growth factor (EGF) family, is associated with increased progression and metastasis in human breast cancer [43, 118, 147]. Approximately, 25-30% of breast cancer patients overexpressing HER2 present with a more aggressive clinical course and decreased disease-free survival due to more invasive tumors [148, 149]. Previously, we have shown that HER2 stimulation induces SLK activity in the human breast cancer cell lines T47D and MCF7 [79]. Additionally, we have shown SLK to be required for Neu-dependent focal adhesion turnover and migration in transformed NMuMG cells [79]. Although we have demonstrated that heregulin-stimulated SLK activity requires signaling from both FAK and Src, the precise mechanism through which SLK contributes to adhesion turnover and migration has yet to be elucidated. Since phosphorylation of paxillin S250 by SLK has been shown to be involved in focal adhesion turnover and cell migration, we wanted to determine whether heregulin-stimulated adhesion turnover and migration was dependent on this phosphorylation event. Cell lysates from various breast cancer cell lines were immunoblotted using the phospho-S250 antibody. Consistent with a role in migration, paxillin S250 phosphorylation was observed to be highest in invasive breast cancer cell lines, BT474 (invasive ductal carcinoma), MDA-MB-231 (metastatic adenocarcinoma) and SKBR3 (metastatic adenocarcinoma) when compared to normal breast epithelia (MCF10A) (**Figure 5.5**) [150-153]. Although cell lines BT474 and SKBR3 are both derived from luminal, Her2 positive breast cancers, the etiology of MDA-MB-231 is that of a triple-negative (ER-, PR-, Her2), basal-like breast cancer (TNBC) [150]. Interestingly, preliminary analyses of a tissue microarray [127] of breast cancer appear to mirror these findings, showing phospho-S250 immuno-reactivity to positively correlate with breast cancer invasiveness **(Figure 5.6 (B))**. Additionally, these TMA results would suggest that the phospho-S250 immuno-reactivity is also not solely dependent on Her2 status. However, a complete statistical analysis of this data is still pending. Consequently, it would appear as though paxillin S250 phosphorylation is not exclusively, Her2-dependent in breast cancer. Irrespective of hormone or growth factor status, the highly invasive and metastatic nature of the breast cancer cell lines and tissue samples that exhibit elevated levels of phospho-S250 would suggest that further investigation is required into the potential use of paxillin serine phosphorylation status as a novel prognostic indicator of breast cancer invasiveness.

Figure 5.5: ***Paxillin S250 is differentially phosphorylated in various breast cancer cell lines.*** Exponentially-growing cells from the human breast cancer cell lines, BT474, MCF-7, MDA-MB-231, SKBR3 and T47D were collected and analyzed for paxillin S250 phosphorylation via SDS-PAGE and immunoblotting using the phospho-S250 antibody. Subsequent blotting with anti-paxillin and tubulin was used to determine total paxillin content and confirm protein loading, respectively. Hormone and HER2 status for the cell lines under investigation is as follows (ER, PR, HER2): BT474 (+, +, +); MCF7 (+, +, -); MDA-MB-231 (-, -, -); SKBR3 (-, -, +); T47D (+, +, -).

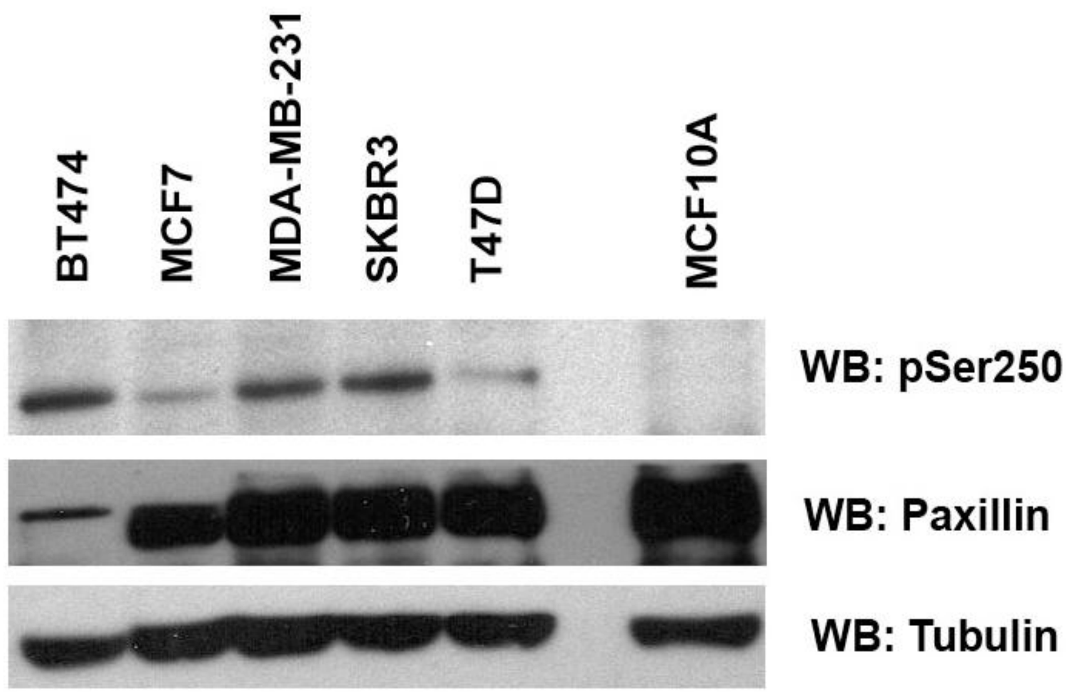
BT474
MCF7
MDA-MB-231
SKBR3
T47D
MCF10A
WB: pSer250
WB: Paxillin
WB: Tubulin

<u>Figure 5.6</u>: *Paxillin phospho-S250 immuno-reactivity is high in invasive breast cancer*. (A) Sample section of a tissue microarray [127] stained by IHC using the phospho-S250 antibody. **(B)** Magnification of 3 independent samples illustrating the variation in phospho-S250 staining (1-3; where 1 is low) intensity described in **Appendix F**. Specifically, sample B12, derived from a benign tumor shows a staining intensity of 1- <1. Sample D10 however, is derived from invasive ductal carcinoma (Her2 and AR positive, ER and PR negative), and is represented by a staining intensity of 2 while sample C8, also derived from invasive ductal carcinoma (Her2, AR, ER, PR positive) exhibits the highest staining intensity of 3. Please note that a complete statistical analysis of all 96 tissue samples contained within this TMA is currently underway.

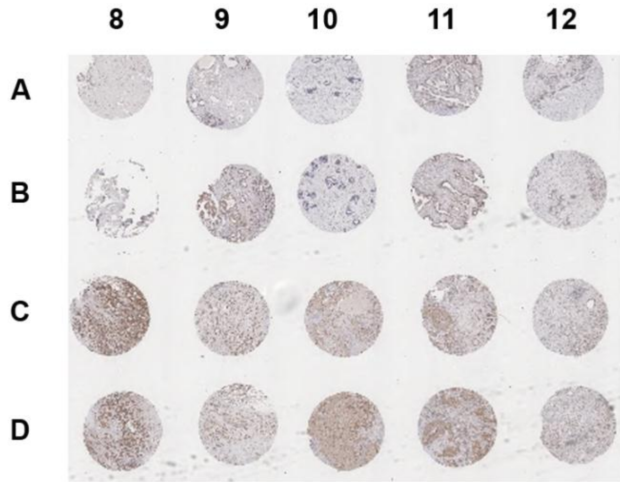

B12

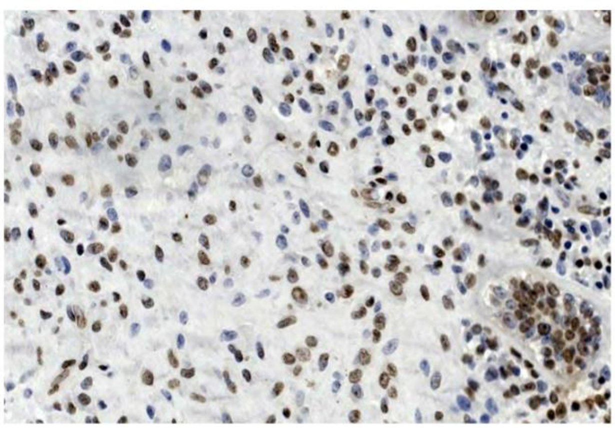

D10

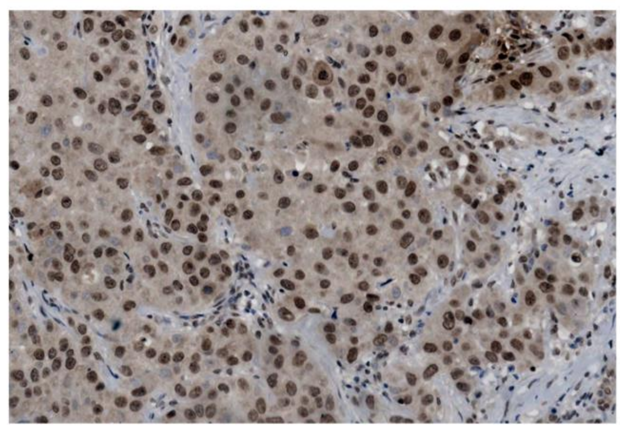

C8

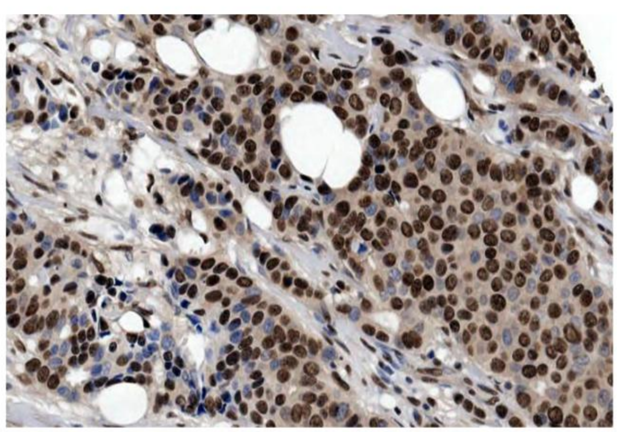

Chapter 6:

General Discussion

General Discussion

Metastasis is the process by which malignant cells spread from a primary tumor to colonize at distant secondary sites [154-156]. Throughout the metastatic process, the highly migratory phenotype required for successful invasion is a function of the dysregulation of signals involved in conventional cell migration [16, 156]. The development of new therapies directed against metastasizing cancers is therefore, reliant on a better understanding of the mechanisms regulating migration-dependent signaling.

Cell migration is a complex, multi-step process that involves the dynamic interconversion between focal adhesion assembly and disassembly that culminates in the reorganization of the cytoskeleton [7, 44]. Consistent with a role in migration, the Ste20-like kinase SLK has been shown to affect actin remodelling and microtubule-induced focal adhesion turnover [69, 78]. We have shown that localization and activation of the kinase at the leading edge of migrating cells in response to scratch-wounding or heregulin stimulation, is dependent on FAK/Src/MAPK signaling [69, 79]. Although we have shown SLK activity to be regulated by the LDB1/2 complex and required for efficient cell migration, the precise mechanism through which SLK exerts its effects on motility has yet to be elucidated [69, 76, 78].

Since the primary role of kinases is to phosphorylate downstream targets to modulate function, the identification of an SLK substrate was required to further characterize the role of SLK in adhesion dynamics and migration [157]. Prior to the start of this project, a natural substrate for SLK had yet to be identified. Through the use of *in vitro* kinase assays we have shown the focal adhesion protein paxillin to be phosphorylated by SLK. Moreover, we were able to pinpoint the exact location of this phosphorylation event to serine 250 within the LD3 domain of paxillin. Interestingly, there are no known binding partners or confirmed phosphorylation sites described for the LD3 domain, although S231 is a predicted ERK phosphorylation site [66, 121]. In addition to being required for SLK-mediated phosphorylation, the altered conformation of paxillin resulting from the mutation of serines 243 and 244 to glycines would suggest that LD3 is important in maintaining the integrity of the tertiary structure of the protein. Although the crystal structures of paxillin motifs LD2 and LD4 have been resolved, the crystal structure of the entire protein has yet to be determined [103, 158, 159]. Consequently, it is difficult to draw any definitive conclusions about the paxillin structure from these results alone.

Previous data suggests that SLK is a focal adhesion disassembly signal transported to the adhesions by the microtubule network [69, 78]. However, the mechanism through which SLK induces turnover still remains unclear. With the identification of paxillin, a critically important focal adhesion protein, as an SLK substrate, we suggest that the phosphorylation of paxillin by SLK is in part, responsible for inducing adhesion turnover. Through the use of overexpression assays that focused on cell spreading, migration and adhesion dynamics, we have shown that SLK phosphorylation of paxillin at S250 is required for efficient focal adhesion turnover and cell migration.

Upon the induction of migration, we have shown SLK to co-localize with paxillin to the leading edge and membrane ruffle of cells. This, taken with the activation of SLK and subsequent phosphorylation of paxillin S250 at approximately 60 minutes post scratching, suggests that SLK phosphorylates paxillin S250 *in vivo*. Interestingly, mutant paxillin (S250T) is no longer able to co-localize with SLK to the membrane ruffle and is instead found exclusively in the adhesion. Since cells that overexpress this mutant exhibit more persistent adhesions and a reduced rate of migration, we suggest that SLK phosphorylates paxillin S250 at the membrane ruffle and that this phosphorylation is required for focal adhesion turnover and cell migration.

Additionally, our data would suggest that the LDBs may function as a sort of docking motif/specificity filter that function to concentrate substrate in a location and time that the kinase is active. Consequently, the paxillin S250T mutant may fail to localize with SLK to the membrane ruffle because it may no longer be able to associate with the LDBs.

An SLK-specific consensus sequence:

Although a consensus sequence for SLK autophosphorylation has recently been identified, it is understood that these sequences are rarely applicable to the identification or verification of physiological substrates [77]. In fact, the determination of a kinase consensus sequence is usually based on information collected from known substrates of the kinase in question [160]. Since SLK has up until now, lacked a known substrate, no known consensus sequence exists. Therefore, using data collected from Ste20 family members as well as the sequence flanking the S250 phosphorylation site in paxillin, we will propose a novel SLK substrate consensus sequence.

Ste20 kinases comprise a superfamily of 27 identified mammalian kinases that are divided into p21-activating kinase (PAK) or germinal center kinase (GCK) subfamilies (**Appendix G**) [161, 162]. Since SLK is classified as a GCK-V kinase, our analysis of current Ste20 phosphorylation literature will focus on the GCK subfamily. An interesting trait of the GCK subfamily is the absence of an acidic residue within the catalytic loop of the kinase domain present within PAKs as an aspartic acid [162, 163]. The resulting reduction in acidic content negates the need for basic residues such as arginine, at P(-2) and P(-5) in the substrate. This however, is a requirement of the basophilic PAK subfamily [162, 163]. Although some GCKs such as Mst1, still phosphorylate substrates containing a basic residue at P(-2), phosphorylation of the GCKs SPAK (Ste20/SPS1-related proline alanine-rich kinase) and OSR1 (oxidative stress-response 1), further confirms that GCKs do not require basic residues in the consensus sequence of their substrates [161, 162, 164]. Those GCKs that maintain the preference for a basic residue in the substrate at P-2 however, have been shown to contain a basic residue at P(-2) with respect to their primary site of autophosphorylation [162]. Since the autophosphorylation sequence of SLK (X-X-X-Y-X-T*-ϕ-R/K-X-X-X) does not have a basic residue at P(-2), it is tempting to speculate that SLK does not require such a residue at P(-2) in its substrate consensus sequence.

Although this thesis represents the first account of an SLK substrate, preliminary data in the lab would suggest that SLK is also capable of phosphorylating the membrane-cytoskeleton linker, ezrin (NCBI accession # P15311) on threonine 576. Since in most cases, the active site of a phosphorylating kinase interacts with four amino acids on either side of the substrate phosphorylation site, a comparison of the sequence flanking paxillin S250 and ezrin T576, may provide insight into an SLK substrate consensus sequence. Interestingly, both sequences show a preference for an uncharged, polar glutamine (Q) at P(+2), while containing a partiality for a hydrophobic residue at P(-2). This is consistent with the hypothesis that SLK may not require a basic residue at P(-2). Taken in combination with the fact that neither sequence shows a predilection for proline directed phosphorylation, leaves us with the very tentative SLK substrate consensus sequence: X-X-ϕ-X-S/T*-X-Q-X-X (where ϕ and * is indicative of a hydrophobic residue and substrate phosphorylation site, respectively).

However, studies would suggest that GCKs are more highly regulated by the molecular interactions that increase substrate concentration than the requirement of a consensus sequence that may not apply to all substrates [49, 163]. Interestingly, Pike *et al.* (2008) shows SLK to require additional mechanisms in order to maintain itself in a dimerized and active state since activation segment phosphorylation appears to weaken SLK self-association [77]. Recently, a study by Storbeck *et al*. (2009) found that the stoichiometry of the LIM domain binding proteins LDB1 and LDB2, which bind directly to the ATH domain of the kinase, dictates the status of SLK activation [76]. Specifically, knockdown of LDB1 resulted in a 5-fold increase in kinase activity, while reducing the amount of LDB2 that associated with the kinase suggesting that LDB1 may be important for the assembly or stability of this complex [76]. Although we have shown paxillin to bind, albeit weakly, to the kinase, we have also demonstrated a direct and high affinity interaction between paxillin and both of the LDBs. Additionally, preliminary data suggests that increased LDB2 expression results in increased paxillin phosphorylation *in vivo* (data not shown). Taken together, we believe that the LDBs may function not only to stabilize the kinase in its dimerized state, but to tether paxillin to the complex, increasing the concentration of the substrate to facilitate efficient phosphorylation. The exact mechanism regulating the stoichiometry of these factors and hence the activation status of the kinase has yet to be determined. However, preliminary data suggests a role for the LIM only protein, LMO4 in the regulation of this complex (unpublished).

A possible mechanism for paxillin phospho-S250-dependent adhesion turnover:

As previously mentioned, an association between FAK and paxillin is required following the autoactivation of FAK at Y397 for the kinase to become fully activated and induce adhesion turnover [30, 51, 67]. Interestingly, we have shown that the dominant negative paxillin S250T mutation ablates the ability of paxillin to interact with FAK. If paxillin recruitment is required for total FAK activation which in turn, is essential for the disassembly of focal adhesions, it is logical that we observe S250T-overexpressing cells migrating at a reduced rate. This observation is not altogether novel: studies have shown that cells overexpressing FAK mutants incapable of binding paxillin exhibit the same phenotype [123]. Since FAK-null cells have also been documented to have more persistent adhesions and a reduced rate of migration when compared to reconstituted cells, we would suggest that with respect to adhesion dynamics, an inability of FAK to bind paxillin, is similar to a FAK-null phenotype [165]. Alternatively, the observation that the S250 phospho-isoform is present along peripheral actin stress fibres but absent from adhesions would suggest that this FAK-paxillin interaction takes place outside of the focal adhesion. Since paxillin-FAK binding has been shown to be required for the proper subcellular localization and consequently, activation of FAK, it is possible that we see an accumulation of stable adhesions in mutant S250T overexpressing cells because FAK can no longer localize to the adhesions with the same efficiency [51]. It is therefore, of interest to determine whether overexpression of the S250T mutant actually has an effect on the distribution of FAK to focal adhesions before more definitive conclusions can be suggested. This being said, we believe our present data supports a role for SLK-mediated paxillin phosphorylation in the regulation of FAK-dependent adhesion turnover.

<u>Figure 6.1</u>: *Proposed mechanism of paxillin S250-dependent adhesion disassembly.* Paxillin is sequestered by SLK through its association with the LIM domain binding proteins, LDB1/2. As a complex, the LDBs, paxillin and SLK are observed co-localizing to the membrane ruffle in actively migrating cells. It is at the membrane ruffle that SLK phosphorylates paxillin at S250, the consequence of which being subsequent ubquitylation via an unknown E3 ligase. Ubiquitylated, phosphorylated paxillin then binds FAK and re-localizes to actin stress fibres that terminate in focal adhesions. Delivery of FAK to focal adhesions facilitates complete FAK activation and adhesion turnover.

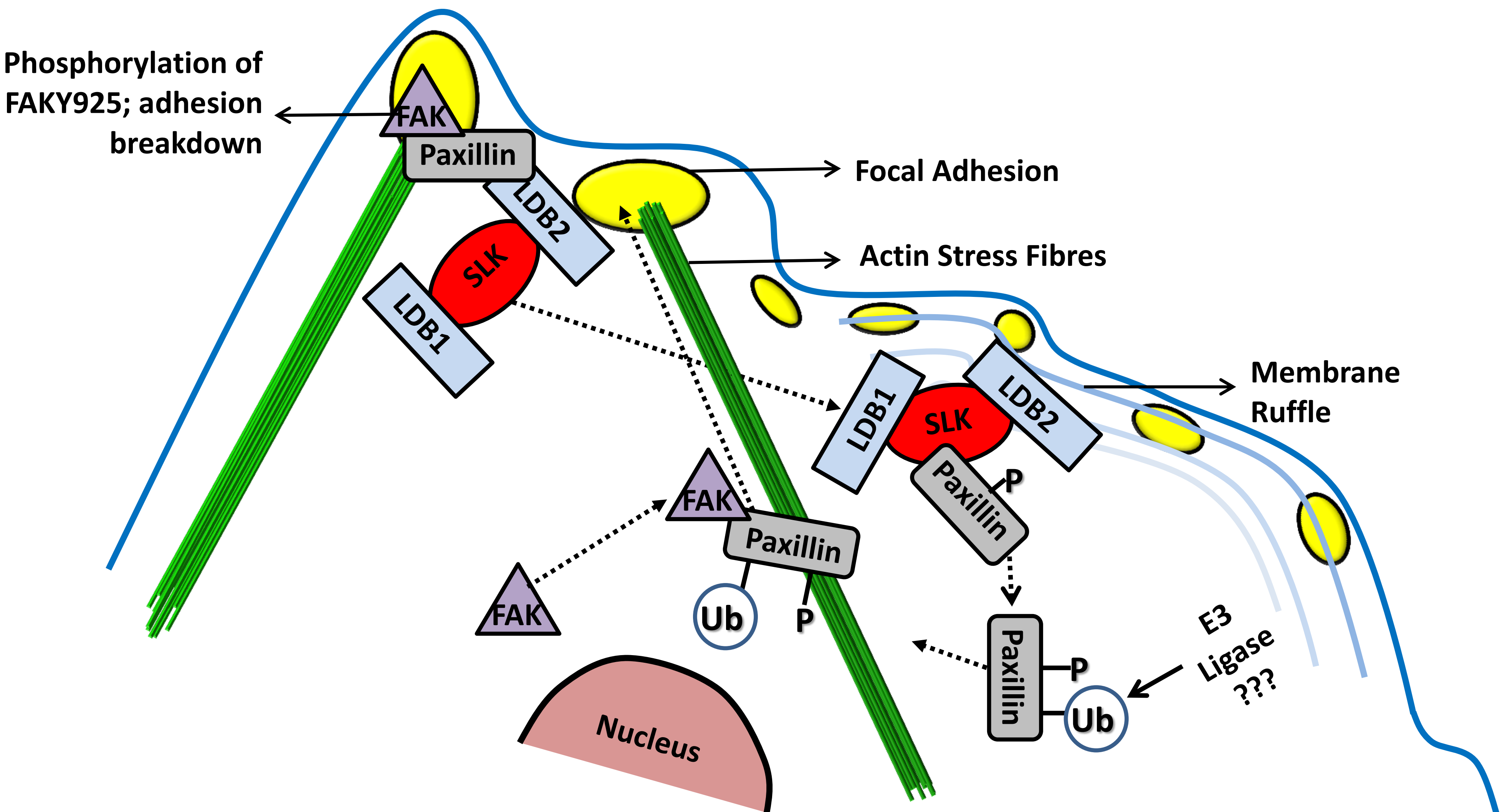

Phosphorylation of FAKY925; adhesion breakdown
FAK
Paxillin
LDB2
SLK
LDB1
Focal Adhesion
Actin Stress Fibres
Membrane Ruffle
LDB1
SLK
LDB2
Paxillin
P
FAK
Paxillin
Ub
P
FAK
Nucleus
Paxillin
P
Ub
E3 Ligase ???

Alternatively, we have shown that overexpression of the paxillin S250T mutant results in a complete ablation of paxillin ubiquitylation. Since paxillin has been shown to contain a veritable duality in function, one that corresponds with the membrane ruffle and one that is related to the adhesion, we believe that instead of targeting paxillin to the proteasome for degradation, ubiquitylation results in the redistribution of paxillin from the ruffle to focal adhesions. The ability of wildtype paxillin to interact with FAK where our mutant cannot, would therefore, suggest that FAK associates with a phosphorylated and possibly ubiquitylated form of paxillin. Moreover, our data suggests that the interaction of FAK with this modified paxillin is required for FAK-mediated adhesion turnover.

The significance of paxillin S250 phosphorylation in breast cancer:

Taken together, we believe that the development of the phospho-S250 antibody and its selective immunoreactivity in breast cancer cell lines warrants further investigation into possible clinical applications. Previous studies have set precedence for investigating paxillin serine phosphorylation within the context of HER2 status in breast cancer. Specifically, Vadlamundi *et al*. (1999) have shown paxillin serine phosphorylation to be induced upon activation of the HER2 pathway following stimulation of MCF-7 cells with heregulin [117]. Interestingly, paxillin expression has also been shown to correlate with the induction of HER2 activity in MCF-7 cells as well as HER2 amplification in breast cancer patients [118, 166]. The significance of these findings can be surmised from a 2007 study by Short *et al*. which showed that the loss of paxillin expression in HER2 positive patients was related to a decrease in the efficacy of chemotherapy and consequently, disease free and overall survival [167]. The determination that phosphorylated paxillin S250 is more prevalent in invasive, Her2-expressing cell lines would suggest that the phosphorylation status of S250 may prove to be a useful prognostic indicator of invasive potential in breast cancer.

Although the highly invasive, basally-derived MDA-MB-231 cell line does not express HER2, it too has been shown to require paxillin expression for its invasive capacity [168]. Paxillin-deficient MDA-MB-231, which is characterized as a triple-negative breast cancer cell line, showed a significant reduction in invasiveness, persistent migration and migration velocity [168]. As a possible substitute to HER2, EGFR expression has been documented in 45-70% of TNBCs [169]. Like the HER2 pathway, induction of EGFR by its ligand EGF, has been also been shown to stimulate paxillin serine phosphorylation in a MAPK-dependent manner [170, 171]. Despite the fact that SLK activity does not seem to be affected by EGF stimulation in 293 cells, it may be because 293 do not express very high levels of endogenous EGFR [70, 172]. Therefore, the increased paxillin S250 phosphorylation seen in the MDA-MB-231 cell line in may in fact be the result of an alternative mechanism of SLK activation, possibly the activation of EGFR. Consequently, this suggests that phosphorylation status of S250 may be useful as a prognostic indicator of invasiveness in non-Her2 positive breast cancers as well.

Future Directions

Although we have verified the use of our custom antibody for Western blot and immunofluorescence analysis, further validation of the phospho-specific paxillin S250 antibody (immunohistochemistry (IHC)) is currently under way. The observation that highly invasive breast cancer cells exhibit a higher level of phospho-S250 immunoreactivity has prompted us to investigate whether or not this translates to actual patient samples. Very preliminary experiments suggest that a differential pattern of phospho-S250 staining exists between highly metastatic disease and normal breast tissue. If the results we observed with the breast cancer cells is mirrored in tissue samples, then the ultimate future work of this project would be to develop this antibody for use as a prognostic indicator of breast cancer invasiveness.

In addition to this, a spin-off project has emerged from this body of work to produce a knock-in mouse line that conditionally expresses the paxillin S250 mutation. When crossed with a breast cancer producing mouse background (NIC mouse model; also described as MMTV-Cre Neu^{NDL} +), it is our hypothesis that we will observe a decrease in the frequency of metastases. If we find that this is in fact the case, this would provide irrefutable support for the development and testing of an SLK kinase inhibitor for use as a novel therapeutic approach to treating metastatic disease.

Mechanistically speaking, a variety of questions remain unanswered. The contribution of the LIM domain binding proteins LDB1 and 2 in mediating the interaction between SLK and paxillin represents an interesting question. Can phosphorylation occur in the absence of one or both of these factors? Moreover, are paxillin and SLK capable of co-localizing to the membrane ruffle without these potential molecular tethers? By determining the exact location of binding between LDB1/2 and paxillin or LDB1/2 and SLK, we will have the means to disrupt this complex and in doing so, will evaluate the consequences *in vivo* on focal adhesion turnover and migration.

Additionally, despite the strong evidence to support the importance of FAK binding to paxillin, not much is known about the modification status of the paxillin involved in this interaction. For example, it would be of interest to determine whether it is the S250 phosphorylation of paxillin that facilitates its interaction with FAK, or whether the S250 phosphorylation is important because it results in the ubiquitylated form of the protein.

Conclusion:

Overall, our data describe a role for the Ste20-like kinase, SLK in regulating adhesion dynamics through phosphorylation of the focal adhesion protein paxillin at S250. Our data shows that phosphorylation of paxillin at serine 250 by SLK is required for adhesion turnover and consequently, efficient cell migration. Moreover, our data suggests that this phosphorylation is critical to the ubquitylation of paxillin which may play a role in its redistribution between the membrane ruffle and the adhesion. Additionally, we have shown that the failure of paxillin to interact with FAK, as is the case with the paxillin S250T mutant, results in a delay in adhesion turnover and migration. Consequently, our results suggest that SLK phosphorylation of paxillin S250 is required for efficient focal adhesion turnover and cell migration.

Appendix:

<u>Appendix A</u>: ***Results of phospho-MALDI-mass spectrometry with IMAC enrichment.*** Immunoprecipitated SLK from MEF3T3 was incubated in the presence GST-paxillin and ATP. Samples were run on SDS-PAGE, and stained with colloidal coomassie prior to the excision of the GST-paxillin band from the gel. Gel slice(s) were frozen at -20°C for storage until MALDI-mass spectrometry with phospho-enrichment could be performed by the Proteomics Research Center, Ottawa Institute of Systems Biology (Ottawa, Ontario, Canada). **(A)** Identification of phosphorylated S272 (serine 8) and **(B)** identification of phosphorylated S274 (serine 10) within the same peptide fragment.

A)

Mascot Search Results

Peptide View

MS/MS Fragmentation of **ELDELMASLṠDFK**
Found in **gi|119618583**, paxillin, isoform CRA_c [Homo sapiens]

Match to Query 1587: 1577.085448 from(789.550000,2+) intensity(42107.7420)
Title: 787: Scan 3077 (rt=2109.07) [P:\Input\Julian\2008\18JAN2008\band2prime.RAW]
Data file P:\Output\Julian\2008\18JAN2008\band2prime.mgf

Click mouse within plot area to zoom in by factor of two about that point
Or, Plot from 200 to 1600 Da Full range

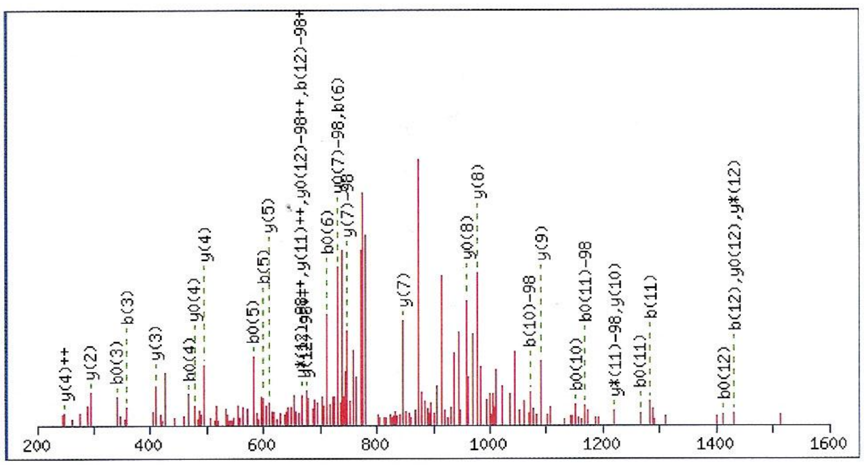

Monoisotopic mass of neutral peptide Mr(calc): 1576.6732
Fixed modifications: Carbamidomethyl (C)
Variable modifications:
S8 : Phospho (ST), with neutral losses 0.0000(shown in table), 97.9769
Ions Score: 37 **Expect:** 0.76
Matches (Bold Red): 35/178 fragment ions using 51 most intense peaks

#	b	b^{++}	b^{0}	b^{0++}	Seq.	y	y^{++}	y*	y^{*++}	y^{0}	y^{0++}	#
1	130.0499	65.5286	112.0393	56.5233	E							13
2	243.1339	122.0706	225.1234	113.0653	L	1448.6379	724.8226	**1431.6113**	716.3093	**1430.6273**	715.8173	12
3	**358.1609**	179.5841	**340.1503**	170.5788	D	1335.5538	**668.2805**	1318.5273	659.7673	1317.5432	659.2753	11
4	487.2035	244.1054	**469.1929**	235.1001	E	**1220.5269**	610.7671	1203.5003	602.2538	1202.5163	601.7618	10
5	**600.2875**	300.6474	**582.2770**	291.6421	L	**1091.4843**	546.2458	1074.4577	537.7325	1073.4737	537.2405	9
6	**731.3280**	366.1676	**713.3175**	357.1624	M	**978.4002**	489.7037	961.3737	481.1905	**960.3896**	480.6985	8
7	802.3651	401.6862	784.3546	392.6809	A	**847.3597**	424.1835	830.3332	415.6702	829.3492	415.1782	7
8	969.3635	485.1854	951.3529	476.1801	S	776.3226	388.6649	759.2961	380.1517	758.3120	379.6597	6
9	1082.4475	541.7274	1064.4370	532.7221	L	**609.3243**	305.1658	592.2977	296.6525	591.3137	296.1605	5
10	1169.4796	585.2434	**1151.4690**	576.2381	S	**496.2402**	**248.6237**	479.2136	240.1105	**478.2296**	239.6185	4
11	**1284.5065**	642.7569	**1266.4960**	633.7516	D	**409.2082**	205.1077	392.1816	196.5944	391.1976	196.1024	3
12	**1431.5749**	716.2911	**1413.5644**	707.2858	F	**294.1812**	147.5942	277.1547	139.0810			2
13					K	147.1128	74.0600	130.0863	65.5468			1

B)

Mascot Search Results

Peptide View

MS/MS Fragmentation of **ELDELMASLSDFKFMAQGK**
Found in **gi|119618583**, paxillin, isoform CRA_c [Homo sapiens]

Match to Query 2739: 2269.075932 from(757.365920,3+) intensity(90690.8790)
Title: 852: Sum of 2 scans in range 3235 (rt=2198.32) to 3239 (rt=2201.68) [P:\Input\Julian\2008\18JAN2008\band2.RAW]
Data file P:\Output\Julian\2008\18JAN2008\band2.mgf

Click mouse within plot area to zoom in by factor of two about that point
Or, Plot from 200 to 1400 Da Full range

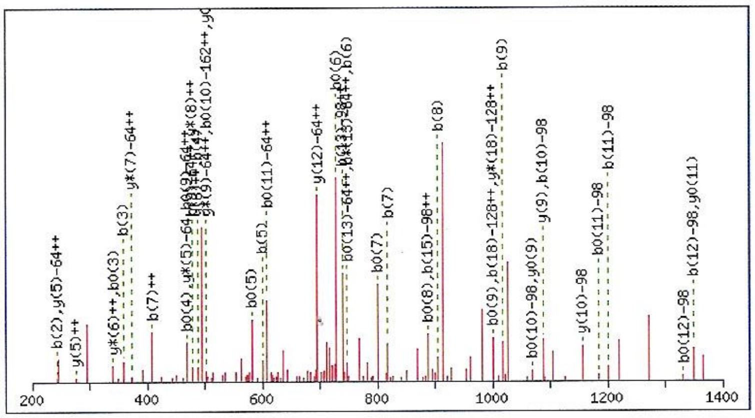

Monoisotopic mass of neutral peptide Mr(calc): 2270.9840
Fixed modifications: Carbamidomethyl (C)
Variable modifications:
M6 : Oxidation (M), with neutral losses 0.0000(shown in table), 63.9983
S10 : Phospho (ST), with neutral losses 97.9769(shown in table), 0.0000
M15 : Oxidation (M), with neutral losses 0.0000(shown in table), 63.9983
Ions Score: 48 **Expect:** 0.056
Matches (Bold Red): 46/520 fragment ions using 54 most intense peaks

#	b	b^{++}	b^{*}	b^{*++}	b^{0}	b^{0++}	Seq.	y	y^{++}	y^{*}	y^{*++}	y^{0}	y^{0++}	#
1	130.0499	65.5286			112.0393	56.5233	E							19
2	**243.1339**	122.0706			225.1234	113.0653	L	2044.9718	1022.9896	2027.9453	1014.4763	2026.9613	1013.9843	18
3	**358.1609**	179.5841			**340.1503**	170.5788	D	1931.8878	966.4475	1914.8612	957.9342	1913.8772	957.4422	17
4	**487.2035**	244.1054			**469.1929**	235.1001	E	1816.8608	908.9340	1799.8343	900.4208	1798.8503	899.9288	16
5	**600.2875**	300.6474			**582.2770**	291.6421	L	1687.8182	844.4128	1670.7917	835.8995	1669.8077	835.4075	15
6	**747.3229**	374.1651			**729.3124**	365.1598	M	1574.7342	787.8707	1557.7076	779.3574	1556.7236	778.8654	14
7	**818.3601**	**409.6837**			**800.3495**	400.6784	A	1427.6988	714.3530	1410.6722	705.8397	1409.6882	705.3477	13
8	**905.3921**	453.1997			**887.3815**	444.1944	S	1356.6616	678.8345	1339.6351	670.3212	1338.6511	669.8292	12
9	**1018.4761**	509.7417			**1000.4656**	500.7364	L	1269.6296	635.3184	1252.6031	626.8052	1251.6191	626.3132	11
10	**1087.4976**	544.2524			**1069.4870**	535.2472	S	**1156.5456**	578.7764	1139.5190	570.2631	1138.5350	569.7711	10
11	**1202.5245**	601.7659			**1184.5140**	592.7606	D	**1087.5241**	544.2657	1070.4975	535.7524	**1069.5135**	535.2604	9
12	**1349.5930**	675.3001			**1331.5824**	666.2948	F	972.4972	**486.7522**	955.4706	**478.2389**			8
13	1477.6879	**739.3476**	1460.6614	730.8343	1459.6774	730.3423	K	825.4287	413.2180	808.4022	404.7047			7
14	1624.7563	812.8818	1607.7298	804.3685	1606.7458	803.8765	F	697.3338	349.1705	680.3072	**340.6573**			6
15	1771.7917	**886.3995**	1754.7652	877.8862	1753.7812	877.3942	M	550.2654	**275.6363**	533.2388	267.1230			5
16	1842.8289	921.9181	1825.8023	913.4048	1824.8183	912.9128	A	403.2300	202.1186	386.2034	193.6053			4
17	1970.8874	985.9474	1953.8609	977.4341	1952.8769	976.9421	Q	332.1928	166.6001	315.1663	158.0868			3
18	2027.9089	1014.4581	2010.8823	1005.9448	2009.8983	1005.4528	G	204.1343	102.5708	187.1077	94.0575			2
19							K	147.1128	74.0600	130.0863	65.5468			1

__Appendix B__*: **Despite mass spectrometry results, paxillin S272 and/or 274 are not phosphorylated in vitro by SLK.*** Endogenous SLK was immunoprecipitated from MEF3T3, incubated with either wildtype GST-paxillin or mutant GST-PaxillinS272/274A prior to being subjected to an *in vitro* kinase assay. Coomassie stain and autoradiography (AUTORAD) were used to visualize protein content and kinase signal, respectively. Despite mass spectrometry results, neither S272 nor S274 are phosphorylated by SLK *in vitro*. Misidentification is not uncommon when it comes to phosphorylation mapping using mass spectrometry-related protocols [133]. Due to the limitations of these protocols such as the inability to detect low signal intensity and the inherent loss of phospho-serine/threonine residues due to collision induced dissociation, phosphopeptides can be overlooked and false-positives generated [133, 173].

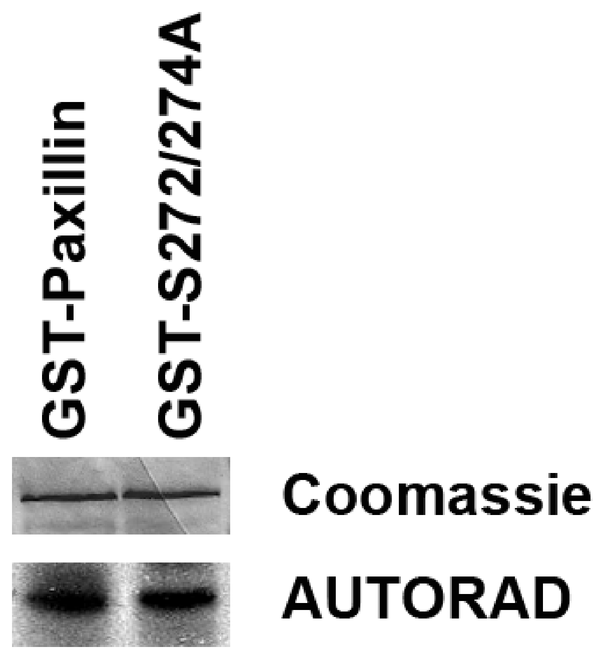
GST-Paxillin
GST-S272/274A
Coomassie
AUTORAD

__Appendix C__: ***Alignment of human, mouse and chicken paxillin sequences in the vicinity of human paxillin S250.***

```
                 S243 S244                S250
Human    GGCGAGATGAGCAGCCCGCAGCGCGTCACCTCCACCCAACAGCAGACACGCATCTCGGCC
Mouse    GGAGAGATGAGCAGTCCGCAGCGAGTCACCTCCAGCCAGCAGCAGACCCGGATCTCGGCC
Chicken  GGGGAGGTGAGCAGCCCCCAGCGTGTCAACGCCAGTCAGCAGCAGACCCGTATCTCTGCT
         ** *** ******* ** ***** **** * ***  ** ******** ** ***** ** 
```

<u>Appendix D</u>: *Expression levels of the paxillin homologue Hic-5 in paxillin-null and wildtype fibroblasts.* Scratch-wounded (S), wildtype (WT) MEF3T3 were scratched and left to incubate for one prior to collection. Cell lysates were then collected and quantified prior to being resolved using SDS-PAGE. Anti-Hic-5, and tubulin antibodies show a higher incidence of Hic-5 expression in paxillin-null (-/-) fibroblasts then in confluent (unscratched; US), wildtype (WT) MEF3T3. However, lane 3 shows Hic-5 expression in WT-MEF3T3 to increase to paxillin -/- levels upon the induction of migration.

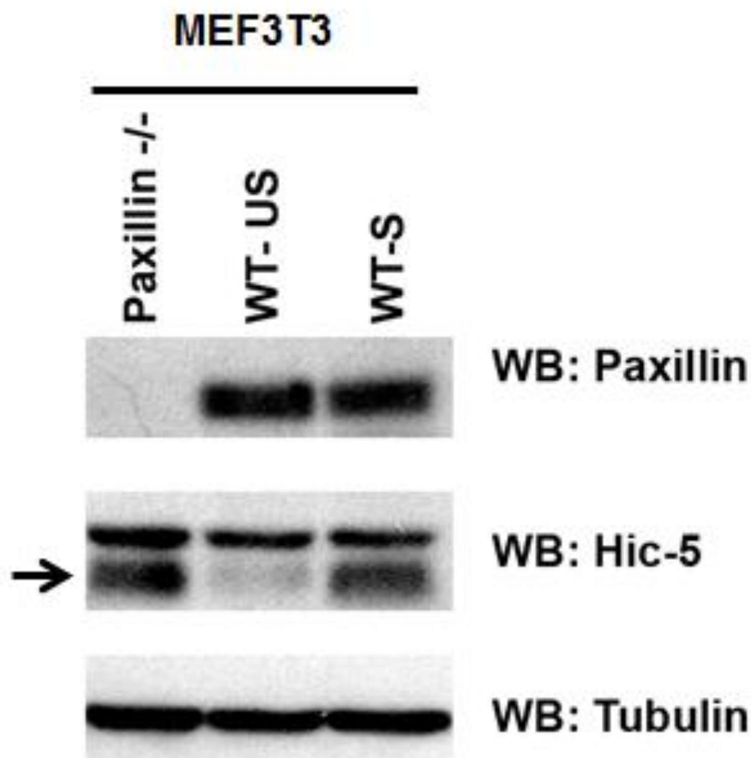
MEF3T3
Paxillin -/-
WT- US
WT-S
WB: Paxillin
WB: Hic-5
WB: Tubulin

<u>Appendix E</u>: *Validation of the phospho-paxillinS250 antibody for Western blot, immunofluorescence and immunohistochemistry*. (A) *In vitro* verification of the paxillin S250 phospho-specific antibody. A non-radioactive kinase assay was conducted using 10 mM of unlabelled ATP in the presence of immunoprecipitated SLK, recombinant GST-wildtype and mutant paxillin for 30 minutes at 30°C. Phosphorylated paxillin S250 was detected via immunoblotting with the anti-phospho-S250 antibody. Total paxillin was determined by ponceau staining the PVDF membrane. **(B)** Phosphatase treatment of scratch-activated (60 minutes) MEF3T3 using λ protein phosphatase and subsequent blotting for paxillin S250 phosphorylation and total paxillin. **(C)** *In vivo* verification of the phospho-S250 antibody. Equal amounts of protein derived from paxillin-null (-/-) MEF and wildtype MEF lysate were run in tandem using SDS-PAGE. Transferred proteins were immunoblotted for phospho-S250, total paxillin and tubulin with the respective antibodies. **(D)** The phospho-S250 antibody and immunofluorescence. Paxillin-null cells were fixed with 4% PFA and immunostained for the presence of total paxillin and phospho-S250. **(E)** The phospho-S250 antibody and immunohistochemistry. The phospho-S250 antibody was tested for use in both murine and human (shown) samples. Negative controls correspond to the incubation of samples with secondary antibody in the absence of primary antibody and incubation of tissues with primary antibody that underwent peptide block. Samples were counterstained with hematoxylin, scanned and the phospho-S250 antibody was validated for use by pathologist, Dr. Manijeh Daneshmand, M. D.

A)

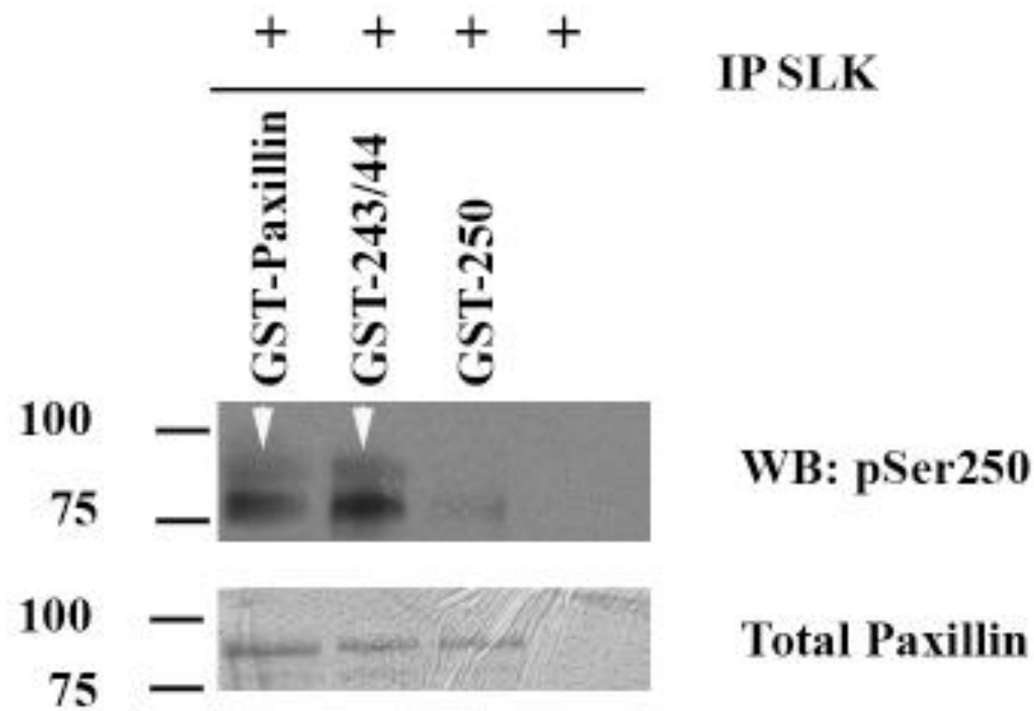
+ + + +
IP SLK
GST-Paxillin
GST-243/44
GST-250
100
75
WB: pSer250
100
75
Total Paxillin

B)

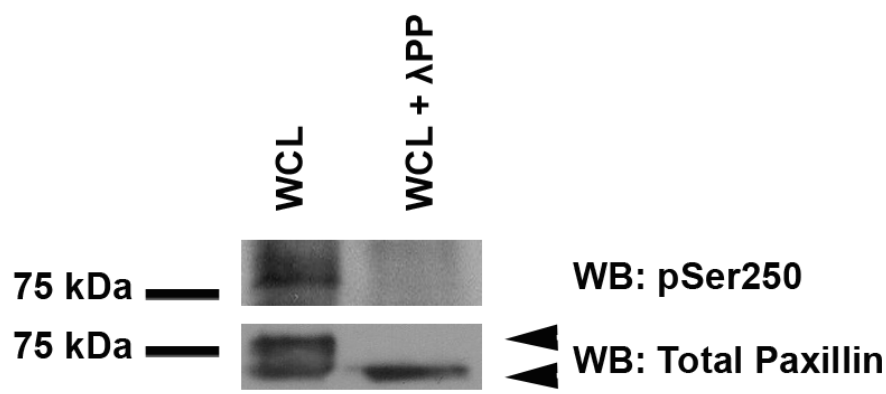
WCL
WCL + λPP
75 kDa
WB: pSer250
75 kDa
WB: Total Paxillin

C)

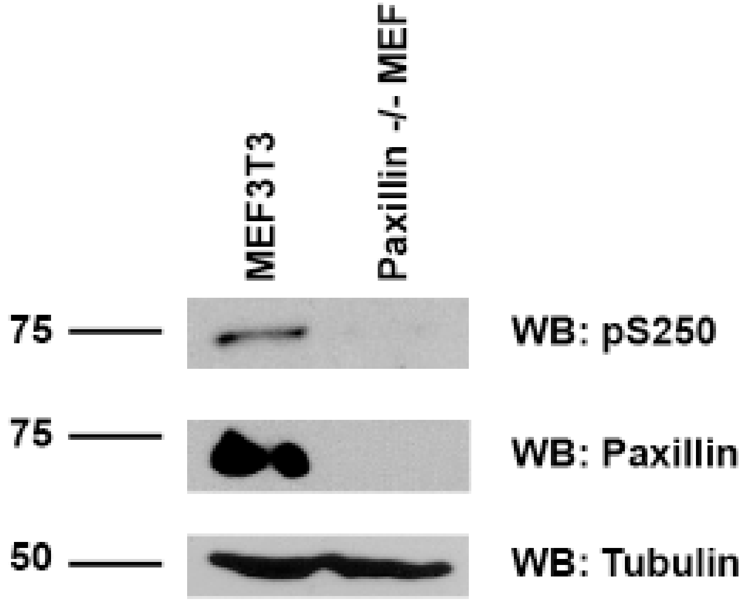
MEF3T3
Paxillin -/- MEF
75
75
50
WB: pS250
WB: Paxillin
WB: Tubulin

D)

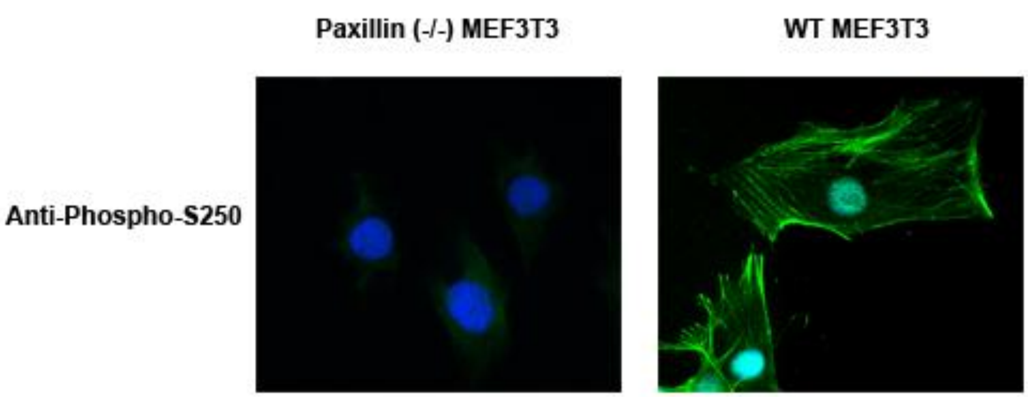
Paxillin (-/-) MEF3T3
WT MEF3T3
Anti-Phospho-S250

E)

Phospho-PaxillinS250

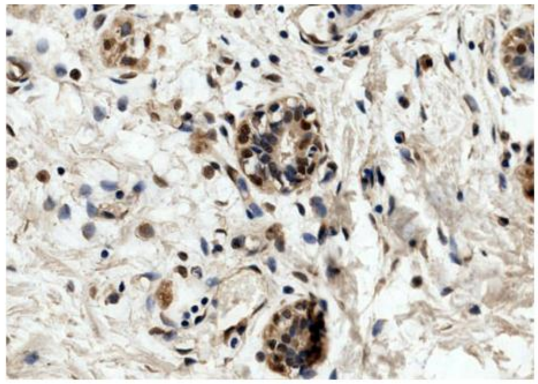

Secondary Control

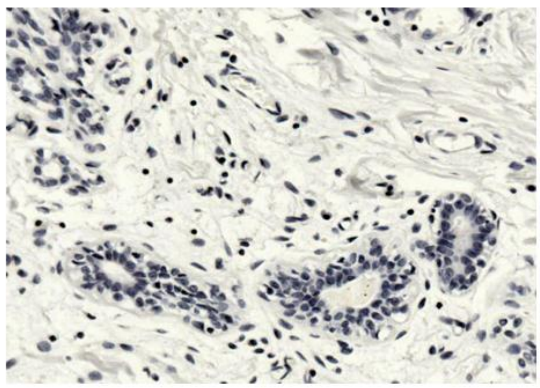

Phospho-Peptide Block

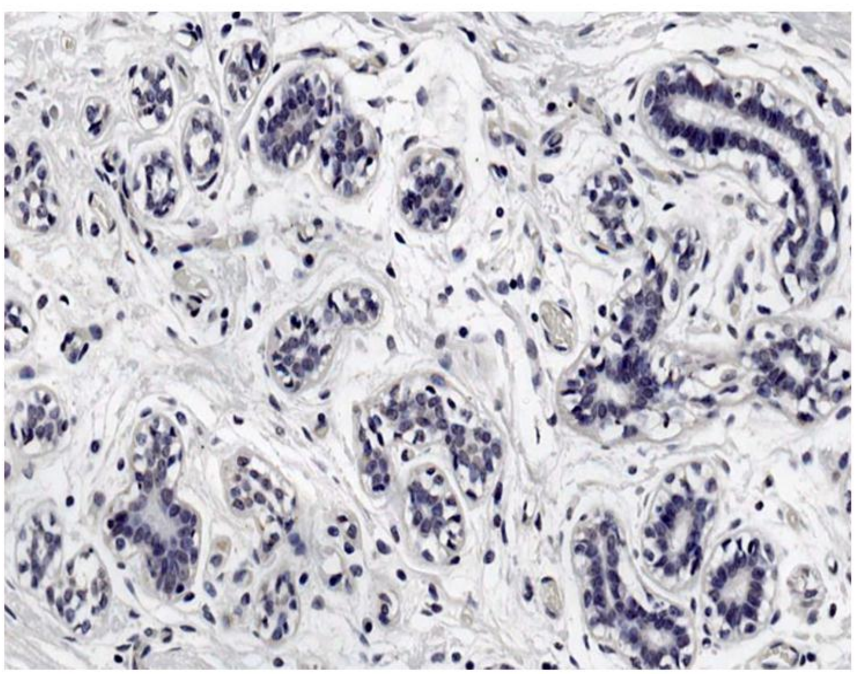

Appendix F: ***Classification of paxillin phospho-S250 IHC staining.*** **(A)** IHC of normal breast epithelia using total paxillin and phospho-S250 antibodies. **(B)** Assessment of phospho-S250 staining intensity as evaluated by pathologist Dr. Manijeh Daneshmand, M.D. A value of staining intensity has been assigned for 3 tissue samples to show the difference between high (3), moderate (2) and low (1) immuno-reactivity of tissues to the phospho-S250 antibody. Samples originate from a TMA containing a spectrum of normal, benign and malignant breast tissues.

Staining Intensity = 1

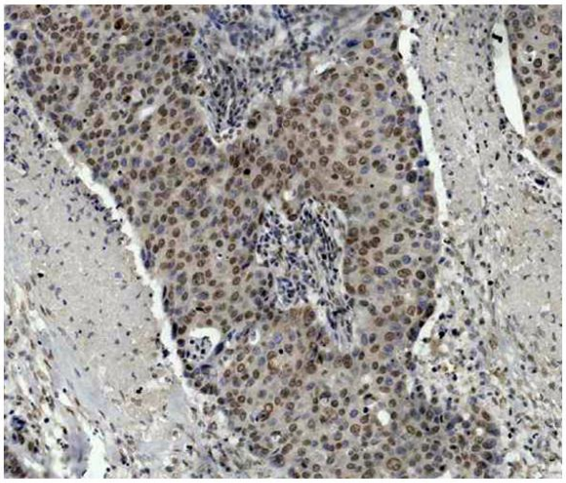

Staining Intensity = 2

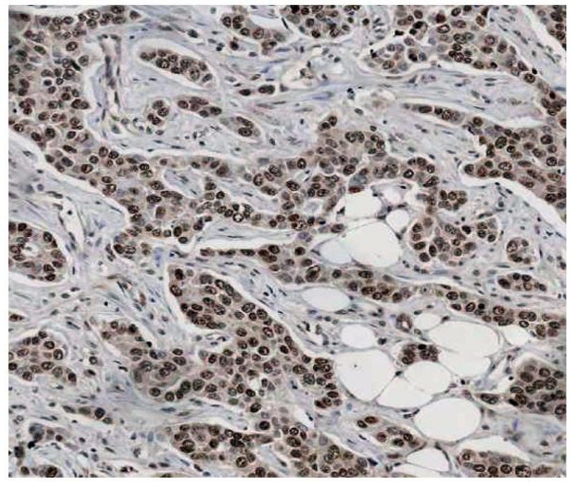

Staining Intensity = 3

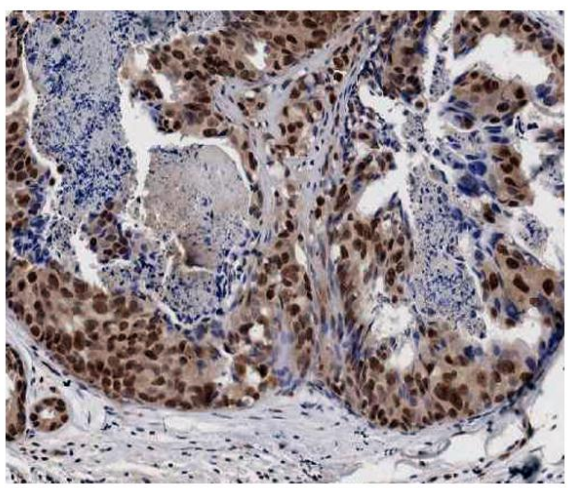

<u>Appendix G</u>: *Dendogram of all 28 Ste20 family kinases.* Figure adapted from Delpire (2009) [162].

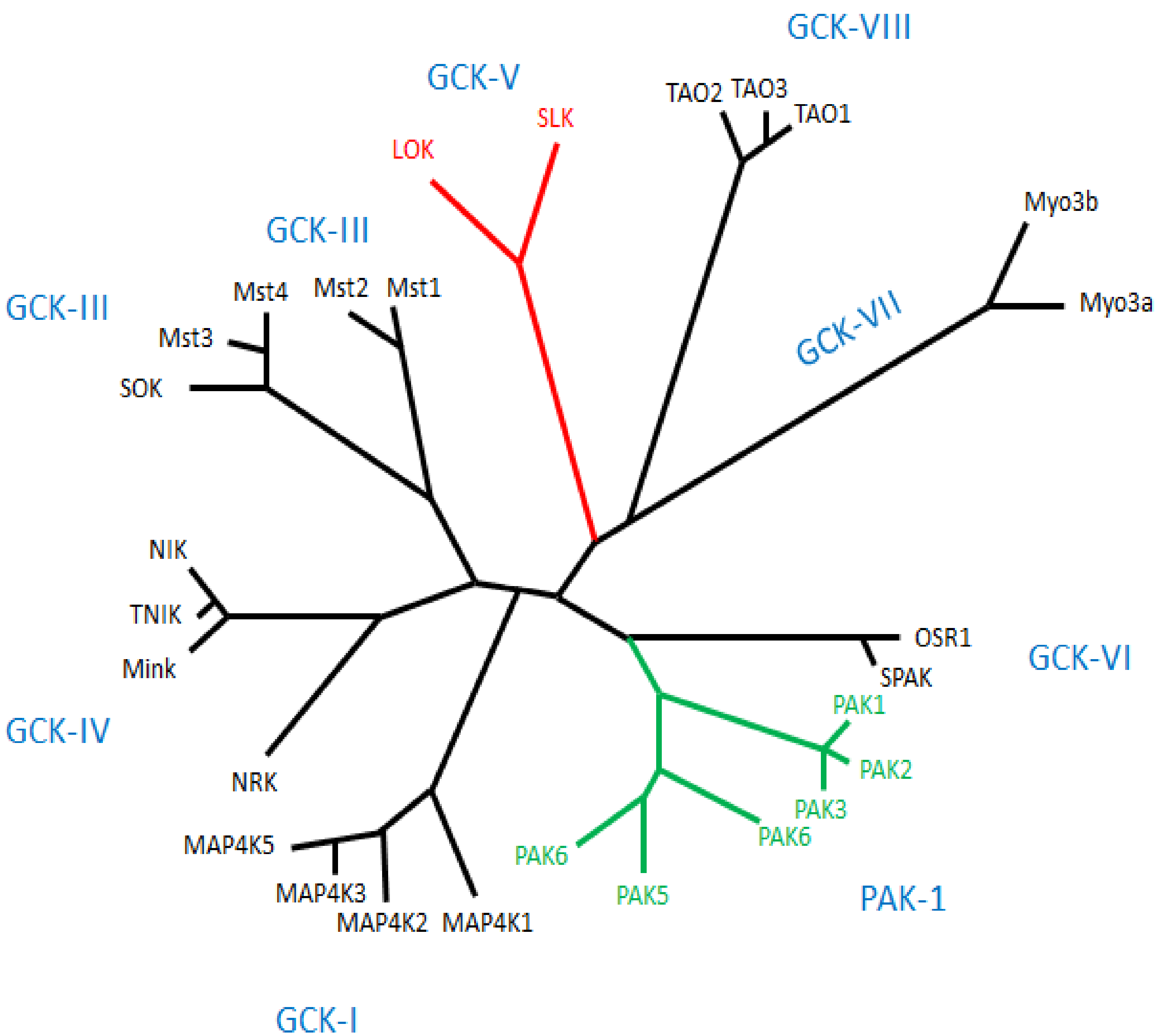
GCK-VIII
GCK-V
TAO2
TAO3
TAO1
SLK
LOK
Myo3b
GCK-III
Myo3a
GCK-VII
GCK-III
Mst4
Mst2
Mst1
Mst3
SOK
NIK
TNIK
Mink
OSR1
GCK-VI
SPAK
PAK1
GCK-IV
PAK2
NRK
PAK3
PAK6
MAP4K5
PAK6
PAK5
MAP4K3
PAK-1
MAP4K2
MAP4K1
GCK-I

References:

1. Franz, C.M., G.E. Jones, and A.J. Ridley, *Cell Migration in Development and Disease.* Developmental cell, 2002. **2**(2): p. 153-158.
2. Moissoglu, K. and M.A. Schwartz, *Integrin signalling in directed cell migration.* Biol. Cell, 2006. **98**(9): p. 547-555.
3. Lo, C.-M., et al., *Cell Movement Is Guided by the Rigidity of the Substrate.* Biophysical journal, 2000. **79**(1): p. 144-152.
4. Ridley, A.J., et al., *Cell Migration: Integrating Signals from Front to Back.* Science, 2003. **302**(5651): p. 1704-1709.
5. Parsons, J.T., A.R. Horwitz, and M.A. Schwartz, *Cell adhesion: integrating cytoskeletal dynamics and cellular tension.* Nat Rev Mol Cell Biol. **11**(9): p. 633-643.
6. Thibault, M.M., C.D. Hoemann, and M.D. Buschmann, *Fibronectin, Vitronectin, and Collagen I Induce Chemotaxis and Haptotaxis of Human and Rabbit Mesenchymal Stem Cells in a Standardized Transmembrane Assay.* Stem Cells and Development, 2007. **16**(3): p. 489-502.
7. Manes, S., et al., *Cells on the Move: A Dialogue Between Polarization and Motility.* IUBMB Life, 2000. **49**(2): p. 89-96.
8. Ulrich, F. and C.-P. Heisenberg, *Trafficking and Cell Migration.* Traffic, 2009. **10**(7): p. 811-818.
9. Biname, F., et al., *What makes cells move: requirements and obstacles for spontaneous cell motility.* Molecular BioSystems. **6**(4): p. 648-661.
10. Watanabe, T., J. Noritake, and K. Kaibuchi, *Regulation of microtubules in cell migration.* Trends in Cell Biology, 2005. **15**(2): p. 76-83.
11. Pollard, T.D., *Cellular Motility Driven by Assembly and Disassembly of Actin Filaments.* Cell, 2003. **112**(453-465).
12. Park, S., D. Koch, et al., *Cell Motility and Local Viscoelasticity of Fibroblasts.* Biophysical Journal, 2005. **89**: p. 4330-4342.
13. Caldieri, G., et al., *Chapter 1 Cell and Molecular Biology of Invadopodia*, in *International Review of Cell and Molecular Biology*. 2009, Academic Press. p. 1-34.
14. Naumanen, P., P. Lappalainen, and P. Hotulainen, *Mechanisms of actin stress fibre assembly.* Journal of Microscopy, 2008. **231**(3): p. 446-454.
15. Yamaguchi, H. and J. Condeelis, *Regulation of the actin cytoskeleton in cancer cell migration and invasion.* Biochimica et Biophysica Acta (BBA) - Molecular Cell Research, 2007. **1773**(5): p. 642-652.
16. Yilmaz, M. and G. Christofori, *EMT, the cytoskeleton, and cancer cell invasion.* Cancer and Metastasis Reviews, 2009. **28**(1): p. 15-33.
17. Block, J., et al., *Filopodia formation induced by active mDia2/Drf3.* Journal of Microscopy, 2008. **231**(3): p. 506-517.
18. Yang, C., et al., *Novel Roles of Formin mDia2 in Lamellipodia and Filopodia Formation in Motile Cells.* PLoS Biol, 2007. **5**(11): p. e317.
19. Honore, S., E. Pasquier, and D. Braguer, *Understanding microtubule dynamics for improved cancer therapy.* Cellular and Molecular Life Sciences, 2005. **62**(24): p. 3039-3056.
20. Vasquez, R.J., et al., *Nanomolar concentrations of nocodazole alter microtubule dynamic instability in vivo and in vitro.* Mol Biol Cell, 1997. **8**(6): p. 973-985.
21. Kaverina, I., O. Krylyshkina, and J.V. Small, *Microtubule Targeting of Substrate Contacts Promotes Their Relaxation and Dissociation.* The Journal of Cell Biology, 1999. **146**(5): p. 1033-1044.
22. Zaidel-Bar, R., et al., *Early molecular events in the assembly of matrix adhesions at the leading edge of migrating cells.* Journal of Cell Science, 2003. **116**(22): p. 4605-4613.
23. Papusheva, E. and C.-P. Heisenberg, *Spatial organization of adhesion: force-dependent regulation and function in tissue morphogenesis.* EMBO J. **29**(16): p. 2753-2768.

24. Yu, J.A., Nicholas O. Deakin and Christopher E. Turner, *The Focal Adhesion: A Network of Molecular Interactions*, in *Handbook of Cell Signaling*. 2010, Elsevier Inc.
25. Hotulainen, P. and P. Lappalainen, *Stress fibers are generated by two distinct actin assembly mechanisms in motile cells.* The Journal of Cell Biology, 2006. **173**(3): p. 383-394.
26. Hu, Y.-L., et al., *Roles of microfilaments and microtubules in paxillin dynamics.* Biochemical and Biophysical Research Communications, 2006. **348**(4): p. 1463-1471.
27. Todaro, G.J. and H. Green, *QUANTITATIVE STUDIES OF THE GROWTH OF MOUSE EMBRYO CELLS IN CULTURE AND THEIR DEVELOPMENT INTO ESTABLISHED LINES.* The Journal of Cell Biology, 1963. **17**(2): p. 299-313.
28. Chhabra, E.S. and H.N. Higgs, *The many faces of actin: matching assembly factors with cellular structures.* Nat Cell Biol, 2007. **9**(10): p. 1110-1121.
29. Kaverina, I., O. Krylyshkina, and J.V. Small, *Regulation of substrate adhesion dynamics during cell motility.* International Journal of Biochemistry and Cell Biology, 2002. **34**(7): p. 746-761.
30. Zimerman, B., T. Volberg, and B. Geiger, *Early molecular events in the assembly of the focal adhesion-stress fiber complex during fibroblast spreading.* Cell Motility and the Cytoskeleton, 2004. **58**(3): p. 143-159.
31. Smilenov, L.B., et al., *Focal Adhesion Motility Revealed in Stationary Fibroblasts.* Science, 1999. **286**(5442): p. 1172-1174.
32. Bellis, S.L., J. A. Perotta, M. S. Curtis and C. E. Turner, *Adhesion of fibroblasts to fibronectin stimulates both serine and tyrosine phosphorylation of paxillin.* Journal of Biochemistry, 1997. **325**: p. 375-381.
33. Horwitz, A.R. and J.T. Parsons, *Cell Migration--Movin' On.* Science, 1999. **286**(5442): p. 1102-1103.
34. Horwitz, A.R. and J.T. Parsons, *Cell migration - Movin' on.* Science, 1999. **286**(5442): p. 1102-1103.
35. Kaverina, I., K. Rottner, and J.V. Small, *Targeting, Capture, and Stabilization of Microtubules at Early Focal Adhesions.* The Journal of Cell Biology, 1998. **142**(1): p. 181-190.
36. Quintela-Fandino, M., A. GonzÃ¡lez-MartÃ-n, and R. Colomer, *Targeting cytoskeleton reorganisation as antimetastatic treatment.* Clinical and Translational Oncology. **12**(10): p. 662-669.
37. Friedl, P. and D. Gilmour, *Collective cell migration in morphogenesis, regeneration and cancer.* Nature Reviews Molecular Cell Biology, 2009. **10**(7): p. 445-457.
38. Guo, W. and F.G. Giancotti, *Integrin signalling during tumour progression.* Nat Rev Mol Cell Biol, 2004. **5**(10): p. 816-826.
39. Soung, Y.H., J.L. Clifford, and J. Chung, *Crosstalk between integrin and receptor tyrosine kinase signaling in breast carcinoma progression.* BMB Reports. **43**(5): p. 311-318.
40. Gilcrease, M.Z., *Integrin signaling in epithelial cells.* Cancer letters, 2007. **247**(1): p. 1-25.
41. Kornberg, L.J., *Focal adhesion kinase and its potential involvement in tumor invasion and metastasis.* Head & Neck, 1998. **20**(8): p. 745-752.
42. Gabarra-Niecko, V., M.D. Schaller, and J.M. Dunty, *FAK regulates biological processes important for the pathogenesis of cancer.* Cancer and Metastasis Reviews, 2003. **22**(4): p. 359-374.
43. Benlimame, N., et al., *FAK signaling is critical for ErbB-2/ErbB-3 receptor cooperation for oncogenic transformation and invasion.* The Journal of Cell Biology, 2005. **171**(3): p. 505-516.
44. Petit, V. and J.-P. Thiery, *Focal adhesions: structure and dynamics.* Biology of the Cell, 2000. **92**(7): p. 477-494.
45. Wang, Y., Gilmore, Thomas D., *Zyxin and paxillin proteins: focal adhesion plaque LIM domain proteins go nuclear.* Biochimica et Biophysica Acta (BBA) - Molecular Cell Research, 2003. **1593**(2-3): p. 115-120.

46. Romer, L.H., K.G. Birukov, and J.G.N. Garcia, *Focal Adhesions: Paradigm for a Signaling Nexus.* Circ Res, 2006. **98**(5): p. 606-616.
47. Abou Zeid, N., A.-M. Valles, and B. Boyer, *Serine phosphorylation regulates paxillin turnover during cell migration.* Cell Communication and Signaling, 2006. **4**(1): p. 8.
48. Richardson, A. and J.T. Parsons, *Signal transduction through integrins: A central role for focal adhesion kinase?* BioEssays, 1995. **17**(3): p. 229-236.
49. Ubersax, J.A. and J.E. Ferrell Jr, *Mechanisms of specificity in protein phosphorylation.* Nat Rev Mol Cell Biol, 2007. **8**(7): p. 530-541.
50. Yano, H., et al., *Paxillin α and Crk-associated substrate exert opposing effects on cell migration and contact inhibition of growth through tyrosine phosphorylation.* Proceedings of the National Academy of Sciences, 2000. **97**(16): p. 9076-9081.
51. Scheswohl, D., et al., *Multiple paxillin binding sites regulate FAK function.* Journal of Molecular Signaling, 2008. **3**(1): p. 1.
52. Wade, R.a.S.V.P., *Minimal features of paxillin that are required for the tyrosine phosphorylation of focal adhesion kinase.* Journal of Biochemistry, 2005. **393**: p. 565-573.
53. Ezratty, E.J., M.A. Partridge, and G.G. Gundersen, *Microtubule-induced focal adhesion disassembly is mediated by dynamin and focal adhesion kinase.* Nat Cell Biol, 2005. **7**(6): p. 581-590.
54. Broussard, J.A., D.J. Webb, and I. Kaverina, *Asymmetric focal adhesion disassembly in motile cells.* Current Opinion in Cell Biology, 2008. **20**(1): p. 85-90.
55. Johnson, L.N. and R.J. Lewis, *Structural basis for control by phosphorylation.* Chemical Reviews, 2001. **101**(8): p. 2209-2242.
56. Gomperts, B.D., Kramer, Ijsbrand M., Tatham, Peter E. R., *Signal Transduction*. 2nd ed. 2009, Burlington, MA USA: Academic Press.
57. Cohen, P., *The origins of protein phosphorylation.* Nature Cell Biology, 2002. **4**(5): p. E127-E130.
58. Bendetz-Nezer, S. and R. Seger, *Role of Non-phosphorylated Activation Loop Residues in Determining ERK2 Dephosphorylation, Activity, and Subcellular Localization.* Journal of Biological Chemistry, 2007. **282**(34): p. 25114-25122.
59. Pervin, S., et al., *MKP-1-Induced Dephosphorylation of Extracellular Signal-Regulated Kinase Is Essential for Triggering Nitric Oxide-Induced Apoptosis in Human Breast Cancer Cell Lines.* Cancer Research, 2003. **63**(24): p. 8853-8860.
60. Hanks, S.K. and T. Hunter, *Protein kinases 6. The eukaryotic protein kinase superfamily: kinase (catalytic) domain structure and classification.* The FASEB Journal, 1995. **9**(8): p. 576-596.
61. Zhu, H., et al., *Analysis of yeast protein kinases using protein chips.* Nature Genetics, 2000. **26**(3): p. 283-289.
62. Martin, J., K. Anamika, and N. Srinivasan, *Classification of Protein Kinases on the Basis of Both Kinase and Non-Kinase Regions.* PLoS ONE. **5**(9): p. e12460.
63. Brown, N.R., et al., *The structural basis for specificity of substrate and recruitment peptides for cyclin-dependent kinases.* Nat Cell Biol, 1999. **1**(7): p. 438-443.
64. Hanks, S.K., *Genomic analysis of the eukaryotic protein kinase superfamily: A perspective.* Genome Biology, 2003. **4**(5).
65. Mochly-Rosen, D., *Localization of Protein Kinases by Anchoring Proteins: A Theme in Signal Transduction.* Science, 1995. **268**(5208): p. 247-251.
66. Brown, M.C.a.C.E.T., *Paxillin: Adapting to Change.* Physiological Reviews, 2004. **84**(4): p. 1315-1339.
67. Deramaudt, T.B., et al., *FAK phosphorylation at Tyr-925 regulates cross-talk between focal adhesion turnover and cell protrusion.* Mol. Biol. Cell. **22**(7): p. 964-975.

68. Schouest, K.R., et al., *The Germinal Center Kinase GCK-1 Is a Negative Regulator of MAP Kinase Activation and Apoptosis in the <italic>C. elegans</italic> Germline.* PLoS ONE, 2009. **4**(10): p. e7450.
69. Wagner, S., et al., *FAK/src-Family Dependent Activation of the Ste20-Like Kinase SLK Is Required for Microtubule-Dependent Focal Adhesion Turnover and Cell Migration.* PLoS ONE, 2008. **3**(4): p. e1868.
70. Sabourin, L.A. and M.A. Rudnicki, *Induction of apoptosis by SLK, a Ste20-related kinase.* Oncogene, 1999. **18**(52): p. 7566.
71. Dan, I., N.M. Watanabe, and A. Kusumi, *The Ste20 group kinases as regulators of MAP kinase cascades.* Trends in Cell Biology, 2001. **11**(5): p. 220-230.
72. Nicholson, D.W., et al., *Identification and inhibition of the ICE/CED-3 protease necessary for mammalian apoptosis.* Nature, 1995. **376**(6535): p. 37-43.
73. Schaar, D.G., et al., *The identification of a novel cDNA preferentially expressed in the olfactory-limbic system of the adult rat.* Brain Research, 1996. **721**(1-2): p. 217-228.
74. Pawson, T. and J.D. Scott, *Signaling Through Scaffold, Anchoring, and Adaptor Proteins.* Science, 1997. **278**(5346): p. 2075-2080.
75. Sabourin, L.A., et al., *Caspase 3 Cleavage of the Ste20-Related Kinase SLK Releases and Activates an Apoptosis-Inducing Kinase Domain and an Actin-Disassembling Region.* Mol. Cell. Biol., 2000. **20**(2): p. 684-696.
76. Storbeck, C.J., et al., *The Ldb1 and Ldb2 Transcriptional Cofactors Interact with the Ste20-like Kinase SLK and Regulate Cell Migration.* Mol. Biol. Cell, 2009. **20**(19): p. 4174-4182.
77. Pike, A.C.W., et al., *Activation segment dimerization: a mechanism for kinase autophosphorylation of non-consensus sites.* EMBO J, 2008. **27**(4): p. 704-714.
78. Wagner, S., et al., *Association of the Ste20-like Kinase (SLK) with the Microtubule.* Journal of Biological Chemistry, 2002. **277**(40): p. 37685-37692.
79. Roovers, K., et al., *The Ste20-like kinase SLK is required for ErbB2-driven breast cancer cell motility.* Oncogene, 2009. **28**(31): p. 2839-2848.
80. O'Reilly, P.G., et al., *The Ste20-like Kinase SLK Is Required for Cell Cycle Progression through G2.* Journal of Biological Chemistry, 2005. **280**(51): p. 42383-42390.
81. Burakov, A.V., et al., *Ste20-related Protein Kinase LOSK (SLK) Controls Microtubule Radial Array in Interphase.* Mol. Biol. Cell, 2008. **19**(5): p. 1952-1961.
82. Wagner, S.M. and L.A. Sabourin, *A novel role for the Ste20 kinase SLK in adhesion signaling and cell migration.* Cell Adhesion and Migration, 2009. **3**(2): p. 182-184.
83. Turner, C.E., J.R. Glenney, and K. Burridge, *Paxillin: a new vinculin-binding protein present in focal adhesions.* The Journal of Cell Biology, 1990. **111**(3): p. 1059-1068.
84. Turner, C.E. and J.T. Miller, *Primary sequence of paxillin contains putative SH2 and SH3 domain binding motifs and multiple LIM domains: identification of a vinculin and pp125Fak-binding region.* J Cell Sci, 1994. **107**(6): p. 1583-1591.
85. Turner, C.E., *Paxillin and focal adhesion signalling.* Nat Cell Biol, 2000. **2**(12): p. E231-E236.
86. Schaller, M.D., *Paxillin: a focal adhesion-associated adaptor protein.* Oncogene, 2001. **20**(44): p. 6459-6472
87. Tumbarello, D.A. and C.E. Turner, *Hic-5 contributes to epithelial-mesenchymal transformation through a RhoA/ROCK-dependent pathway.* Journal of Cellular Physiology, 2007. **211**(3): p. 736-747.
88. Tumbarello, D.A., et al., *Regulation of paxillin family members during epithelial-mesenchymal transformation: a putative role for paxillin {delta}.* J Cell Sci, 2005. **118**(20): p. 4849-4863.

89. Sen, A., et al., *Paxillin Regulates Androgen- and Epidermal Growth Factor-induced MAPK Signaling and Cell Proliferation in Prostate Cancer Cells.* Journal of Biological Chemistry, 2010. **285**(37): p. 28787-28795.
90. Kaulfus, S., et al., *Leupaxin acts as a mediator in prostate carcinoma progression through deregulation of p120catenin expression.* Oncogene, 2009. **28**(45): p. 3971-3982.
91. Kaulfuss, S., et al., *Leupaxin, a Novel Coactivator of the Androgen Receptor, Is Expressed in Prostate Cancer and Plays a Role in Adhesion and Invasion of Prostate Carcinoma Cells.* Mol Endocrinol, 2008. **22**(7): p. 1606-1621.
92. Heitzer, M.D.a.D.B.D., *Hic-5, an adatpor-like nuclear receptor co-activator.* Journal of the Nuclear Receptor Signaling Atlas, 2006. **4**: p. 1-3.
93. Yuminamochi, T., Yutaka Yatomi, Makoto Osada, Tsukasa Ohmori, Yoshio Ishii, Kumiko Nakazawa, Shigemi Hosogaya, Yukio Ozaki, *Expression of the LIM Proteins Paxillin and Hic-5 in Human Tissues.* Journal of Histochemistry & Cytochemistry, 2003. **51**(4): p. 513-521.
94. Thomas, S.M., M. Hagel, and C.E. Turner, *Characterization of a focal adhesion protein, Hic-5, that shares extensive homology with paxillin.* J Cell Sci, 1999. **112**(2): p. 181-190.
95. Dawid, I.B., J.J. Breen, and R. Toyama, *LIM domains: multiple roles as adapters and functional modifiers in protein interactions.* Trends in Genetics, 1998. **14**(4): p. 156-162.
96. Hagel, M., et al., *The Adaptor Protein Paxillin Is Essential for Normal Development in the Mouse and Is a Critical Transducer of Fibronectin Signaling.* Mol. Cell. Biol., 2002. **22**(3): p. 901-915.
97. Dong, J.-M., et al., *Paxillin nuclear-cytoplasmic localization is regulated by phosphorylation of the LD4 motif: evidence that nuclear paxillin promotes cell proliferation.* Biochem J, 2009. **418**(1): p. 173-184.
98. Hervy, M., L. Hoffman, and M.C. Beckerle, *From the membrane to the nucleus and back again: bifunctional focal adhesion proteins.* Current Opinion in Cell Biology, 2006. **18**(5): p. 524-532.
99. Brown, M.C., J.A. Perrotta, and C.E. Turner, *Serine and Threonine Phosphorylation of the Paxillin LIM Domains Regulates Paxillin Focal Adhesion Localization and Cell Adhesion to Fibronectin.* Mol. Biol. Cell, 1998. **9**(7): p. 1803-1816.
100. Tong, X., et al., *The Bovine Papillomavirus E6 Protein Binds to the LD Motif Repeats of Paxillin and Blocks Its Interaction with Vinculin and the Focal Adhesion Kinase.* Journal of Biological Chemistry, 1997. **272**(52): p. 33373-33376.
101. Brown, M.C., M.S. Curtis, and C.E. Turner, *Paxillin LD motifs may define a new family of protein recognition domains.* Nat Struct Mol Biol, 1998. **5**(8): p. 677-678.
102. Tumbarello, D.A., M.C. Brown, and C.E. Turner, *The paxillin LD motifs.* FEBS Letters, 2002. **513**(1): p. 114-118.
103. Bertolucci, C.M., C.D. Guibao, and J. Zheng, *Structural features of the focal adhesion kinase–paxillin complex give insight into the dynamics of focal adhesion assembly.* Protein Science, 2005. **14**(3): p. 644-652.
104. Deakin, N.O., et al., *An integrin-α-4-14-3-3-ζ-paxillin ternary complex mediates localised Cdc42 activity and accelerates cell migration.* Journal of Cell Science, 2009. **122**(10): p. 1654-1664.
105. Brown, M.C. and C.E. Turner, *Characterization of paxillin LIM domain-associated serine threonine kinases: Activation by angiotensin II in vascular smooth muscle cells.* Journal of Cellular Biochemistry, 2000. **76**(1): p. 99-108.
106. Sanchez-Garcia, I.a.T.H.R., *The LIM domain: a new structural motif found in zinc-finger-like proteins.* Trends in Genetics, 1994. **10**(9): p. 315-320.
107. Wade, R., J. Bohl, and S. Vande Pol, *Paxillin null embryonic stem cells are impaired in cell spreading and tyrosine phosphorylation of focal adhesion kinase.* Oncogene, 2002. **21**(1): p. 96-107.

108. Deakin, N.O. and C.E. Turner, *Paxillin comes of age.* Journal of Cell Science, 2008. **121**(15): p. 2435-2444.
109. Glenney, J.R., Jr. and L. Zokas, *Novel Tyrosine Kinase Substrates from Rous Sarcoma Virus-Transformed Cells Are Present in the Membrane Skeleton.* The Journal of Cell Biology, 1989. **108**(6): p. 2401-2408.
110. Zaidel-Bar, R., et al., *A paxillin tyrosine phosphorylation switch regulates the assembly and form of cell-matrix adhesions.* Journal of Cell Science, 2007. **120**(1): p. 137-148.
111. Sachdev, S., Y. Bu, and I. Gelman, *Paxillin-Y118 phosphorylation contributes to the control of Src-induced anchorage-independent growth by FAK and adhesion.* BMC Cancer, 2009. **9**(1): p. 12.
112. Roy, S., P.J. Ruest, and S.K. Hanks, *FAK regulates tyrosine phosphorylation of CAS, paxillin, and PYK2 in cells expressing v-Src, but is not a critical determinant of v-Src transformation.* Journal of Cellular Biochemistry, 2002. **84**(2): p. 377-388.
113. Thomas, S.M., P. Soriano, and A. Imamoto, *Specific and redundant roles of Src and Fyn in organizing the cytoskeleton.* Nature, 1995. **376**(6537): p. 267-271.
114. Vallés, A.M., M. Beuvin, and B. Boyer, *Activation of Rac1 by Paxillin-Crk-DOCK180 Signaling Complex Is Antagonized by Rap1 in Migrating NBT-II Cells.* Journal of Biological Chemistry, 2004. **279**(43): p. 44490-44496.
115. Romanova, L.Y., et al., *Phosphorylation of paxillin tyrosines 31 and 118 controls polarization and motility of lymphoid cells and is PMA-sensitive.* Journal of Cell Science, 2004. **117**(17): p. 3759-3768.
116. Schaller, M.D. and J.T. Parsons, *pp125FAK-dependent tyrosine phosphorylation of paxillin creates a high- affinity binding site for Crk.* Mol. Cell. Biol., 1995. **15**(5): p. 2635-2645.
117. Vadlamudi, R., Liana Adam, Amjad Talukder, John Mendelsohn and Rakesh Kumar, *Serine phosphorylation of paxillin by heregulin-B1: role of p38 mitogen activated protein kinase.* Oncogene, 1999. **18**: p. 7253-7246
118. Vadlamudi, R., et al., *Transcriptional Up-Regulation of Paxillin Expression by Heregulin in Human Breast Cancer Cells.* Cancer Research, 1999. **59**(12): p. 2843-2846.
119. Yamaguchi, R., et al., *Mitosis specific serine phosphorylation and downregulation of one of the focal adhesion protein, paxillin.* Oncogene, 1997. **15**(15): p. 1753.
120. Nayal, A., et al., *Paxillin phosphorylation at Ser273 localizes a GIT1-PIX-PAK complex and regulates adhesion and protrusion dynamics.* The Journal of Cell Biology, 2006. **173**(4): p. 587-589.
121. Webb, D.J., et al., *Paxillin phosphorylation sites mapped by mass spectrometry.* Journal of Cell Science, 2005. **118**(21): p. 4925-4929.
122. Huang, C., et al., *JNK phosphorylates paxillin and regulates cell migration.* Nature, 2003. **424**(6945): p. 219-223.
123. Donais, K., et al., *FAK-Src signalling through paxillin, ERK and MLCK regulates adhesion disassembly.* Nature Cell Biology, 2004. **6**(2): p. 154-161.
124. Stratagene, *QuikChange Site-Directed Mutagenesis Kit: Instruction Manual*. 2011; Revision #063008, Stratagene/Agilent Technologies.
125. Walker, J.M. and J.M. Walker, *Nondenaturing Polyacrylamide Gel Electrophoresis of Proteins*, in *The Protein Protocols Handbook*. 2002, Humana Press. p. 57-60.
126. Duclos, B., et al., *[2] Chemical properties and separation of phosphoamino acids by thin-layer chromatography and/or electrophoresis*, in *Methods in Enzymology*. 1991, Academic Press. p. 10-21.
127. Ghogomu, S.M., et al., *HIC-5 Is a Novel Repressor of Lymphoid Enhancer Factor/T-cell Factor-driven Transcription.* Journal of Biological Chemistry, 2006. **281**(3): p. 1755-1764.

128. Chiara, L. and N. Paolo, *Immunohistochemistry protocol for γH2AX detection (formalin-fixed paraffin-embedded sections).* 2006.
129. Storbeck, C.J., et al., *Ste20-like kinase SLK displays myofiber type specificity and is involved in C2C12 myoblast differentiation.* Muscle & Nerve, 2004. **29**(4): p. 553-564.
130. Rochlin, K., et al., *Myoblast fusion: When it takes more to make one.* Developmental Biology. **341**(1): p. 66-83.
131. Blom, N., S. Gammeltoft, and S. Brunak, *Sequence- and structure-based prediction of eukaryotic protein phosphorylation sites.* Journal of Molecular Biology, 1999. **294**(5): p. 1351-1362.
132. Loyet, K.M., J.T. Stults, and D. Arnott, *Mass Spectrometric Contributions to the Practice of Phosphorylation Site Mapping through 2003.* Molecular & Cellular Proteomics, 2005. **4**(3): p. 235-245.
133. Delom, F. and E. Chevet, *Phosphoprotein analysis: from proteins to proteomes.* Proteome Science, 2006. **4**(1): p. 15.
134. Ross, H., C.G. Armstrong, and P. Cohen, *A non-radioactive method for the assay of many serine/threonine-specific protein kinases.* Biochem J, 2002. **366**: p. 977-981.
135. Alberts, B., Alexander Johnson, Julian Lewis, Martin Raff, Keith Roberts, Peter Walter, *Molecular Biology of the Cell*. 4th edition ed. 2002, New York: Garland Science (Taylor and Francis Group).
136. Graur, D.a.W.-H.L., *Fundamentals of Molecular Evolution*. 2nd ed. 2000, Sunderland, MA: Sinauer Associates Inc. 18-20.
137. Pixley, F.J., et al., *Protein Tyrosine Phosphatase {phi} Regulates Paxillin Tyrosine Phosphorylation and Mediates Colony-Stimulating Factor 1-Induced Morphological Changes in Macrophages.* Mol. Cell. Biol., 2001. **21**(5): p. 1795-1809.
138. Becker, T., et al., *Multiple functions of LIM domain-binding CLIM/NLI/Ldb cofactors during zebrafish development.* Mechanisms of Development, 2002. **117**(1-2): p. 75-85.
139. Efimov, A. and I. Kaverina, *Significance of microtubule catastrophes at focal adhesion sites.* Cell adhesion & migration, 2009. **3**(3): p. 285-7.
140. Efimov, A., et al., *Paxillin-dependent stimulation of microtubule catastrophes at focal adhesion sites.* Journal of Cell Science, 2008. **121**(2): p. 196-204.
141. West, K.A., et al., *The LD4 motif of paxillin regulates cell spreading and motility through an interaction with paxillin kinase linker (PKL).* The Journal of Cell Biology, 2001. **154**(1): p. 161-176.
142. Hu, Y.-L. and S. Chien, *Dynamic motion of paxillin on actin filaments in living endothelial cells.* Biochemical and Biophysical Research Communications, 2007. **357**(4): p. 871-876.
143. Anan, T., et al., *Human ubiquitin-protein ligase Nedd4: expression, subcellular localization and selective interaction with ubiquitin-conjugating enzymes.* Genes to Cells, 1998. **3**(11): p. 751-763.
144. Chen, Z.J. and L.J. Sun, *Nonproteolytic Functions of Ubiquitin in Cell Signaling.* Molecular cell, 2009. **33**(3): p. 275-286.
145. Yang, W.L., X. Zhang, and H.K. Lin, *Emerging role of Lys-63 ubiquitination in protein kinase and phosphatase activation and cancer development.* Oncogene. **29**(32): p. 4493-4503.
146. Didier, C., et al., *RNF5, a RING Finger Protein That Regulates Cell Motility by Targeting Paxillin Ubiquitination and Altered Localization.* Mol. Cell. Biol., 2003. **23**(15): p. 5331-5345.
147. Dankort, D., et al., *Grb2 and Shc Adapter Proteins Play Distinct Roles in Neu (ErbB-2)-Induced Mammary Tumorigenesis: Implications for Human Breast Cancer.* Mol. Cell. Biol., 2001. **21**(5): p. 1540-1551.
148. Mansour, E.G., P. M. Ravdin and L. Dressler, *Prognostic factors in early breast carcinoma.* Cancer, 1994. **74**: p. 381-400.
149. Chan, C., M. Metz, and S. Kane, *Differential sensitivities of trastuzumab (Herceptin®)-resistant human breast cancer cells to phosphoinositide-3*

kinase (PI-3K) and epidermal growth factor receptor (EGFR) kinase inhibitors. Breast Cancer Research and Treatment, 2005. **91**(2): p. 187-201.
150. Kao, J., et al., *Molecular Profiling of Breast Cancer Cell Lines Defines Relevant Tumor Models and Provides a Resource for Cancer Gene Discovery.* PLoS ONE, 2009. **4**(7): p. e6146.
151. (ATCC), A.T.C.C., *BT-474*.
152. (ATCC), A.T.C.C., *SK-BR-3*.
153. (ATCC), A.T.C.C., *MDA-MB-231*.
154. O'Shaughnessy, J., *Extending Survival with Chemotherapy in Metastatic Breast Cancer.* The Oncologist, 2005. **10**(suppl 3): p. 20-29.
155. Geiger, T.R. and D.S. Peeper, *Metastasis mechanisms.* Biochimica et Biophysica Acta (BBA) - Reviews on Cancer, 2009. **1796**(2): p. 293-308.
156. Baker, E.L., et al., *Cancer Cell Migration: Integrated Roles of Matrix Mechanics and Transforming Potential.* PLoS ONE. **6**(5): p. e20355.
157. Amano, M., et al., *A Proteomic Approach for Comprehensively Screening Substrates of Protein Kinases Such as Rho-Kinase.* PLoS ONE. **5**(1): p. e8704.
158. Hoellerer, M.K., et al., *Molecular Recognition of Paxillin LD Motifs by the Focal Adhesion Targeting Domain.* Structure (London, England : 1993), 2003. **11**(10): p. 1207-1217.
159. Lorenz, S., et al., *Structural Analysis of the Interactions Between Paxillin LD Motifs and ±-Parvin.* Structure (London, England : 1993), 2008. **16**(10): p. 1521-1531.
160. Mok, J., et al., *Deciphering Protein Kinase Specificity Through Large-Scale Analysis of Yeast Phosphorylation Site Motifs.* Sci. Signal. **3**(109): p. ra12-.
161. Falin, R.A., et al., *Identification of regulatory phosphorylation sites in a cell volume- and Ste20 kinase-dependent ClC anion channel.* The Journal of general physiology, 2009. **133**(1): p. 29-42.
162. Delpire, E., *The mammalian family of sterile 20p-like protein kinases.* Pflügers Archiv European Journal of Physiology, 2009. **458**(5): p. 953-967.
163. Zhu, G., et al., *A Single Pair of Acidic Residues in the Kinase Major Groove Mediates Strong Substrate Preference for P-2 or P-5 Arginine in the AGC, CAMK, and STE Kinase Families.* Journal of Biological Chemistry, 2005. **280**(43): p. 36372-36379.
164. Villa, F., et al., *Structural insights into the recognition of substrates and activators by the OSR1 kinase.* EMBO Rep, 2007. **8**(9): p. 839-845.
165. Owen, J.D., et al., *Induced Focal Adhesion Kinase (FAK) Expression in FAK-Null Cells Enhances Cell Spreading and Migration Requiring Both Auto- and Activation Loop Phosphorylation Sites and Inhibits Adhesion-Dependent Tyrosine Phosphorylation of Pyk2.* Mol. Cell. Biol., 1999. **19**(7): p. 4806-4818.
166. Han, S.-W., et al., *Expression of HER-2/neu and Paxillin in Ductal Carcinoma in situ, Invasive Ductal Carcinoma with Ductal Carcinoma in situ and Mucinous Carcinoma.* J Breast Cancer, 2008. **11**(3): p. 109-115.
167. Short, S.M., et al., *The Expression of the Cytoskeletal Focal Adhesion Protein Paxillin in Breast Cancer Correlates with HER2 Overexpression and May Help Predict Response to Chemotherapy: A Retrospective Immunohistochemical Study.* The Breast Journal, 2007. **13**(2): p. 130-139.
168. Deakin, N.O. and C.E. Turner, *Distinct roles for paxillin and Hic-5 in regulating breast cancer cell morphology, invasion, and metastasis.* Mol. Biol. Cell. **22**(3): p. 327-341.
169. Bosch, A., et al., *Triple-negative breast cancer: Molecular features, pathogenesis, treatment and current lines of research.* Cancer treatment reviews. **36**(3): p. 206-215.
170. Terfera, D.R., M.C. Brown, and C.E. Turner, *Epidermal growth factor stimulates serine/threonine phosphorylation of the focal adhesion protein paxillin in a MEK-dependent manner in normal rat kidney cells.* Journal of Cellular Physiology, 2002. **191**(1): p. 82-94.

171. Sen, A., et al., *Paxillin regulates androgen- and epidermal growth factor-induced MAPK signaling and cell proliferation in prostate cancer cells.* Journal of Biological Chemistry. **285**(37): p. 28787-28795.
172. Sakai, K., et al., *Dimerization and the signal transduction pathway of a small in-frame deletion in the epidermal growth factor receptor.* The FASEB Journal, 2006. **20**(2): p. 311-313.
173. Wu, H.-Y. and P.-C. Liao, *Analysis of Protein Phosphorylation Using Mass Spectrometry.* Med J, 2007. **31**(3): p. 217-227.

SLK-mediated Phosphorylation of Paxillin is Required for Focal Adhesion Turnover and Cell Migration

Jennifer L. Quizi[1,2], Paul O'Reilly[1] and Luc A. Sabourin[1,2]

[1]Department of Cellular and Molecular Medicine, University of Ottawa, 451 Smyth Rd., Ottawa, ON, Canada, K1H8M5.

[2]Ottawa Hospital Research Institute, Cancer Therapeutics Program, 501 Smyth Rd, Ottawa, ON, Canada, K1H8L6

Condensed Title: "SLK regulates migration through paxillin"

Number of Characters: 25,582

Corresponding Author: Luc A. Sabourin, Senior Scientist
Ottawa Hospital Research Institute
Cancer Therapeutics, 501 Smyth Rd, Box 926
Ottawa, ON, Canada
K1H8L6

ABSTRACT

Focal adhesion turnover is a complex process required for cell migration. We have previously shown that the Ste20-like kinase SLK is required for cell migration and efficient focal adhesion turnover in a FAK-dependent manner. However, the role of SLK in this process remains unclear. Using a candidate substrate approach, we show that SLK phosphorylates the adhesion adapter protein paxillin on serine 250. Serine 250 phosphorylation is required for paxillin ubiquitylation, redistribution and interaction with FAK. Mutation of paxillin serine 250 prevents its phosphorylation by SLK *in vitro* and results in impaired adhesion turnover and migration *in vivo* as evidenced by an accumulation of phospho-FAK-Tyr397 and impaired focal adhesion turnover rates. Together, our data suggest that SLK phosphorylation of paxillin on serine 250 is required for FAK-dependent focal adhesion dynamics.

INTRODUCTION

Cell migration is a complex, multi-step process that is essential for embryonic development, inflammatory response, wound repair, tumorigenesis and metastasis (Horwitz and Parsons 1999). The integrin family of transmembrane proteins initiates this process by binding extracellular matrix ligands such as fibronectin and vitronectin, catalyzing the formation of mulitprotein complexes known as focal adhesions (FA) (Parsons, Horwitz et al.; Bellis 1997; Hoellerer, Noble et al. 2003; Abou Zeid, Valles et al. 2006). Cycles of attachment at the cell front, release at the rear and traction in between, are mediated by these adhesion complexes and are required to generate the force necessary for translocation in a specific direction (Manes, Mira et al. 2000; Zaidel-Bar, Ballestrem et al. 2003). At the molecular level, adhesions are a dynamic assembly of cytoplasmic proteins whose composition varies over time to include differential proportions of FAK, Src, vinculin, paxillin and zyxin (Zaidel-Bar, Ballestrem et al. 2003; Ezratty, Partridge et al. 2005; Romer, Birukov et al. 2006; Gilcrease 2007; Broussard, Webb et al. 2008; Efimov, Schiefermeier et al. 2008). As an integrin-interacting unit, these proteins transduce the nature of the extracellular environment throughout the cell by initiating a number of downstream signaling cascades that ultimately feedback onto the adhesions themselves, regulating the rate at which they turnover (Parsons, Horwitz et al.; Abou Zeid, Valles et al. 2006). Consequently, adhesion turnover represents a critical rate limiting step in the acquisition of a migratory phenotype.

Although the molecular mechanisms involved in the assembly of FAs are well documented, the same cannot be said about their dissolution. However, the destabilization of focal adhesions appears to be mediated in part, by the microtubule network. It is believed that microtubule targeting of FAs delivers a 'destabilizing' signal to nascent adhesions at the leading edge as well as mature adhesions at the rear of the cell (Kaverina, Krylyshkina et al. 1999; Efimov, Schiefermeier et al. 2008; Efimov and Kaverina 2009). We have previously shown that the Ste20-like kinase SLK is a microtubule-associated protein that can be activated during cell migration in a FAK-dependent manner (Wagner, Flood et al. 2002; Wagner, Storbeck et al. 2008). Specifically, SLK, a serine/threonine kinase that is ubiquitously expressed in adult tissues and cell lines, has been shown to co-immuoprecipitate with tubulin and localize with polymerized microtubules during normal adhesion and spreading (Wagner, Flood et al. 2002). Interestingly, SLK overexpression has also been shown to disrupt the organization of actin stress fibres and the stability of focal adhesions (Wagner, Flood et al. 2002). Recently, we have demonstrated that SLK activation, through FAK signalling, is required for microtubule-dependent focal adhesion turnover and cell migration (Wagner, Storbeck et al. 2008; Roovers, Wagner et al. 2009). Although this is consistent with a role for SLK in focal adhesion disassembly, the precise mechanisms by which SLK affects adhesion turnover has yet to be elucidated.

Here we provide evidence that SLK mediates adhesion turnover through the phosphorylation of the focal adhesion protein, paxillin (Brown 2004). Defined by an amino-terminal LD and carboxy-terminal LIM domain respectively, paxillin is a 68 kDa multi-domain adaptor protein that localizes predominantly to FAs (Brown 2004). Interestingly, the phosphorylation status of paxillin has been implicated in the regulation of adhesion formation, disassembly and signaling (Brown and Turner 2002; Brown 2004). Accordingly, our results show that phosphorylation of paxillin within the LD3 domain (serine 250) by SLK is required for focal adhesion turnover and efficient cell migration. Moreover, we provide evidence that this phosphorylation event is required for paxillin ubiquitylation and FAK interaction. Overall, our data suggest that SLK regulates FAK-dependent adhesion turnover through the phosphorylation of paxillin.

RESULTS

SLK phosphorylates paxillin on Serine 250 *in vitro*

We have previously shown that SLK is required for efficient focal adhesion turnover (Wagner, Flood et al. 2002). Supporting a role for SLK in cytoskeletal dynamics and cell migration, confocal microscopy studies show that SLK can be co-localized with paxillin and other adhesion proteins in membrane ruffles and at the leading edge of migrating cells (**Figure 1**) (Wagner, Flood et al. 2002; Wagner, Storbeck et al. 2008). Interestingly, SLK can also be co-localized with the microtubule network at the leading edge of migrating cells (**Figure 1**).

Serine/threonine phosphorylation of paxillin has been shown to regulate adhesion dynamics in migrating cells (Abou Zeid, Valles et al. 2006). Therefore, using a candidate approach we tested the possibility that paxillin could be phosphorylated by SLK. To determine whether SLK could phosphorylate paxillin *in vitro*, endogenous SLK was immunoprecipitated (IP) from scratch-wounded monolayers of MEF-3T3 and incubated with full length purified recombinant GST-paxillin protein in the presence of [^{32}P]-γ-ATP (Etienne-Manneville and Hall 2001). Subsequent SDS-PAGE and autoradiography shows that SLK phosphorylates human paxillin *in vitro* **(Figure 2a)**.

The use of endogenous SLK from scratch wounded MEF-3T3 cells as the source of active SLK raises the possibility that paxillin phosphorylation may be due to the activity of an associated kinase. To test this, wildtype (HA-SLK) and kinase dead (HA-K63R) SLK were transiently transfected into 293 cells and immunoprecipitated using anti-HA (12CA5) antibodies. Immune complexes were then subjected to *in vitro* kinase assays using recombinant GST-paxillin. As seen in **Figure 2b**, GST-paxillin phosphorylation can be observed in the presence of wildtype HA-SLK but not with the kinase inactive mutant HA-K63R, suggesting that SLK-mediated phosphorylation of GST-paxillin is not due to another kinase co-immunoprecipitating with SLK. Further characterization of this phosphorylation event by phospho-amino acid analysis revealed that SLK exclusively phosphorylates paxillin on serine residue(s) **(Figure 2c).**

Perhaps due to a low efficiency of phosphorylation *in vitro*, multiple rounds of mass spectrometry failed to identify a site of phosphorylation in GST-paxillin. Therefore, the critical region was narrowed down using deletion constructs. Subsequent *in vitro* kinase assays showed SLK to phosphorylate the amino terminal LD domain of paxillin, exclusively (**Figure 3b**). Additional N-terminal deletions of the LD domain were then generated within the context of the full length protein. Further *in vitro* kinase assays using three amino-terminal deletions of paxillin showed that SLK phosphorylates paxillin within its LD3 domain, specifically within a region of 20 amino acids encompassing serine residues S243, S244 and S250 **(Figure 3c)**.

Each of the candidate serine residue within this 20 amino acid stretch were mutated to a non-phosphorylatable glycine or alanine residue (S243G, S244G or S250A). Paxillin point mutants were then subjected to an *in vitro* kinase assay using SLK immunoprecipitated from scratch wounded MEF-3T3. Interestingly, all three phospho-inactivating mutations resulted in a complete loss of paxillin phosphorylation (**Figure 3d**), suggesting that some or all of these sites are important for SLK-mediated paxillin phosphorylation. To rule out possible effects of the point mutations on conformation, each serine was mutated to a conserved threonine residue. Whereas the phosphorylation of the S243T and S244T mutants is still observed, the paxillin S250T mutant can no longer be phosphorylated by SLK *in vitro*, suggesting that SLK phosphorylates paxillin exclusively on serine 250 **(Figure 3e).** Interestingly, no threonine phosphorylation was observed in the S250T mutant, suggesting that it cannot substitute for a serine residue in the SLK recognition site (**Figure 3f**). Furthermore, these results suggest that these serines may also be critical for substrate recognition or paxillin conformation.

Paxillin serine 250 is phosphorylated *in vivo*

To investigate whether paxillin is phosphorylated *in vivo* on serine 250, a peptide-affinity purified paxillin S250-specific phospho-antibody was generated against a murine paxillin phosphopeptide corresponding to amino acids 244-255 (CSPQRVT**pS**SQQQT). Anti-phopsho paxillin S250 (pPxnS250) immunoblotting shows a single reactive species at the predicted paxillin molecular weight. However, in paxillin-null cells, no reactivity was observed suggesting that the pPxnS250 polyclonal is specific to phospho-paxillin **(Figure 4a)**.

We have previously shown that SLK kinase activity is upregulated in scratch wounded MEF-3T3 within 60 min (**Figure 4b**) (Wagner, Flood et al. 2002). To survey the status of paxillin S250 phosphorylation during cell migration, confluent MEF-3T3 were scratch wounded and the levels of pPxnS250 were assessed by Western blot. As shown in Figure 4b, the kinetics of pPxnS250 phosphorylation were strikingly similar to that of SLK activity, reaching a maximum at around 60 min post wounding **(Figure 4c)**. Additionally, short hairpin-directed knockdown of SLK in MEF-3T3 resulted in a marked decrease in pPxnS250 in both confluent monolayers and at 60 minutes post wounding.

Interestingly, the levels of phospho-paxillin were reduced whereas total paxillin was upregulated in the SLK knockdown samples, suggesting that this modification may also regulate paxillin levels (**Figure 4c**). This, taken together with the observation that residual SLK activity appears to be sufficient to maintain a low level of paxillin phosphorylation, suggests that SLK phosphorylates paxillin at 250 *in vivo*.

Interestingly, immunofluorescence studies show that both total and phospho-S250 paxillin can be localized to membrane ruffles. However, pPxnS250 predominantly localizes to focal adhesions and along actin stress fibres (**Figure 4d and Suppl. Fig. 1**). In addition, a strong signal can be observed in the nucleus, suggesting that pPxnS250 may also have a nuclear-specific function**.**

Paxillin S250 phosphorylation is required for adhesion turnover and efficient cell migration

Although conflicting reports exist on the role of paxillin in the formation of adhesions (Brown, Perrotta et al. 1998; Wade, Bohl et al. 2002), we tested the involvement of serine 250 phosphorylation in this process. To determine whether S250 is required for cell adhesion, GFP-Paxillin S250T and wildtype paxillin were transiently transfected into MEF-3T3 cells, GFP-sorted using flow cytometry and plated onto uncoated surfaces. Enumeration of the adherent cells at specific time points revealed no significant differences in the rate of adhesion between cells over-expressing the S250T mutation when compared to wildtype paxillin (**Suppl. Fig. 2**).

Since paxillin-deficient cells have been observed to spread and migrate at reduced rates (Hagel, George et al. 2002), we also investigated the role of S250 phosphorylation in cell spreading. GFP fusion expressing MEF-3T3 cells were flow sorted prior to plating on fibronectin coated plates. Phase contrast and fluorescence microscopy was used at 30 minute intervals to capture the extent of spreading of the fibroblasts. Cell spreading measurements revealed that expression of a GFP-S250T mutant results in a significant delay in cell spreading when compared to both wildtype paxillin and the GFP control **(Figure 5a)**. Phase contrast images of cells at 90 minutes post-plating **(Figure 5b)**, further illustrate this defect.

Deficiencies in cell spreading often result in reduced rates of cell migration. Therefore, we tested whether expression of the S250T mutant could impair cell motility. To investigate the migratory capacity of the paxillin S250T mutant, MEF-3T3 stably over-expressing Myc-S250T, Myc-paxillin or vector control were subjected to wound closure and haptotaxis assays on fibronectin-coated substrates. Expression of the S250T mutant resulted in a 2-fold decrease in migration when compared to wildtype paxillin (**Figure 5c**)**.** Similarly, a significant delay in wound closure was observed in S250T-expressing cells (**Figure 5d**). Together, these data suggests that serine 250 phosphorylation is required for cell spreading and efficient cell migration.

Adhesion dynamics play a critical role in the regulation of cell migration. Furthermore, paxillin has been previously shown to be required for efficient focal adhesion turnover (Webb, Brown et al. 2003). Therefore, we tested whether paxillin S250 phosphorylation was required for focal adhesion turnover. To investigate this, MEF-3T3 were transiently transfected with the GFP-fusion proteins S250T or wildtype paxillin prior to plating onto a fibronectin-coated dish and live-cell imaging. Area measurements of disassembling focal adhesions revealed a 5-fold decrease in the rate of adhesion turnover in cells expressing the S250T mutant paxillin when compared to wildtype **(Figure 6)**. Specifically, adhesions were found to persist over a 9 minute period in the GFP-PaxillinS250T mutant whereas cells expressing wildtype GFP-paxillin exhibit signs of dissociation in less than 6 minutes **(Figure 6a and Suppl. Fig. 3 & 4)**. Together these results suggest that paxillin phosphorylation at serine 250 is critical for adhesion turnover and cell motility.

Focal adhesion turnover has been correlated with decreased levels of phospho-FAKY397 immunoreactivity whereas stable adhesions show persistent elevated levels (Ezratty, Partridge et al. 2005; Scheswohl, Harrell et al. 2008). Additionally, turnover has been correlated with increased FAK-Y925 phosphorylation (Deramaudt, Dujardin et al.; Brown 2004). To further support a role for S250 phosphorylation in adhesion turnover, nocodazole wash-out experiments show microtubule repolymerization to induce phosphorylation of paxillin S250 and FAK-Y925 within 15 and 30 minutes, respectively (**Figure 7a**). The incidence of S250 phosphorylation preceding that of FAK-Y925 suggests that paxillin S250 phosphorylation may be a rate limiting step in the kinetics of adhesion turnover. Furthermore, consistent with a reduced rate of turnover, cells expressing the Myc-PaxillinS250T mutant display higher levels of phospho-FAKY397 but reduced FAK phosphorylation at tyrosine 925 when compared to wildtype Myc-Paxillin (**Figure 7b**). Consequently, these results suggest that microtubule-mediated adhesion turnover requires paxillin phosphorylation by SLK.

Studies involving paxillin-null fibroblasts demonstrated that while paxillin is not absolutely necessary for the localization of FAK to focal adhesions, their interaction is required for the complete activation of FAK (Deramaudt, Dujardin et al.; Zimerman, Volberg et al. 2004; Scheswohl, Harrell et al. 2008). Therefore, we tested the possibility that serine 250 phosphorylation may play a role in paxillin recruitment to the FAK-adhesion complex. Expression and immunoprecipitation of Myc-PaxillinS250T or Myc-Paxillin shows that FAK is unable to co-precipitate with the paxillin S250T mutant (**Figure 7b**), suggesting that paxillin S250 phosphorylation is required for its recruitment to the FAK complex and adhesion turnover.

Although ubiquitylation is best known for its role in the selective degradation and/or processing of intracellular proteins in eukaryotic cells (Anan, Nagata et al. 1998), recent evidence suggests a non-proteolytic role for ubiquitin in the regulation of protein localization and activation (Yang, Zhang et al.; Chen and Sun 2009). Supporting this, paxillin ubiquitylation has previously been shown to alter its cellular distribution (Didier, Broday et al. 2003). Therefore, we tested the possibility that paxillin S250 phosphorylation acts as a signal for ubiquitylation and recruitment to adhesions. Immunoprecipitation of Myc-Paxillin or Myc-Paxillin S250T followed by anti-ubiquitin immunoblotting reveals undetectable levels of ubiquitylated protein in the Myc-PaxillinS250T immunoprecipitation, suggesting that serine 250 phosphorylation is required for paxillin ubiquitylation **(Figure 7c)**. Supporting this, nocodazole wash-out experiments reveal the presence of a higher molecular weight paxillin at 30 and 45 minutes post-wash **(Figure 7a)** which may correspond to further modifications of paxillin such as ubiquitylation **(Figure 7a)**. Together, these findings suggest that paxillin may require to be phosphorylated and ubiquitylated in order to interact with FAK and induce adhesion turnover.

Discussion

Cell migration is a complex, multi-step process that requires a dynamic balance between focal adhesion assembly and disassembly that culminates in the reorganization of the cytoskeleton (Manes, Mira et al. 2000; Petit and Thiery 2000). Consistent with a role in migration, the Ste20-like kinase SLK has been shown to affect actin remodelling and microtubule-dependent focal adhesion turnover (Wagner, Flood et al. 2002; Wagner, Storbeck et al. 2008). To gain insights into the role of SLK in focal adhesion turnover, we tested its ability to phosphorylate paxillin, a protein implicated in the regulation of adhesion turnover (Amano, Tsumura et al.). Using *in vitro* kinase assays we have shown that SLK can phosphorylate human paxillin within the LD3 domain on serine 250. Interestingly, there are no known binding partners or confirmed phosphorylation sites described for the LD3 domain, although S231 is a predicted ERK phosphorylation site (Brown 2004; Webb, Schroeder et al. 2005).

As SLK can associate with the microtubule network, our results suggest that it is part of the microtubule-associated focal adhesion disassembly signal (Wagner, Flood et al. 2002; Wagner, Storbeck et al. 2008). Interestingly, our previous findings and the data presented here suggest that SLK cannot be localized to focal adhesions, rather, it can co-localize with adhesion proteins in membrane ruffles, in close proximity to focal adhesions. Therefore, we propose that SLK is delivered by the microtubule network in proximity to focal adhesions where it can phosphorylate paxillin. This phosphorylation then induces paxillin ubiquitylation and recruitment to FAK-containing adhesion complexes, allowing for further signalling and turnover. Alternatively, SLK may phosphorylate tubulin-bound and/or free cytosolic paxillin at the membrane ruffle (Brown and Turner 2002; Scheswohl, Harrell et al. 2008). This, in turn, facilitates its distribution to focal adhesions through the association of pPxn250 with the actin stress fibre network. Moreover, the localization of mutant GFP-Paxillin S250T to focal adhesions exclusively (**Figure 6**), suggests that this phosphorylation event is not required for focal adhesion targeting but rather for interaction with the signalling complex.

Our previous results show that SLK is activated in a FAK/c-src-dependent manner following scratch wounding of confluent monolayers (Wagner, Storbeck et al. 2008). Conversely, in the absence of activated SLK, fibroblasts have been shown to exhibit a delay in migration (Wagner, Storbeck et al. 2008; Roovers, Wagner et al. 2009). Interestingly, expression of the paxillin S250T mutation in fibroblasts mirrors this migration defect, suggesting that SLK regulates migration through the phosphorylation of paxillin at S250.

Following FAK autophosphorylation, an association between FAK and paxillin is required for FAK to become fully activated and induce adhesion turnover (Deramaudt, Dujardin et al.; Zimerman, Volberg et al. 2004; Scheswohl, Harrell et al. 2008). In the absence of this association, FAK exhibits altered Src-mediated phosphorylation at Y576 and Y577 which prevents the subsequent phosphorylation of Y925, a focal adhesion disassembly signal. Accordingly, our results show that the expression of PxnS250T impairs the phosphorylation status of FAKY925 resulting in more persistent adhesions in these transfected cells. Furthermore, nocodazole wash-out results in serine 250 phosphorylation followed by FAK-Y925 phosphorylation, suggesting that SLK-mediated phosphorylation of paxillin may be required for FAK-dependent adhesion turnover as previously reported (Deramaudt, Dujardin et al.; Zimerman, Volberg et al. 2004;

Scheswohl, Harrell et al. 2008). Interestingly, we have shown that the dominant negative paxillin S250T mutation ablates the ability of paxillin to interact with FAK. This supports previous observations whereby the paxillin-FAK interaction is required for full activation of FAK (Deramaudt, Dujardin et al.; Brown 2004).

Lastly, we have shown that the paxillin S250T mutant exhibits undetectable levels of ubiquitylation, suggesting that S250 phosphorylation precedes ubiquitylation. Supporting this, nocodazole wash-out triggers the phosphorylation of serine 250 which is accompanied by a mobility shift of the paxillin protein, perhaps as a result of ubiquitylation. The ability of wildtype, but not mutant paxillin, to interact with FAK suggests that FAK associates with a phosphorylated and ubiquitylated form of paxillin. We propose that the phosphorylation of paxillin by SLK in the vicinity of adhesion complexes induces its ubiquitylation and recruitment to the FAK complex. This interaction in turn, stimulates further intracellular signalling and FAK-mediated adhesion turnover **(Figure 8)**. Overall, our data suggest that SLK regulates FAK-mediated adhesion turnover through the phosphorylation of paxillin at S250 and its subsequent interaction with the adhesion complex.

AKNOWLEDGEMENTS

This work was supported by the Canadian Institute for Health Research and the Canadian Breast Cancer Foundation. JQ is the recipient of a Canadian Breast Cancer Foundation scholar award. LAS is the recipient of a CIHR scholar award. PO is the recipient of an OGSST studentship.

Materials and Methods

Purified recombinant GST-fusion protein preparations:

Low density cultures of glutathione-S-transferase (GST)-tagged fusion protein were grown from bacterial stocks in 3 ml of Luria-Bertani broth (LB) containing 50 µg/ml ampicillin in a 37°C shaker. Cultures were induced for 2h with 1 mM isopropyl-beta-D-thiogalactopyranoside (IPTG; Sigma). Following induction, bacteria were collected and lysed in RIPA buffer containing inhibitors (50 mM Tris-HCl (pH 7.4), 150 mM NaCl, 1 mM EDTA, 1% TritonX-100, 0.5% sodium deoxycholate, 0.1% SDS, 1% Nonidet P-40, 2 mM DTT, 10 µg/ml leupeptin, 10 µg/ml pepstatin, 10 µg/ml aprotinin, 1mM phenylmethylsulphonylfluoride (PMSF) and 100 µM benzamidine). Protein lysates were cleared by centrifugation (10 minutes at 14,000*g*) and transferred to glutathione sepharose beads (GE Healthcare Life Sciences) for 30 minutes at room temperature. Beads were recovered by pulse centrifugation at maximum speed and washed 4X in NETN ((20 mM Tris-HCl pH 8.0, 1 mM EDTA, 200 mM NaCl, 0.5% Noniodet P-40) buffer prior to being used in other assays.

Immunoprecipitation and *in vitro* kinase assays

For immunoprecipitation, 200-400 µg of protein lysate was used in combination with 2 µg of SLK antibody in the presence of 20 µl of protein A sepharose beads (GE Health Care, Piscataway, NJ, USA) and inverted for 2 h at 4°C. Immune complexes were collected by pulse centrifugation at maximum speed and washed 4 times in NETN buffer (20 mM Tris-HCl pH 8.0, 1 mM EDTA, 200 mM NaCl, 0.5% Noniodet P-40).

In vitro kinase assays were performed as previously described in (Sabourin and Rudnicki 1999) on SLK immunoprecipitations obtained from scratch-wounded cell lysates (ref 15, 17). In the case of the *in vitro* kinase assays where purified recombinant GST protein is added, the recombinant protein on glutathione beads was combined with the immunoprecipitated SLK on protein A sepharose prior to the first wash in NETN buffer. The kinase reaction was halted by the addition of 4X SDS sample buffer and resolved using 4-20% SDS-PAGE. Gels were either stained with coomassie brilliant blue and dried, or transferred to PVDF prior to exposure to X-ray film at -80°C for autoradiography. Transferred membranes were then subjected to Western blot analysis to normalize for SLK levels.

Phosphoamino acid analysis:

Amino acid hydrolysis of [^{32}P]-labelled phosphorylated protein was achieved by excising metabolically labeled proteins from PVDF membranes post kinase assay and incubation at 100°C in 6M HCL for 1h. Samples were then lyophilized before phospho-amino acid standards were added (1mg/ml). Phosphoamino acids were separated using 2-D thin layer electrophoresis as described (Duclos, Marcandier et al. 1991). Phosphoamino acids were then detected using ninhydrin staining and autoradiography.

Antibodies and reagents

Paxillin, FAK and phospho-FAKY397 were purchased from BD transduction laboratories and used at dilutions ranging from 1:1000 to 1:5000 (Mississauga, ON, Canada). Other antibodies used in these studies were γ-tubulin (Sigma-Aldrich, Oakville, Ontario, Canada), Myc (Sigma-Aldrich; 9E10 mouse ascites), HA (Sigma-Aldrich; 12CA5 mouse ascites), GFP (Santa Cruz Biotechnology, Santa Cruz, California, USA), ubiquitin

(Abgent Inc., San Diego, California, USA) and DAPI (nucleic acid stain; Invitrogen, Carlsbad, California, USA). Anti-SLK and phospho-paxillinS250 antibodies were custom made by Dr. Toshi Myazaki (Medical & Biological Laboratories, Co., Ltd., Nagoya, Japan).

Cell Culture, Plasmids and Transient Transfections/Infections:

Paxillin cDNA encoding full length human paxillin4 (accession # U14588) was kindly provided by Dr. Victor Small (Vienna, Austria). The human-paxillin-4 coding region was amplified by PCR with complimentary oligonucleotides containing a 5' *BglII* and a 3' *EcoRI* restriction site. The PCR products were subcloned into *BamHI*/*EcoRI*-digested pGex (Promega), pCAN-HA (Clontech), pCAN-Myc (Clonetech) and GFP vectors (Clontech). Point mutations were made using and according to the protocol from Stratagene's (Agilent; Santa Clara, California, USA) 'QuikChange XL Site-Directed Mutagenesis Kit' using GST-tagged paxillin cDNA as the template. Myc-tagged paxillin cDNA in a hygromycin vector was also used as template to make point mutants for use in the generation of stable cell lines.

Transient transfections in HEK293 cells were performed with 5 µg of plasmid DNA per 10 cm plate of cells using Lipofectamine/Plus transfection reagents as per the manufacturer's instructions (Invitrogen). Adenovirus Infections of MEF-3T3 were performed at an MOI of 10. Infections in 10 cm plates were carried out in serum-free DMEM for 1.5 h at 37°C and 5% CO_2. Plates were then topped up to 10 ml with DMEM with 10% FBS and left at 37°C and 5% CO_2 for 48h prior to being collected and used in subsequent experiments.

For microtubule-dependent adhesion turnover assays, subconfluent MEF-3T3 were serum-starved overnight prior to being treated with 10 µM nocodazole for 3 hours. The cultures were then washed 3 times in tissue culture grade phosphate-buffered saline (PBS) and refed with 10% DMEM for the duration of the time course. Cells were collected at various time points and surveyed for pFAKY925, pFAKY397 and pPxnS250 immunoreactivity by Western blotting.

Spreading and Migration Assays

For transwell Boyden chamber migration assays, cells were seeded at a density of 5 X 10^4 cells per transwell (Fisher, Ottawa, Ontario, Canada) migration chamber in 10% FBS DMEM. Migration chambers were pre-coated with 10 µg/ml fibronectin for one hour prior to plating. Cells were allowed to migrate for 6 h toward 10% FBS DMEM in the bottom chamber. Cells remaining on the upper side of the filter were removed and cells that migrated through to the underside of the filter were fixed in 4% paraformaldehyde (PFA) and stained with 0.5 µg/ml DAPI (4,6-diamidino-2-phenylindole; Sigma). DAPI-stained nuclei were visualized using fluorescent microscopy and counted from four random fields of view using a Zeiss Axiocam digital camera. For each cell line, three independent experiments were performed in triplicate.

Wound healing experiments were also conducted using stable cell lines. Cells were seeded at a density of 3 x 10^5 cells per well in a 24-well, fibronectin-coated plate and grown to confluency. Artificial wounds were introduced in the confluent monolayer using a micropipette tip. The wounds were visualized using phase contrast microscopy and photographed using a Zeiss Axiocam digital camera. For each wound, five predetermined and independent points were photographed at 0 and 10h to measure the distance between converging wound fronts. Measurements made using ImageJ software were averaged among 4 independent experiments to calculate the percent wound closure.

Westen Blotting and Immunofluorescence

For Western blotting, cells were washed once in cold PBS and lysed in RIPA buffer containing 50 mM Tris-HCl (pH 7.4), 150 mM NaCl, 1 mM EDTA, 1% TritonX-100, 0.5% sodium deoxycholate, 0.1% SDS, 1% Nonidet P-40. Equal amounts of protein (20-40 µg) were resolved on an 8-12% acrylamide gel then transferred to PVDF (polyvinylidene difluoride) membrane. Membranes were blocked and probed with the indicated antibodies in the presence of 5% BSA or milk powder at 4°C in 1X TBST (50mM Tris pH 7.4, 150 mM NaCl, 0.1% Tween 20). Proteins were visualized following the addition of horseradish peroxidase-coupled secondary antibody, chemiluminescence (Perkin-Elmer, Waltham, MA, USA), and exposure to X-ray film.

For immunofluorescence, cells were plated onto fibronectin-coated (10 µg/ml) coverslips and incubated overnight at 37°C prior to being fixed with 4% paraformaldehyde (PFA). Following permeablization (0.3% Triton X-100 in 1X modified PBS:; StoPBS, 4mM Na_2HPO_4, 2mM NaH_2PO_4, 140mM NaCl, 3mM KCl), cells were washed and incubated with primary antibodies at room temperature for 1 h or overnight at 4°C. Primary antibodies were detected using anti-mouse and/or anti-goat secondaries conjugated to either fluorescein isothiocyanate (FITC; Alexa Fluor 488, Invitrogen) or tetramethyl rhodamine isothiocyanate (TRITC; Alexa Fluor 594, Invitrogen). Slides were visualized with a Zeiss LSM5 laser-scanning confocal microscope and photographed using LSM5 Pascal software and a Sony Corporation HB050 digital camera.

GFP Sorting, Cell Spreading and Live Imaging Microscopy:

MEF-3T3 were transfected with GFP-fusion proteins and 1-2 X 10^7 cells were collected the next day and sorted for GFP content. For cell spreading, 1 X 10^4 GFP-positive cells were plated onto fibronectin-coated dishes and allowed to spread for 2 h at 37°C and 5% CO_2. Phase contrast and fluorescent images (488 nm) were obtained every 30 minutes using a Ziess Colibri LED microscope. Eight different frames of view were photographed using AxioVision software for each cell type and time point. Cell spreading was assessed by measuring the surface area of >10 isolated cells per field of view using ImageJ software.

Live cell imaging was performed on 1-5 X 10^4 GFP-positive cells that were plated onto fibronectin-coated dishes and allowed to spread for 12 h at 37°C and 5% CO_2 prior to imaging. Throughout the imaging process, cells were maintained at 37°C and 5% CO_2 using a heated stage and gas hook-up. Fluorescent images were captured at a frequency of one image/minute for 10 minutes at 488 nm using a Zeiss Colibri LED microscope and AxioVision software. The area of at least 20 focal adhesions per cell type was measured over time using ImageJ software. Dissociation constants were then calculated as previously described by Webb et al. (2004) (Donais, Webb et al. 2004; Storbeck, Wagner et al. 2009). Briefly, the ratio of the area of the focal adhesion as observed from the GFP fluorescence at T=0 and T=X was determined. Plotting of the natural log of this quotient ($\ln[I_0/I_t]$) over time and subsequent calculation of the slope was used to obtain the value for K*diss*(min^{-1}). Means of the K*diss* and standard errors of the means of more than 20 adhesions were calculated.

SUPPLEMENTAL MATERIAL

Supplemental Figure 1. Phospho-paxillin S250 localizes to actin fibres. Sub-confluent MEF-3T3 cells were immunostained for pPxnS250 (FITC) and phalloidin (TRITC). Merged image shows co-localization and DAPI stained nuclei.

Supplemental Figure 2. Expression of PxnS250T does not impair adhesion. MEF-3T3 cells expressing GFP fusion proteins were plated and allowed to adhere for the indicated times. After washing and fixing the remaining GFP-positive cells were enumerated.

Supplemental Figure 3. Compiled movie of migrating MEF-3T3 expressing mutant GFP-PxnS250T. Phase contrast and fluorescent images were analyzed by time-lapse microscopy using a Ziess Colibri LED microscope (Carl Zeiss, Inc.). Frames were collected every minute for 12 minutes. Note the absence of adhesion breakdown (Arrowheads) and intense membrane ruffling.

Supplemental Figure 4. Compiled movie of migrating MEF-3T3 expressing wildtype GFP-Pxn. Phase contrast and fluorescent images were analyzed by time-lapse microscopy using a Ziess Colibri LED microscope (Carl Zeiss, Inc.). Frames were collected every minute for 12 minutes.Arrowheads show adhesions breaking down or assembling at the front. Note the nucleus translocating in the direction of migration.

REFERENCES

Abou Zeid, N., A.-M. Valles, et al. (2006). "Serine phosphorylation regulates paxillin turnover during cell migration." Cell Communication and Signaling **4**(1): 8.

Amano, M., Y. Tsumura, et al. "A Proteomic Approach for Comprehensively Screening Substrates of Protein Kinases Such as Rho-Kinase." PLoS ONE **5**(1): e8704.

Anan, T., Y. Nagata, et al. (1998). "Human ubiquitin-protein ligase Nedd4: expression, subcellular localization and selective interaction with ubiquitin-conjugating enzymes." Genes to Cells **3**(11): 751-763.

Bellis, S. L., J. A. Perotta, M. S. Curtis and C. E. Turner (1997). "Adhesion of fibroblasts to fibronectin stimulates both serine and tyrosine phosphorylation of paxillin." Journal of Biochemistry **325**: 375-381.

Broussard, J. A., D. J. Webb, et al. (2008). "Asymmetric focal adhesion disassembly in motile cells." Current Opinion in Cell Biology **20**(1): 85-90.

Brown, M. C., J. A. Perrotta, et al. (1998). "Serine and Threonine Phosphorylation of the Paxillin LIM Domains Regulates Paxillin Focal Adhesion Localization and Cell Adhesion to Fibronectin." Mol. Biol. Cell **9**(7): 1803-1816.

Brown, M. C. and C. E. Turner (2002). "Roles for the tubulin- and PTP-PEST-binding paxillin LIM domains in cell adhesion and motility." The International Journal of Biochemistry & Cell Biology **34**(7): 855-863.

Brown, M. C. a. C. E. T. (2004). "Paxillin: Adapting to Change." Physiological Reviews **84**(4): 1315-1339.

Chen, Z. J. and L. J. Sun (2009). "Nonproteolytic Functions of Ubiquitin in Cell Signaling." Molecular cell **33**(3): 275-286.

Deramaudt, T. B., D. Dujardin, et al. "FAK phosphorylation at Tyr-925 regulates cross-talk between focal adhesion turnover and cell protrusion." Mol. Biol. Cell **22**(7): 964-975.

Didier, C., L. Broday, et al. (2003). "RNF5, a RING Finger Protein That Regulates Cell Motility by Targeting Paxillin Ubiquitination and Altered Localization." Mol. Cell. Biol. **23**(15): 5331-5345.

Donais, K., D. J. Webb, et al. (2004). "FAK-Src signalling through paxillin, ERK and MLCK regulates adhesion disassembly." Nature Cell Biology **6**(2): 154-161.

Duclos, B., S. Marcandier, et al. (1991). [2] Chemical properties and separation of phosphoamino acids by thin-layer chromatography and/or electrophoresis. Methods in Enzymology, Academic Press. **Volume 201:** 10-21.

Efimov, A. and I. Kaverina (2009). "Significance of microtubule catastrophes at focal adhesion sites." Cell adhesion & migration **3**(3): 285-7.

Efimov, A., N. Schiefermeier, et al. (2008). "Paxillin-dependent stimulation of microtubule catastrophes at focal adhesion sites." Journal of Cell Science **121**(2): 196-204.

Etienne-Manneville, S. and A. Hall (2001). "Integrin-Mediated Activation of Cdc42 Controls Cell Polarity in Migrating Astrocytes through PKCÎ¶." Cell **106**(4): 489-498.

Ezratty, E. J., M. A. Partridge, et al. (2005). "Microtubule-induced focal adhesion disassembly is mediated by dynamin and focal adhesion kinase." Nat Cell Biol **7**(6): 581-590.

Gilcrease, M. Z. (2007). "Integrin signaling in epithelial cells." Cancer letters **247**(1): 1-25.

Hagel, M., E. L. George, et al. (2002). "The Adaptor Protein Paxillin Is Essential for Normal Development in the Mouse and Is a Critical Transducer of Fibronectin Signaling." Mol. Cell. Biol. **22**(3): 901-915.

Hoellerer, M. K., M. E. M. Noble, et al. (2003). "Molecular Recognition of Paxillin LD Motifs by the Focal Adhesion Targeting Domain." Structure (London, England : 1993) **11**(10): 1207-1217.

Horwitz, A. R. and J. T. Parsons (1999). "Cell Migration--Movin' On." Science **286**(5442): 1102-1103.

Kaverina, I., O. Krylyshkina, et al. (1999). "Microtubule Targeting of Substrate Contacts Promotes Their Relaxation and Dissociation." The Journal of Cell Biology **146**(5): 1033-1044.

Manes, S., E. Mira, et al. (2000). "Cells on the Move: A Dialogue Between Polarization and Motility." IUBMB Life **49**(2): 89-96.

Parsons, J. T., A. R. Horwitz, et al. "Cell adhesion: integrating cytoskeletal dynamics and cellular tension." Nat Rev Mol Cell Biol **11**(9): 633-643.

Petit, V. and J.-P. Thiery (2000). "Focal adhesions: structure and dynamics." Biology of the Cell **92**(7): 477-494.

Romer, L. H., K. G. Birukov, et al. (2006). "Focal Adhesions: Paradigm for a Signaling Nexus." Circ Res **98**(5): 606-616.

Roovers, K., S. Wagner, et al. (2009). "The Ste20-like kinase SLK is required for ErbB2-driven breast cancer cell motility." Oncogene **28**(31): 2839-2848.

Sabourin, L. A. and M. A. Rudnicki (1999). "Induction of apoptosis by SLK, a Ste20-related kinase." Oncogene **18**(52): 7566.

Scheswohl, D., J. Harrell, et al. (2008). "Multiple paxillin binding sites regulate FAK function." Journal of Molecular Signaling **3**(1): 1.

Storbeck, C. J., S. Wagner, et al. (2009). "The Ldb1 and Ldb2 Transcriptional Cofactors Interact with the Ste20-like Kinase SLK and Regulate Cell Migration." Mol. Biol. Cell **20**(19): 4174-4182.

Wade, R., J. Bohl, et al. (2002). "Paxillin null embryonic stem cells are impaired in cell spreading and tyrosine phosphorylation of focal adhesion kinase." Oncogene **21**(1): 96-107.

Wagner, S., T. A. Flood, et al. (2002). "Association of the Ste20-like Kinase (SLK) with the Microtubule." Journal of Biological Chemistry **277**(40): 37685-37692.

Wagner, S., C. J. Storbeck, et al. (2008). "FAK/src-Family Dependent Activation of the Ste20-Like Kinase SLK Is Required for Microtubule-Dependent Focal Adhesion Turnover and Cell Migration." PLoS ONE **3**(4): e1868.

Webb, D. J., C. M. Brown, et al. (2003). "Illuminating adhesion complexes in migrating cells: moving toward a bright future." Current Opinion in Cell Biology **15**(5): 614-620.

Webb, D. J., M. J. Schroeder, et al. (2005). "Paxillin phosphorylation sites mapped by mass spectrometry." Journal of Cell Science **118**(21): 4925-4929.

Yang, W. L., X. Zhang, et al. "Emerging role of Lys-63 ubiquitination in protein kinase and phosphatase activation and cancer development." Oncogene **29**(32): 4493-4503.

Zaidel-Bar, R., C. Ballestrem, et al. (2003). "Early molecular events in the assembly of matrix adhesions at the leading edge of migrating cells." Journal of Cell Science **116**(22): 4605-4613.

Zimerman, B., T. Volberg, et al. (2004). "Early molecular events in the assembly of the focal adhesion-stress fiber complex during fibroblast spreading." Cell Motility and the Cytoskeleton **58**(3): 143-159.

Figure Legends:

Figure 1: ***SLK and paxillin co-localize to membrane ruffles and the leading edge of migrating cells.*** Confluent MEF-3T3 fibroblasts were scratch-wounded and co-immunostained for paxillin **(A)** and SLK **(B)**. Scratch-wounded monolayers were also co-stained for α-tubulin **(D)** and SLK **(E)**. Note the absence of SLK/Paxillin co-localization in mature focal adhesions (arrows). Images were captured by confocal microscopy (A-C; 400x, D-F; 630x).

Figure 2: ***SLK phosphorylates paxillin in vitro*****.** **(A)** Endogenous SLK was immunoprecipitated (IP) from scratch-wounded MEF-3T3 and added *in vitro* kinase assays containing purified recombinant GST-paxillin or GST alone. Coomassie stain was used to visualize protein loading. **(B)** HA-tagged SLK or a kinase inactive mutant (K63R) were transiently transfected into 293 cells, immunoprecipitated and used in kinase assays as in (A) The presence of SLK and paxillin was confirmed by immunobloting. **(C)** Phospho-amino acid analysis of *in vitro* phosphorylated GST-paxillin (pGST-paxillin) excised from the gel in (A). The results show that SLK phosphorylates paxillin exclusively on serine residues.

Figure 3: ***SLK phosphorylates paxillin on serine 250 in vitro*****.** **(A)** Schematic representation of the human paxillin deletion constructs used in the mapping of the SLK phosphorylation site. **(B)** *In vitro* kinase assay using immunoprecipitated SLK and recombinant GST-paxillin domain constructs GST-LD1-5 and GST-LIM1-4, as well as full length GST-Paxillin (Pxn). A phosphorylated N-terminal breakdown product was consistently observed in the GST-LD1-5 protein (*). **(C)** *In vitro* kinase assay as in (B) except that the GST constructs consisted in N-terminal deletion constructs. GST-Δ660, Δ699 and Δ758 denote the last nucleotide deleted from the paxillin cDNA. (WT; wildtype). The asterisk denotes an SLK-specific background product in the kinase assay. **(D)** SLK kinase assays showing the absence of phosphorylation in the GST-paxillinS243G, S244G and S250A point mutants. **(E)** SLK kinase assays showing phosphorylation in the GST-paxillinS243T, S244T and S243/244T point mutants. No phosphorylation was observed in the S250T mutant. **(F)** Phospho-amino acid analysis showing that the double mutant S243/244/T is not threonine phosphorylated.

Figure 4: ***SLK phosphorylates paxillin in vivo on S250.*** **(A)** *In vivo* validation of the phospho-S250 antibody. Equal amounts of protein derived from paxillin-null (-/-) MEF and wildtype MEF resolved using SDS-PAGE and immunoblotted for phospho-paxillin S250. Total paxillin and tubulin were assessed as controls. **(B)** MEF3T3 lysate from a scratch-wound time course were subjected to SLK IPs and *in vitro* kinase assays to evaluate SLK kinase activity. Lysates from the same scratch-wound time course was also assessed for paxillin phosphoS250 and total paxillin levels. **(C)** Confluent monolayers were infected with AdshSLK and cell lysates were collected 48h post infection. The extracts were analysed for SLK, pS250 and total paxillin levels. Knock down of SLK results in a reduction of pPxnS250 levels. **(D)** Immunofluorescence staining of endogenous phospho-paxillinS250 and total paxillin in subconfluent MEF3T3 (630x). Phospho-paxillin S250 predominantly localizes along the stress fibers and at

adhesion complexes (arrowheads). Co-localization is also observed in membrane ruffles (arrow)

Figure 5: ***Paxillin S250 phosphorylation is required for cell spreading and efficient cell migration.*** **(A)** GFP-fusion transiently transfected MEF3T3 were assessed for cell spreading using phase contrast and fluorescence microscopy. At least 6 independent fields of view containing more than 200 cells are represented as a mean of pixel units^2 for each time point. Statistical analyses were conducted relative to the paxillin S250T mutant for both assays (*, $p < 0.05$; **, $p < 0.01$; ***, $p < 0.005$). **(B)** Representative phase contrast and corresponding fluorescent (488 nm) field of view at 90 minutes post plating. **(C and D)** Boyden chamber and wound healing migration of stably transfected Myc-PaxillinS250T and Myc-Paxillin MEF3T3. For Boyden chambers, cells were plated onto the upper side of a transwell membrane and allowed to migrate for 6 hours. For wound-healing assays, phase contrast photography was taken of the artificial wounds at T = 0 and at T = 10 hours. Statistical analyses were conducted relative to the paxillin S250T mutant for both assays (*, $p < 0.05$; **, $p < 0.01$; ***, $p < 0.005$).

Figure 6: ***Paxillin S250 phosphorylation is required for adhesion turnover*** **(A)** GFP-fusion transfected MEF3T3 cells were subjected to live imaging using phase contrast and fluorescent (488 nm) microscopy on fibronectin-coated plates. Images are shown at intervals of 3 minutes. Arrowheads denote stable adhesions in GFP-PaxillinS250T or adhesions that are turning over in GFP-Paxillin cells. **(B)** The focal adhesion disassociation constant (K*diss*) were calculated as described in Storbeck et al., (2009) (Storbeck, Wagner et al. 2009). Statistical analyses were conducted relative to the paxillin S250T mutant (*, $p < 0.05$; **, $p < 0.01$; ***, $p < 0.005$).

Figure 7. ***Paxillin S250 phosphorylation is required for FAK association and further signaling.*** **(A)** MEF3T3 cells were subjected to nocodazole wash out experiments and the levels of FAK-Y925, pPxnS250, total FAK and paxillin were evaluated at the indicated time points following wash out. **(B)** Myc fusion proteins from transiently transfected 293 cells were immunoprecipitated and blotted back for FAK and the Myc-tagged fusion. The levels of FAK-Y397 and Y925 were also assessed in the same lysates. Our results show that mutant S250T paxillin cannot interact with FAK and interferes with further FAK phosphorylation at Y925. **(C)** Paxillin S250 phosphorylation is required for ubiquitylation. Immunoprecipitation of the Myc-tagged paxillin S250T mutant (Myc-PxnS250T) shows undetectable levels of ubiquitylation.

Figure 8: ***Proposed model for the role of paxillin S250 phosphorylation in cell migration.*** As paxillin and SLK can both be localized to membrane ruffles in close proximity to adhesion sites, we propose that FAK-dependent activation requires paxillin phosphorylation by SLK. The target may be tubulin-bound paxillin. Paxillin phosphorylation on serine 250 triggers its ubiquitylation and recruitment to focal adhesions/complexes, through the actin network. It can then interact with FAK to promote further signalling and adhesion turnover.

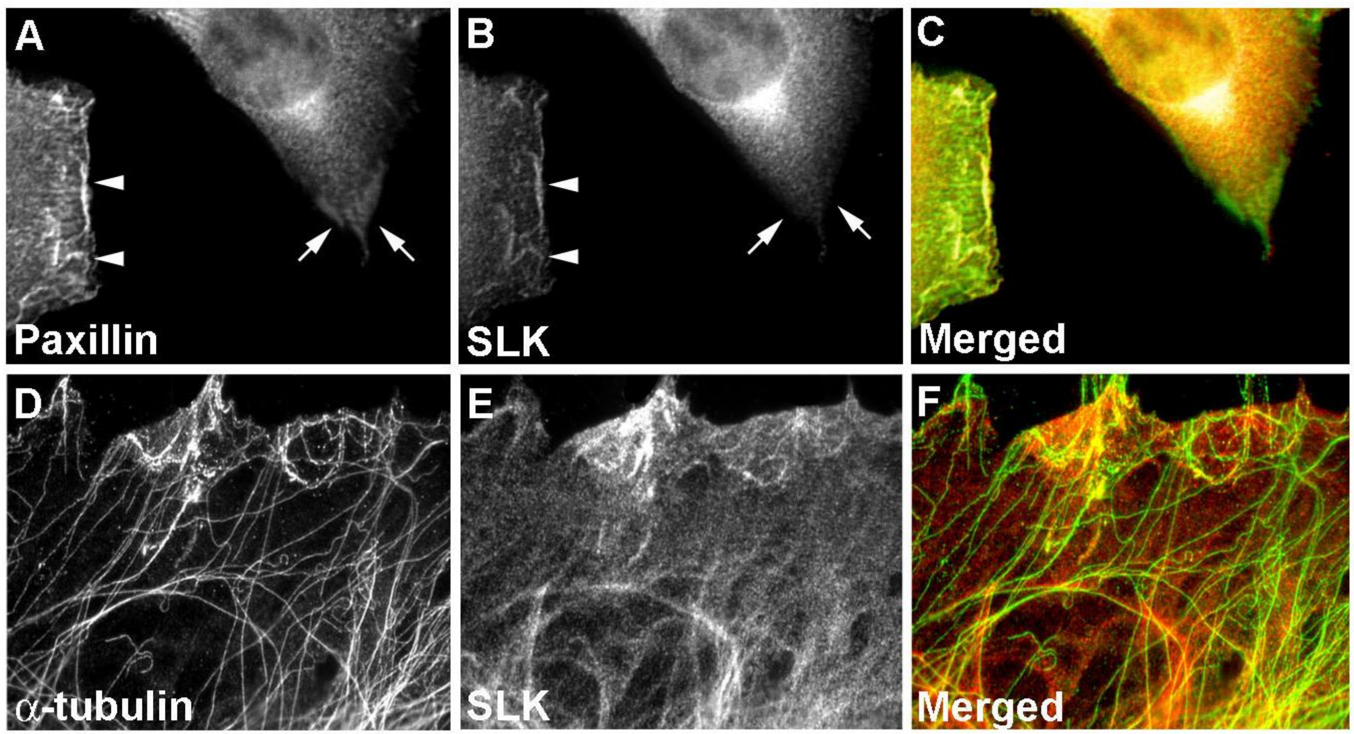

Figure 1-Quizi

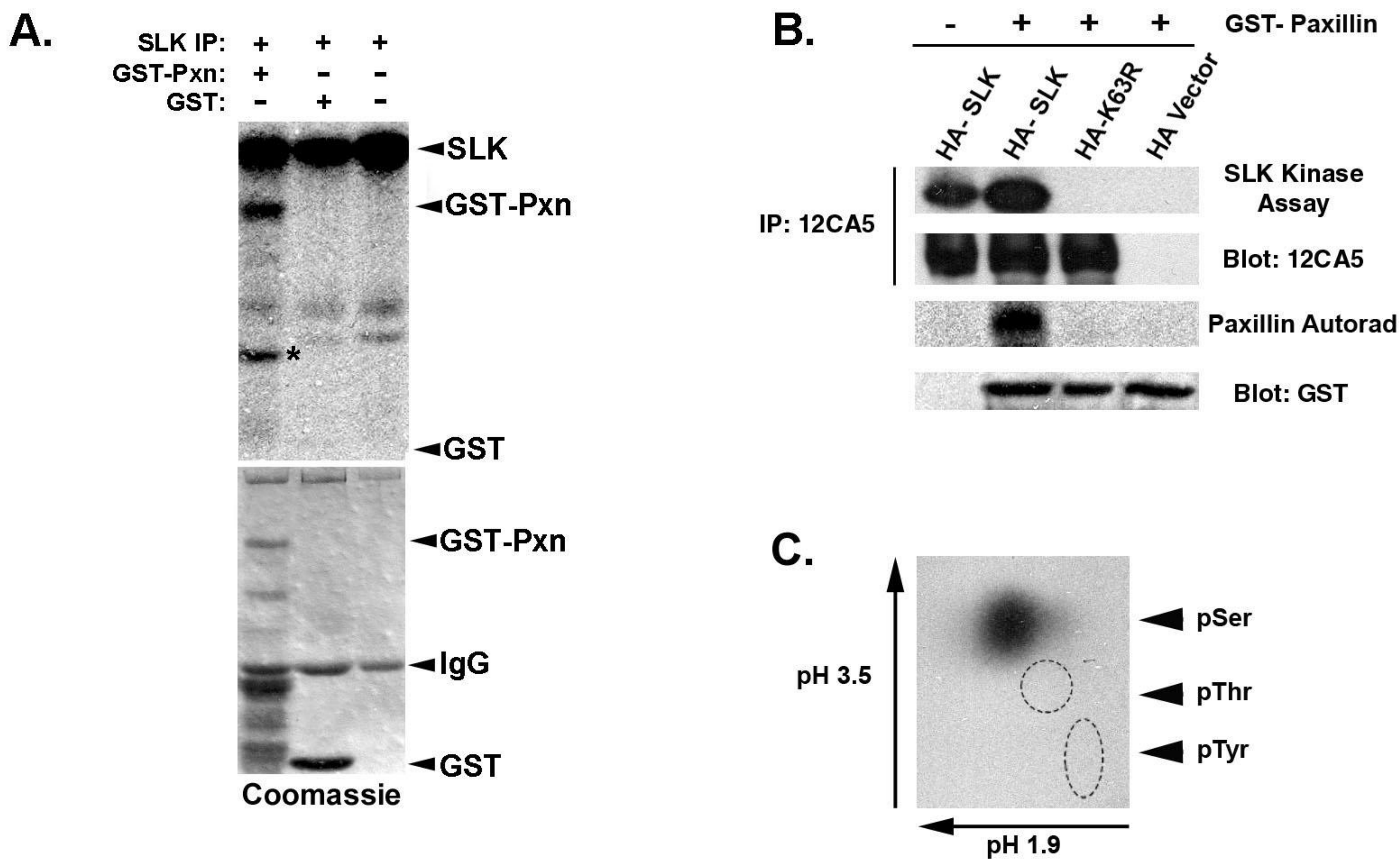

Figure 2- Quizi

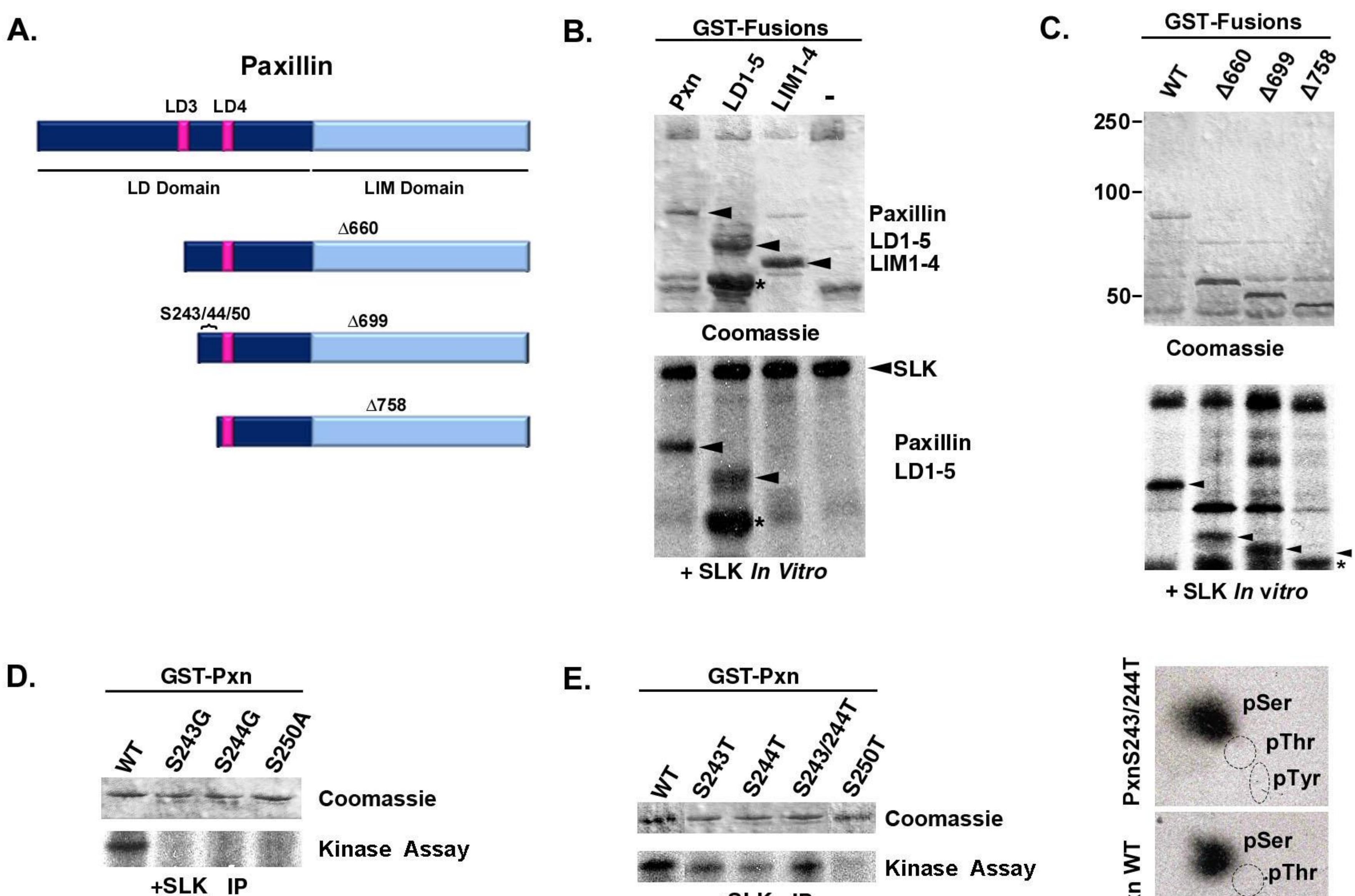

Figure 3- Quizi

A.

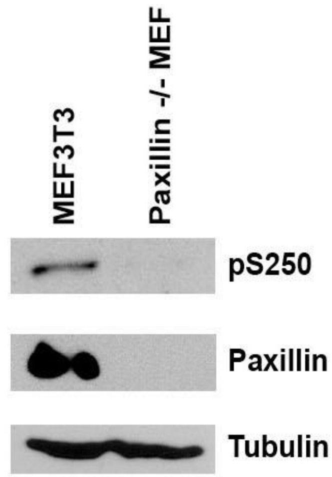

B.

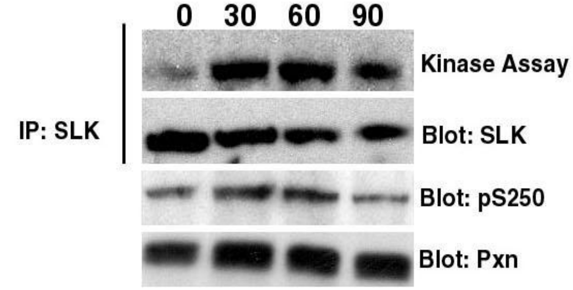

C.

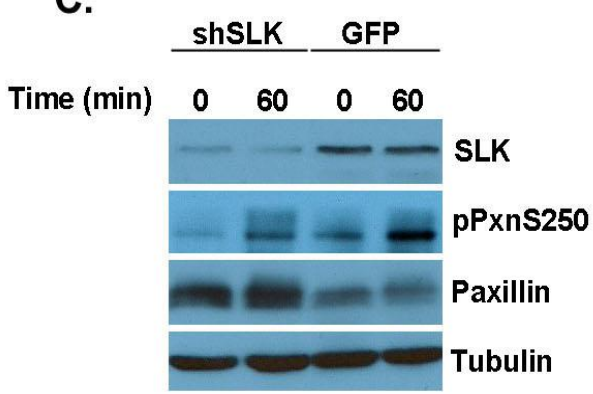

D.

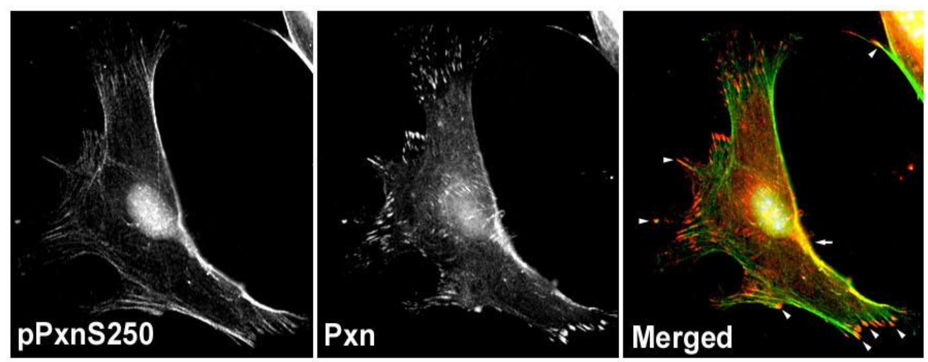

Figure 4- Quizi

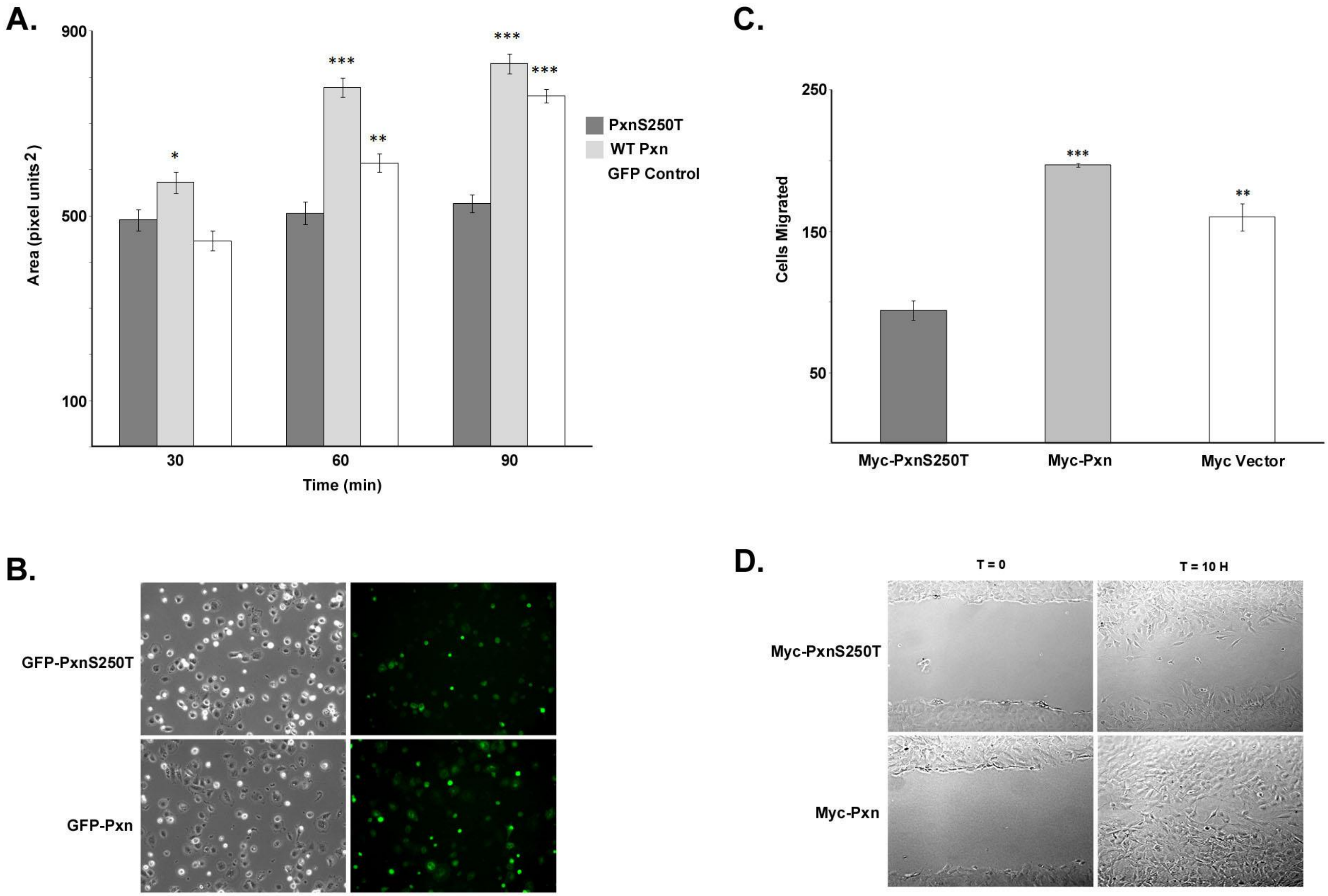

Figure 5 -Quizi

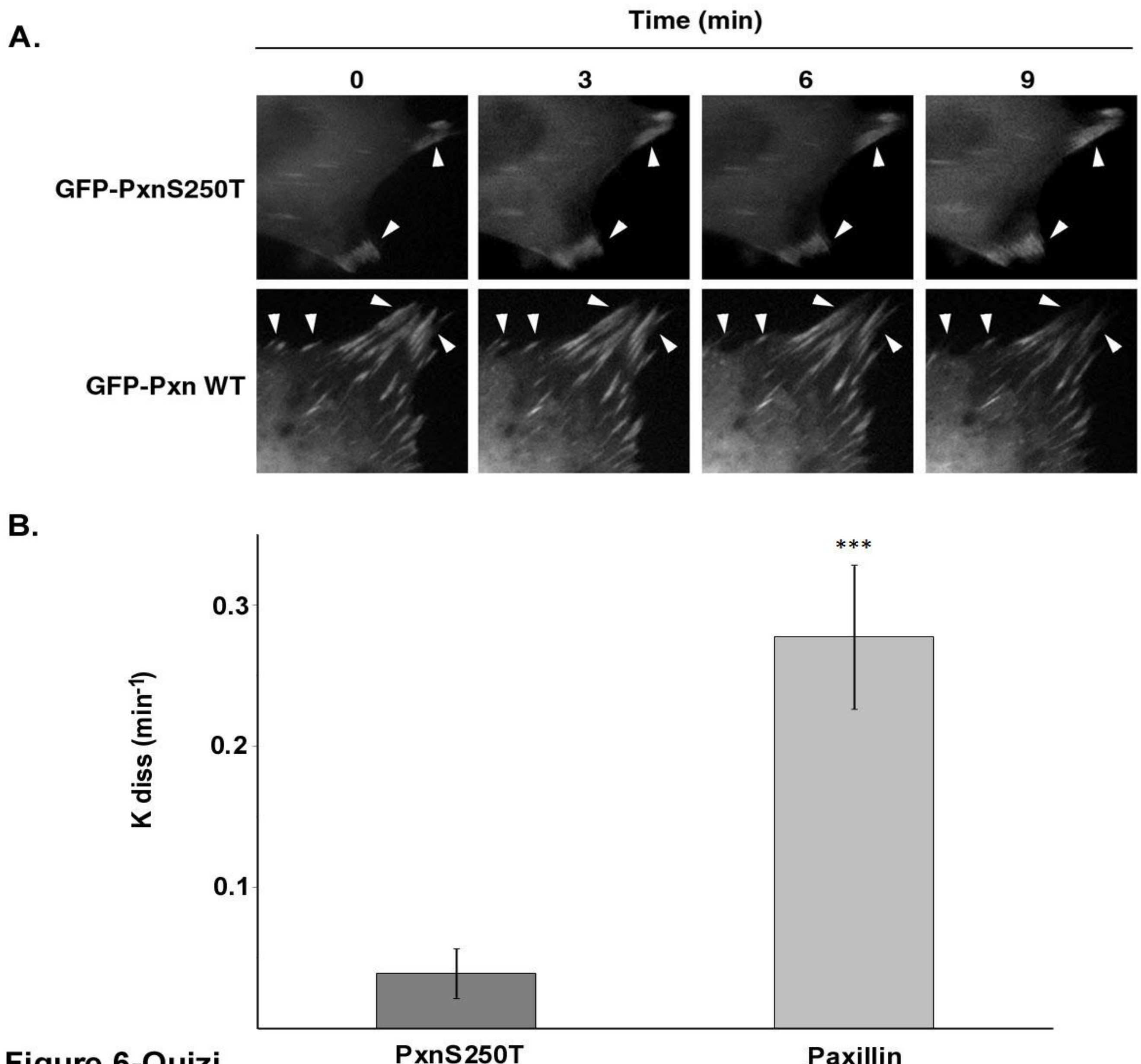

Figure 6-Quizi

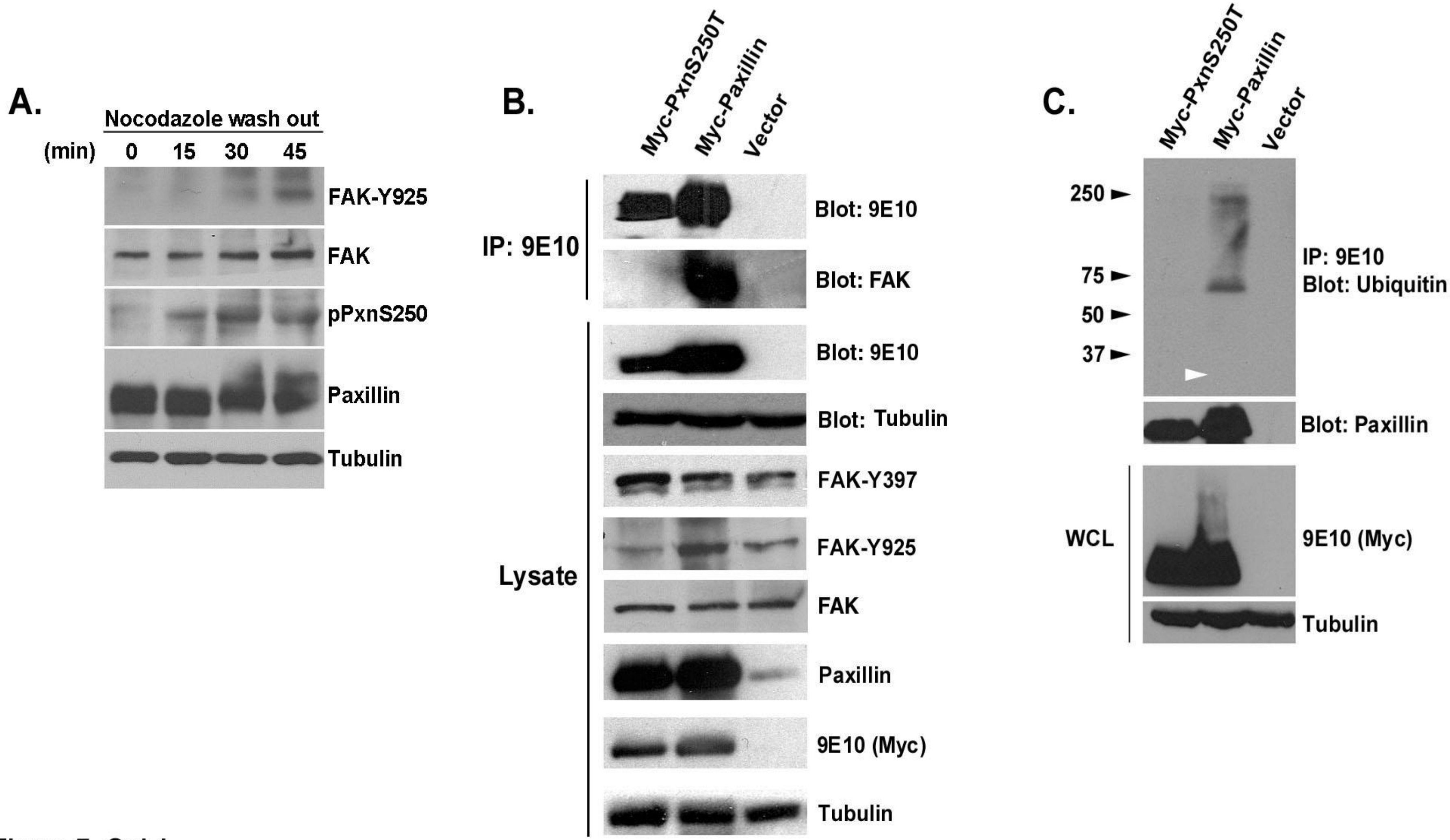

Figure 7- Quizi

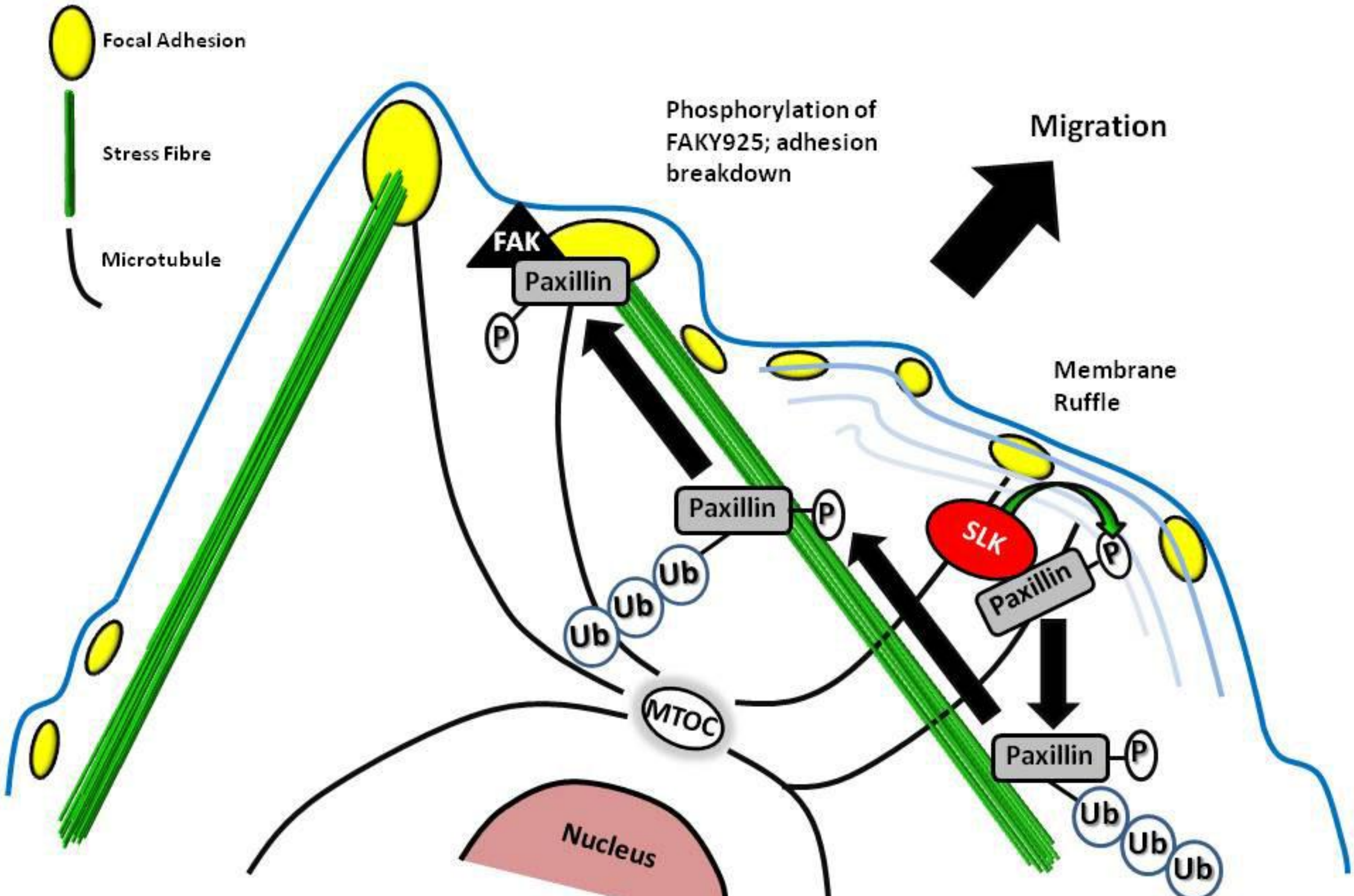

Figure 8- Quizi